POLITECNICO DI MILANO

II Facoltà di Ingegneria

Corso di Laurea Specialistica in Ingegneria Biomedica

AUTOMATIC LABELING AND NOMENCLATURE OF THE TRACHEO-BRONCHIAL TREE RECONSTRUCTED FROM VOLUMETRIC CT LUNG IMAGES

Relatore: Prof. Andrea Aliverti

Correlatore: Dott. Ing. Caterina Salito

Tesi di Laurea di:

Sebastiano Mauriello
Matr. 723441

Anno Accademico 2009/2010

CONTENTS

LIST OF FIGURES 5
LIST OF TABLES 7

ABSTRACT 9
SOMMARIO 15

CHAPTER 1 – Introduction 21
1.1 – NORMAL LUNG ANATOMY 22
1.1.1 – The secondary pulmonary lobule and lung acinus 22
1.1.2 – Airways anatomy 24
GEOMETRY OF THE AIRWAYS TREE 26
BRONCHI NOMENCLATURE 29
THE PROBLEM OF ATUOMATED AIRWAYS LABELING 32
1.2 – CT FEATURES OF THE NORMAL LUNG 33
1.2.1 – Lung arteries and bronchi 33
1.2.2 – Secondary pulmonary lobule 34
1.2.3 – Lung parenchyma 35
1.2.4 – The airways tree extraction from CT images 37
1.3 – VIRTUAL BRONCHOSCOPY 39
1.3.1 – The virtual bronchoscopy applications 41

CHAPTER 2 – Materials and Methods 45
2.1 – STATE OF ART 46
2.1.1 – Association graph 46
2.1.2 – Machine learning and combination optimization 47
LEARNING PHASE 48
TEST PHASE 49
2.2 – METHODS 50
2.2.1 – Main steps 50
2.2.2 – Airways segmentation from thoracic CT 50
THORACIC CT 50
AIRWAYS SEGMENTATION 50
2.2.3 – Preliminary segmentation processing 52
CLOSING OPERATION 52
CARINA DEMASKING 53
2.2.4 – Key points extraction 54
SLICE ANALYSIS 54
CENTROIDS MATRIX 59
CENTROIDS CODE 62
BRANCH RECOGNITION 63
KEY POINTS 66

2.2.5 – Stick diagram 68
SHORT TERMINATION BRANCHES ELIMINATION 68
KEY POINTS LINKING RULES 68
KEY POINTS MATRIX CLASSIFICATION 71
LINKING ALGORITHM 73
Computing of the ideal trace 73
Collision prevention 73
STICK DIAGRAM 76
2.2.6 – Labeling 79
ANATOMICAL MATRIX 80
STICK DIAGRAM ANALYSIS 82
Neighbourhoods theft 83
Branches name codes 84
Upper lobe limits 85
Topologic rules 88
Candidate label reduction 89
Anatomical matrix real time update 89
Branches matrix 90
2.2.7 – Statistical analysis 90

CHAPTER 3 – Results 91
3.1 – EXPERIMENTAL PROTOCOL 92
DATABASE 92
ANATOMICAL MATRIX 92
3.2 – REPRESENTATIVE AUTOMATED AIRWAYS LABELING 93
3.3 – RESULTS 103

Conclusions and future development 119

Appendix 1 – The algorithm flow charts 125
Appendix 2 – User interventions 143

BIBLIOGRAPHY 153

LIST OF FIGURES

CHAPTER 1 – Introduction

1 - Anatomy and dimensions of secondary lobule and pulmonary acinus. 22
2 - Resin cast of a human tracheo-bronchial tree. 25
3 - Organization of the airways tree by functional zones. 25
4 - Patterns of airways branching. 26
5 - Hierarchy of space division of the lung. 30
6 - A typical example of the human bronchial tree. 30
7 - Branching patterns of segmental bronchi arising from the right upper lobar bronchus (UB). 30
8 - Scheme of the bronchial nomenclatures. 31
9 - Normal appearances of large bronchi and arteries. 33
10 - HRCT of the normal lung at suspended deep inspiration. 34
11 - The septa bordering a well defined lobule are partially visible. 35
12 - HRCT of normal lung in supine and in prone body position in suspended deep inspiration. 36
13 - The relationships between the trachea, a paratracheal abscess, and the carotid artery. 40
14 - Example of transbronchial lymph node biopsy. 42
15 - Screen shot of a pulmonary path-finding program. 43

CHAPTER 2 – Materials and Methods

16 - Flowchart and ten feature extracted in method proposed by Mori. 47
17 - Combinatorial optimization approach. 48
18 - Automated labeling of the tracheo-bronchial tree block diagram. 51
19 - Example of closing operation on a segmentation slice. 52
20 - Example of carina de-masking. 53
21 - Example of tracheo-bronchial tree segmentation. 55
22 - Single slice at fixed Z extracted from an airways segmentation. 55
23 - Two consecutive slices of an airways tree segmentation. 56
24 - Five significant steps of branch recognition mechanism. 58
25 - Example of centroids of a group of connected pixels. 59
26 - The real and false central axis for branches like trachea and left upper lobe bronchus. 60
27 - Example of centroid moving. 61
28 - Example of tags assignment and bit C and S utilization. 65
29 - Example of AUX useful. 67
30 - Example of linking rule 4 application. 69
31 - Example of linking rule 5 application. 69
32 - Example of linking rule 6 application. 70
33 - The four step of stick diagram creation. 72
34 - Example of 2D line rasterization. 73
35 - A two-dimensional example of collision avoidance. 74
36 - The rasterization line principle and minimization distance principle. 75

37 - The stick diagram obtained from an airways segmentation. 76
38 - Stick diagram of the left upper lobe bronchus. 77
39 - The airways tree extracted from Netter Atlas of Anatomy. 79
40 - Example of cube for possible ramifications development classification from a target sector. 81
41 - Example of labeling mechanism. 82
42 - The correct 2D ramification classification that avoid the neighbourhood theft phenomena. 83
43 - The complete stick diagram with the correct label on every branch. 84

CHAPTER 3 – Results

44 - Segmented airways tree, key points and stick diagram. 93
45 - Steps of a representative case of automated airways labeling. 100
46 - The airways tree extracted from Netter Atlas of Anatomy and the complete stick diagram. 110
47 - Bars graphs. 111
48 - The total percent of branch recognized zone by zone at TLC and RV volume. 116
49 - The percent of the automatism on the airways tree zone by zone at TLC and RV volume. 117
50 - The percent of branches automatically recognized zone by zone at TLC and RV volume. 118

Appendix 1 – The algorithm flow charts

51 - Linking algorithm flow chart. 126
52 - Carina de-masking algorithm flow chart. 127
53 - Branch recognition algorithm flow chart part 1/2. 128
54 - Branch recognition algorithm flow chart part 2/2. 129
55 - Branch algorithm flow chart. 130
56 - Ramification algorithm flow chart part 1/2. 131
57 - Ramification algorithm flow chart part 2/2. 132
58 - Branch end algorithm flow chart. 133
59 - Stick diagram algorithm flow chart. 134
60 - Stick diagram creation algorithm flow chart part 1/3. 135
61 - Stick diagram creation algorithm flow chart part 2/3. 136
62 - Stick diagram creation algorithm flow chart part 3/3. 137
63 - Labeling algorithm flow chart part 1/3. 138
64 - Labeling algorithm flow chart part 2/3. 139
65 - Labeling algorithm flow chart part 3/3. 140
66 - Dead lobo algorithm flow chart. 141
67 - Ramification finding algorithm flow chart. 142

LIST OF TABLE

CHAPTER 1 – Introduction

1 - Bronchi Nomenclature proposed by Jackson and Huber. 29

CHAPTER 2 – Materials and Methods

2 - Advantages and disadvantages of the state of art methods. 49
3 - Columns composition of centroids matrix. 61
4 - Columns division of key points matrix. 67
5 - The anatomical matrix column division. 80
6 - Characteristic Z value extracted from database stick diagrams at TLC volume. 85
7 - The stick diagrams at TLC volume with the lobe extension out of the range. 86
8 - Characteristic Z value extracted from database stick diagrams at RV volume. 87
9 - The stick diagrams at RV volume with the lobe extension out of the range. 87
10 - Univocal correspondence between particular couples of branches. 88
11 - The branches matrix column composition. 90

CHAPTER 3 – Results

12 - The results of the labeling for each subjects at TLC volume. 104
13 - The results of the labeling for each subjects at RV volume. 105
14 - The total results of the labeling at TLC, RV and on the entire database. 105
15 - The results of the labeling zone by zone at TLC volume. 107
16 - The results of the labeling zone by zone at RV volume. 108
17 - The results of the labeling zone by zone on the entire database. 109

Appendix 2 – User interventions

18 - User interventions during subject 1 tracheo-bronchial tree label at TLC volume. 144
19 - User interventions during subject 2 tracheo-bronchial tree label at TLC volume. 144
20 - User interventions during subject 3 tracheo-bronchial tree label at TLC volume. 145
21 - User interventions during subject 4 tracheo-bronchial tree label at TLC volume. 145
22 - User interventions during subject 5 tracheo-bronchial tree label at TLC volume. 146
23 - User interventions during subject 6 tracheo-bronchial tree label at TLC volume. 147
24 - User interventions during subject 7 tracheo-bronchial tree label at TLC volume. 148
25 - User interventions during subject 8 tracheo-bronchial tree label at TLC volume. 148
26 - User interventions during subject 1 tracheo-bronchial tree label at RV volume. 149
27 - User interventions during subject 2 tracheo-bronchial tree label at RV volume. 149
28 - User interventions during subject 3 tracheo-bronchial tree label at RV volume. 150
29 - User interventions during subject 4 tracheo-bronchial tree label at RV volume. 150
30 - User interventions during subject 5 tracheo-bronchial tree label at RV volume. 151
31 - User interventions during subject 6 tracheo-bronchial tree label at RV volume. 151
32 - User interventions during subject 7 tracheo-bronchial tree label at RV volume. 152
33 - User interventions during subject 8 tracheo-bronchial tree label at RV volume. 152

ABSTRACT

Volume data acquisition for medical imaging is rapidly spreading in the clinical use due to the technological progress in multi-detector CT scanners. 3D image processing techniques have enabled precise structural analysis of living organs. **Anatomical nomenclature** is an important step in sharing a common understanding of organs structure. However, anatomical knowledge used for establishing the nomenclature of biological structure, is challenging when seeking to construct robust computational algorithms, because of the nature of biologic complexity and diversity. Inter-individual and intra-individual comparisons are in fact meaningful only when accurate nomenclatures are applied to the structures. Discrepancy of anatomical nomenclature, even between experts, is not uncommon.

The **human airways tree** is a typical example of the difficulty of nomenclature and labeling because of its hierarchical properties and the considerable variations of branching pattern. Automated airways labeling is extremely important for a large field of applications, ranging from fundamental to clinical imaging investigation. One of the more recent clinical application is virtual bronchoscopy, which is providing a significant contribution to pulmonary practice particularly in the field of interventional pulmonology. Bronchoscopic navigation systems and advanced virtual bronchoscopy include applications such as pulmonary path-finding of peripheral lung lesions, mediastinal biopsies, and surgical planning of increasingly important procedures for the treatment of emphysema, such as endo-bronchial valves and airways bypasses.

The aim of this thesis was to develop a **new method for an automatic labeling of the tracheo-bronchial tree**.

The main innovative aspect of the **proposed method** is a way to extract information from the segmented airways, different from the classical skeletonization. Through the linking of key points, extracted from the tracheo-bronchial tree, is possible to obtain a guide to overlap to the original segmented airways tree. This guide is called “stick diagram” and it is useful to help the labeling of the branches up to the segmental bronchus. This kind of approach introduces less artefacts than a classical skeletonization algorithm.

In order to perform the key points extraction a preliminary branch recognition is realized on the segmented airways. This process starts from a bi-dimensional analysis of the segmented slices. On a single slice pixel regions which represent a section of the airways tree at a fixed quote are visible. Looking at a particular slice, the region which represents the section of the airway followed, is called "*target region*". The intersections between its projections and other regions on the above and on the below slices are considered. If a single intersection is found it means that the branch followed continues without ramifications instead if a multiple intersection is found it means a ramification of the tree. If no intersection is found it means that the end of a branch has been reached. The centroids of the regions that represent feature points of the airways tree, like ramification points or branch ending, are classified as key points. A numeric code that permits to determine the relationship between these new points is assigned to each centroid. This code is fundamental to perform the correct linking of the key points to realize the stick diagram.

The labeling of the stick diagram is performed using information of the relative orientation between a known target branch and an unknown branch to label. Topologic information from the airways anatomy, based on the presence of a particular branch respect to the other, are used only when this particular branch has really been found on the stick diagram. In this way the lack of branches, due to a poor segmentation, doesn't heavily influence the labeling.

The first step of the labeling algorithm is the creation of an "*anatomical matrix*" to associate a specified tag at all the possible directions of the branches. The user intervention is required when an ambiguity is found by the software in anatomical matrix: a list of possible labels candidates, for the unknown branch, is proposed.

The method developed in the frame of this thesis work has been successively applied and tested on the airways trees extracted from whole lung CT images of eight healthy subjects, taken at two different lung volumes: full inspiration at Total Lung Capacity (TLC) and full expiration at Residual Volume (RV).

The **results** obtained in terms of algorithm performance, for automatic branch recognition, were generally highly positive. A detailed multi-factorial quantitative analysis showed that the total percentage of automatically recognized branches, in the right lung, was influenced by lung volume, while, in the left lung, no influence of lung volume was present. The principal sources of error influencing the algorithm performances were the inter-individual anatomical variability of branches generation points in the right upper lobe and in the lingular bronchus and the major anatomical complexity of the airways tree in the lower lobes. As a consequence, the labeling in the lower lobes cannot be accurate as for the upper lobes.

Future developments will be oriented to improve algorithm performances in the critical airways tree zones. The dimension of the matrix, which contains the segmented airways tree, is too small to describe in detail all the regions of the tracheo-bronchial tree: a compromise between computational costs and comprehension of the stick diagram should be necessary. An increase of the database should be very useful to do statistical study in order to find a threshold on the Z coordinate of each generation point, to better control the labeling in particular regions of the tracheo-bronchial tree. Topologic rules on ramification with more than two branches can be introduced to reduce the number of label candidate for the user interventions and, consequently, to improve the autonomy of the software.

Despite some limitations, we believe that the present work represents **an important basis for the development of fully automatic tools for tracheo-bronchial tree nomenclature**.

The thesis is structured in three main chapters.
The **first chapter** is divided in three main sections. The first section describes the CT-based lung anatomy. In particular the geometry of the airways tree is considered with a focus on the bronchi nomenclature and on the difficult problem of the automated tracheo-bronchial tree labeling.

The second section is dedicated to the CT features of the normal lung, in particular on the airways tree reconstruction from CT images. The last part illustrates the virtual bronchoscopy and its application as a main field of interest for the method developed in this thesis.

The **second chapter** presents the method developed in this work for the automatic labeling of the airways tree. In the first part there is a review on the automatic and semi-automatic methods, for anatomical labeling of bronchial branches, published up to now.
The two reported methods start from a skeletonization of the segmented airways tree.
The technique proposed by Kitaoka and Tschirren uses a method based on an association graph. The labeling algorithm is a weighted maximum clique search of an association graph between a reference tree and an object tree. Automated bronchial nomenclature and labeling can be viewed as a tree matching problem between an object tree and a standard airways tree. The nomenclature labeling is then applied to give the same name to a node in the object tree as that of its corresponding node in the reference tree.
The method proposed by Mori and Ota is based on machine learning and combination optimization. The labeling method uses a classifiers that output bronchial branch name candidates with likelihoods using learning datasets. A machine learning approach is utilized here. In the anatomical labeling process, the feature values of bronchial branches extracted from CT images, are computed. Then, for each bronchial branch, the bronchial branch name candidates, with the likelihoods, are computed using the classifiers. Finally, the anatomical names for each branch is determined by a combination optimization technique.
In the second section, the main steps of the developed work are described: the preliminary segmentation processing; the first airways branch recognition necessary to execute the key points extraction; the key points linking necessary to realize the stick diagram and finally the true automated labeling of the diagram extracted from the airways tree.

The **third chapter** reports the results obtained applying the implemented software to a set of CT volumetric data, taken on eight healthy subjects at two different lung volumes (TLC and RV). A representative automated airways labeling is presented to explain better how the software work and the typical sources of error encountered during an airways analysis. The results of the labeling are reported for each subject at TLC and RV volume and the algorithm performances are showed on the airways tree zone by zone. Bars graphs are utilized to better highlight the algorithm performance for each branch of the tracheo-bronchial tree. Scatter graphs are reported to show the software performances variations between two lung volume (TLC and RV).

In addition to the three chapters, **two appendices** are also attached where algorithm flow charts are showed and, additional data, relative to the user interventions during the labeling of the tracheo-bronchial tree, of each subject at two different lung volume (TLC and RV), are reported.

SOMMARIO

L'uso dell'imaging medico, per l'acquisizione di volumi di interesse, si sta rapidamente diffondendo in ambito clinico grazie ai progressi tecnologici nel campo delle apparecchiature TAC. Le tecniche di elaborazione di immagini 3D hanno permesso una precisa analisi strutturale degli organi in vivo. La **nomenclatura anatomica** rappresenta un importante passo nella condivisione di una conoscenza comune della struttura degli organi. La conoscenza anatomica, utilizzata per stabilire la nomenclatura di strutture biologiche, è un aspetto critico quando si cerca di sviluppare robusti algoritmi di calcolo, a causa della complessità e variabilità biologica. I confronti inter e intra individuali sono infatti significativi solo quando viene applicata la nomenclatura corretta alle strutture. L'**albero tracheobronchiale** è un tipico esempio delle difficoltà di nomenclatura e labeling, a causa delle sue proprietà gerarchiche e della considerevole variabilità nei pattern di ramificazione. Il labeling automatico delle vie aeree è estremamente importante nell'ambito di un ampio campo di applicazioni che spazia, dall'analisi basilare di immagini, all'investigazione clinica di immagini. Una delle più recenti applicazioni cliniche è la broncoscopia virtuale, che sta dando un contributo significativo nella pratica pneumologica, in particolare in campo interventistico. I sistemi di navigazione broncoscopica e la broncoscopia virtuale avanzata, aprono la strada a tecniche applicative, come la pianificazione di traiettoria per il raggiungimento di lesioni polmonari periferiche, biopsie mediastinali e la pianificazione chirurgica di procedure di crescente importanza per il trattamento dell'enfisema, come l'impianto di valvole endo-bronchiali e il bypass delle vie aeree.

L'obiettivo di questo lavoro di tesi è di sviluppare un **nuovo metodo per il labeling automatico dell'albero tracheo-bronchiale**.

L'aspetto innovativo principale del **metodo proposto** è il modo, differente dalla classica scheletonizzazione, di estrarre informazione dalle vie aeree ricostruite da immagini TAC. Attraverso l'unione di "*key points*", estratti dall'albero tracheo-bronchiale, è possibile ottenere una guida da sovrapporre all'albero delle vie aeree originariamente segmentato.

Questa guida è denominata "*stick diagram*" ed è utile come ausilio per il labeling dei rami fino ai bronchi segmentali. Questo tipo di approccio introduce meno artefatti di un classico algoritmo di scheletonizzazione.

Per effettuare l'estrazione dei key points viene realizzato un preliminare riconoscimento dei rami, nelle vie aeree segmentate. Questo processo inizia con una analisi bidimensionale delle immagini delle vie aeree segmentate. Su una singola slice sono visibili regioni di pixel, che rappresentano una sezione delle vie aeree ad una quota costante, chiamate "*regioni target*". Per ciascuna regione si osservano le eventuali intersezioni di una sua proiezione con le slice contigue. Se viene trovata una singola intersezione, significa che il ramo considerato continua senza ramificarsi; se viene individuata invece un'intersezione multipla, si è in presenza di una ramificazione di quello specifico tratto di albero. Se non viene individuata nessuna intersezione significa che è stata raggiunta la fine di un ramo. I centroidi delle regioni che rappresentano punti caratteristici dell'albero delle vie aeree, come punti di ramificazione o punti terminali di un ramo, vengono catalogati come key points. Ad ogni centroide viene assegnato un codice numerico che permette di determinare la relazione tra questi nuovi punti. Il codice è poi fondamentale per realizzare il corretto collegamento dei key points, necessario alla costruzione dello stick diagram.

Il labeling dello stick diagram è realizzato utilizzando informazioni sull'orientamento relativo tra un ramo già nominato e un ramo ancora da nominare. Le informazioni topologiche estratte dall'anatomia delle vie aeree, basate sulla presenza o meno di un ramo rispetto ad altri, vengono utilizzate solo quando questo particolare ramo viene effettivamente individuato sullo stick diagram. In questo modo, la mancanza di rami dovuta ad una segmentazione povera, non influenza in maniera pesante il labeling.

Il primo passo dell'algoritmo di labeling è la creazione di una "*matrice anatomica*", per associare un tag specifico a tutte le possibili direzioni dei rami. L'intervento dell'operatore è richiesto quando viene trovata dal software un'ambiguità nella matrice anatomica, in questo caso viene proposta una lista di possibili label candidate a diventare il nome del ramo sconosciuto.

Il metodo sviluppato in questo lavoro di tesi è stato poi applicato e testato su alberi tracheobronchiali estratti da immagini TAC dell'intero volume polmonare, di otto soggetti sani. Le immagini sono state acquisite a due differenti volumi polmonari: fine inspirazione, a capacità polmonare totale (TLC) e fine espirazione, a volume residuo (RV).

I **risultati** ottenuti, in termini di performance dell'algoritmo per quanto riguarda il riconoscimento automatico dei rami, sono in generale molto positivi.
Un'analisi multi fattoriale dettagliata mostra che vi è, nel polmone destro, un'influenza del volume polmonare sulla percentuale totale di rami riconosciuti automaticamente, mentre questo non accade nel polmone sinistro. Le principali fonti di errore che influenzano le performance dell'algoritmo sono la variabilità anatomica inter-individuale dei punti di generazione dei rami nel lobo superiore destro e nella lingula, e la maggiore complessità anatomica dell'albero nei lobi inferiori. Per questo motivo il labeling nei lobi inferiori non è risultato accurato come quello dei lobi superiori.

Sviluppi futuri saranno orientati a migliorare le performance dell'algoritmo nelle zone critiche dell'albero. La matrice che contiene le vie aeree segmentate è sottodimensionata per descrivere nel dettaglio tutte le regioni dell'albero tracheobronchiale: sarebbe necessario aumentarne la dimensione ottenendo un compromesso tra costo computazionale e comprensione nella lettura dello stick diagram. Un database più ricco potrebbe essere molto utile per effettuare uno studio statistico, atto ad identificare soglie sulla coordinata Z, di ogni punto di generazione dei rami, per migliorare il controllo del labeling in regioni particolarmente critiche dell'albero tracheobronchiale. Possono essere studiate regole topologiche sulle ramificazioni con più di due rami, per ridurre il numero di label candidate in ausilio agli interventi dell'operatore e, di conseguenza, aumentare l'autonomia del software.

Nonostante alcune limitazioni, questo lavoro rappresenta **una base importante per lo sviluppo di uno strumento completamente automatico, per la nomenclatura dell'albero tracheobronchiale**.

La tesi è strutturata in tre capitoli principali.

Il **primo capitolo** è diviso in tre sezioni. La prima sezione descrive l'anatomia polmonare basandosi su immagini TAC. Viene analizzata in particolare la geometria delle vie aeree, con un accento sulla nomenclatura dei bronchi e sul difficile problema del labeling automatico dell'albero tracheobronchiale. La seconda sezione è dedicata alle caratteristiche TAC del polmone sano e, in particolare, alla ricostruzione dell'albero tracheobronchiale da immagini TAC. L'ultima parte illustra la broncoscopia virtuale come principale campo d'interesse per il metodo sviluppato in questo lavoro di tesi, e le sue applicazioni.

Nel **secondo capitolo** è presentato il metodo sviluppato in questo lavoro per il labeling automatico delle vie aeree. Nella prima parte è presentata una review sui metodi pubblicati fino ad ora per il labeling anatomico, automatico e semiautomatico, dei rami bronchiali. I due metodi riportati partono entrambi da una scheletonizzazione dell'albero tracheobronchiale. La tecnica proposta da Kitaoka e Tschirren utilizza un metodo basato sull'association graph. La nomenclatura automatica dei bronchi è vista come un problema di corrispondenza tra un albero oggetto e un albero delle vie aeree standard. La nomenclatura è poi applicata allo scopo di dare lo stesso nome ad un nodo dell'albero oggetto e al suo corrispondente nell'albero di riferimento.

Il metodo proposto da Mori e Ota è basato sul machine learning e l'ottimizzazione combinata. Viene utilizzato un classificatore che dia in uscita i nomi dei rami candidati associati ad un coefficiente di verosimiglianza, usando un dataset di apprendimento. A questo punto viene utilizzato l'approccio del machine learning. Nell'operazione di labeling anatomico vengono calcolati dei valori caratteristici dei rami dei bronchi, estratti dalle immagini TAC. Successivamente, usando il classificatore, vengono calcolati i nomi candidati con il loro coefficiente di verosimiglianza. Alla fine vengono determinati i nomi anatomici per ogni ramo trovando la combinazione ottima tra i candidati.

Nella seconda sezione vengono descritti gli step principali del lavoro sviluppato: l'elaborazione preliminare della segmentazione; il primo riconoscimento dei rami delle vie aeree, necessario per effettuare l'estrazione dei key points; il collegamento dei key points per costruire lo stick diagram e in conclusione il labeling automatico del diagramma estratto dall'albero tracheobronchiale.

Nel **terzo capitolo** sono riportati i risultati ottenuti applicando il software implementato ad un set di TAC volumetriche, acquisite su otto soggetti sani a due differenti volumi polmonari (TLC e RV). Viene riportato un caso rappresentativo di labeling automatico, per spiegare meglio le modalità con le quali lavora il software e le tipiche fonti di errore che si incontrano. I risultati del labeling vengono riportati per ogni soggetto a TLC e RV, e le performance dell'algoritmo sulle vie aeree vengono mostrate zona per zona.

Per integrare i tre capitoli si allegano **due appendici** nelle quali sono mostrati i diagrammi di flusso dell'algoritmo e riportati i dati relativi agli interventi dell'operatore durante il labeling dell'albero tracheobronchiale di ogni soggetto, a due differenti volumi polmonari (TLC e RV).

CHAPTER 1

Introduction

1.1 – NORMAL LUNG ANATOMY

1.1.1 - The secondary pulmonary lobule and lung acinus

The lobe is the principal division of the lungs (normally, three lobes on the right and two on the left); each lobe is enveloped by visceral pleura, except at the lung root (hilum) and when an interlobar fissure is incomplete. [1]

A segment is the unit of a lobe ventilated by a segmental bronchus, perfused by a segmental pulmonary artery, and drained by an intersegmental pulmonary vein. There are two to five segments per lobe. [1] The lung is comprised of numerous anatomical units smaller than a lobe or

segment. The secondary pulmonary lobule and lung acinus are widely regarded to be the most important of these subsegmental lung units.

The secondary pulmonary lobule, as defined by Miller [2], refers to the smallest unit of lung structure marginated by connective tissue septa. Secondary pulmonary lobules are irregularly polyhedral in shape and vary in size, measuring from 1 to 2.5 cm in diameter in most locations (Figure 1).

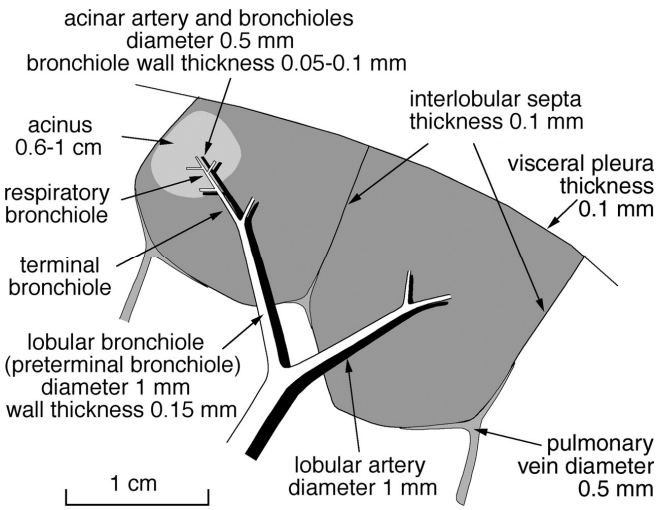

Figure 1 - Anatomy and dimensions of secondary lobule and pulmonary acinus. Two secondary pulmonary lobules in the lung periphery are illustrated, with approximate dimensions of their components indicated [3].

Airways, pulmonary arteries and veins, lymphatics, and the various components of the pulmonary interstitium are all represented at the level of the pulmonary lobule.

Each secondary lobule is supplied by a small bronchiole and pulmonary artery branch, and is variably marginated in different lung regions by connective tissue interlobular septa containing pulmonary veins and lymphatics [4].

The pulmonary acinus is smaller than a secondary lobule. It is defined as the portion of lung distal to a terminal bronchiole (the last purely conducting airways) and supplied by a first-order respiratory bronchiole or bronchioles [5]. Because respiratory bronchioles are the largest airways that have alveoli in their walls, an acinus is the largest lung unit in which all airways participate in gas exchange. Acini are usually described as ranging from 6 to 10 mm in diameter and average 7

to 8 mm in adults. It should be emphasized that all three interstitial fiber systems described by Weibel (axial, peripheral, and septal) are represented at the level of the pulmonary lobule [6], and abnormalities in any can produce recognizable lobular abnormalities on HRCT [6]. Axial (centrilobular) fibers surround the artery and bronchiole in the lobular core, peripheral fibers comprising the interlobular septa marginate the lobule, and septal fibers (the intralobular interstitium) extend throughout the substance of the lobule in relation to the alveolar walls.

1.1.2 – Airways anatomy

The airways are organized as a branching network of tubes that become narrower, shorter, and more numerous as they penetrate deeper into the lung. Air enters the pharynx through the nose and is conducted to the lungs through the trachea. The trachea divides into two main branches, the left and right bronchi, which enter into the right and left lungs [7].

The root of the airways tree is the trachea. The trachea is composed of cartilaginous rings, which are in fact horseshoe shaped and incomplete posteriorly. The posterior portion of the tracheal wall between the open ends of the tracheal cartilages, is a thin fibromuscular membrane, termed the posterior tracheal membrane.

The airways begin as a simple branched tubes whose surface is lined by mucose membrane. As we approach the periphery their structure changes in that more and more alveoli, containing a gas exchange surface, are formed as out-pocketings of their wall until, in the last few generations, the circumference of the alveolar ducts and sacs is totally occupied by alveoli (Figure 2).

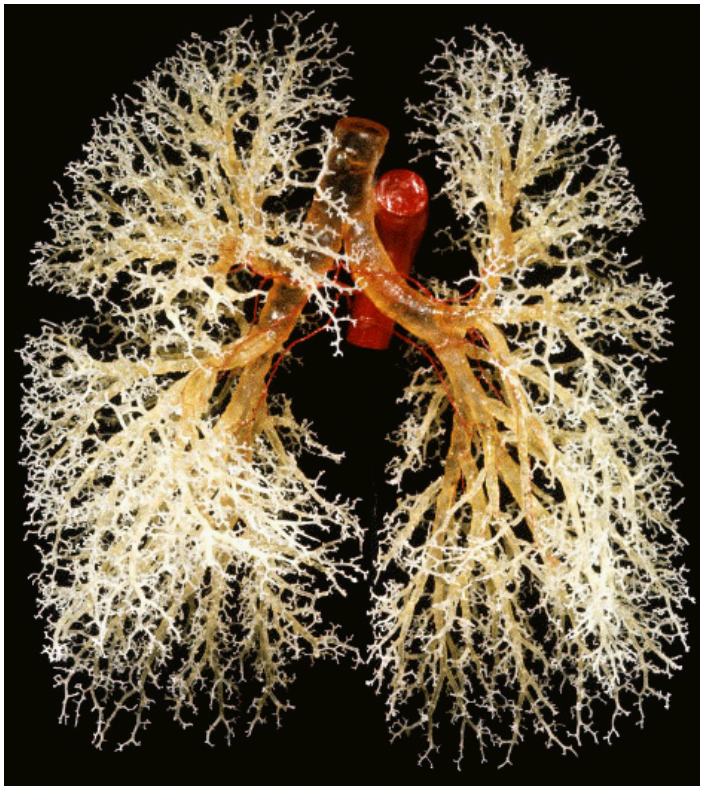

Figure 2 – Resin cast of a human tracheo-bronchial tree.

On the basis of this design features one assigns the airways to different classes of functional zones (Figure 3): bronchi and bronchioles are purely conducting structures whose main function is to distribute the air into peripheral units; respiratory bronchioles and alveolar ducts are transitional elements as they distribute the air into the respiratory zone, the alveoli with which they are intimately associated.

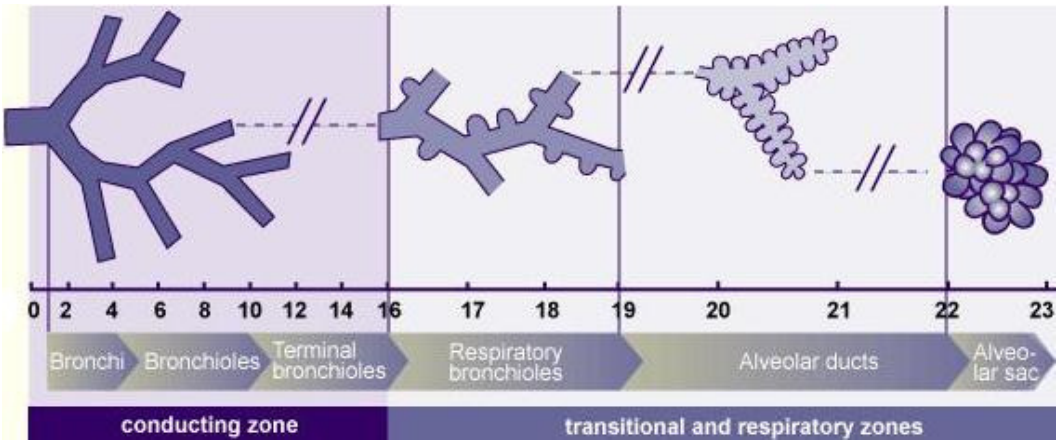

Figure 3 - Organization of the airways tree by functional zones in relation to generation of dichotomous branching.

GEOMETRY OF THE AIRWAYS TREE

If we look at the pattern of airways branching, we observe that each parent branch gives rise to two smaller daughter branches. We observe that the two daughter branches from the same parent branch often differ in diameter and length. This pattern is called *irregular dichotomy*, in contrast to regular dichotomy where all branches in one generation are of the same size (Figure 4). Nonetheless, the morphometric analysis of such trees reveals that the progression of airways dimensions from the trachea to the periphery follows strict laws which are functionally relevant.

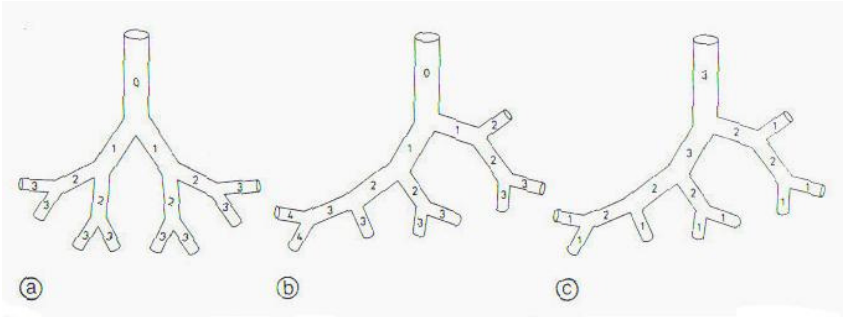

Figure 4 - Patterns of airways branching: (a) regular dichotomy; (b) irregular dichotomy numbered by "generation down"; (c) irregular dichotomy numbered by "orders up" (From Weibel, 1980)

There are two basic ways for classifying branches in a tree.

The first approach is to number the branches progressively by generation as one goes down the (inverted) tree, starting with generation z=0 at the trachea. I would like to call this the morphogenetic approach because it simply follows the pattern of branching as it occurred during lung morphogenesis. Note that the number of branches in any generation z is twice that in the parent generation (z-1):

$$N(z) = 2 \cdot N(z-1) \qquad (1)$$

an obvious consequence of dichotomy. From this we can now immediately derive the total number of branches in generation z to be

$$N(z) = 2^z \qquad (2)$$

a very simple relations that is, in fact, quite useful.

The alternative approach is to start numbering at the end twig which is designated ad "order 1". As we go up the tree the order is increased by 1 when two branches of the same order come together, but it remains unchanged when, for example, an order 2 branch meets an order 3 branch. In this so-called Strahler method on considers the airways as a system of tubes converging from the periphery toward the center, an approach used with success in describing river system. It also makes sense in the lung if we consider, for example, the acini as the fundamental ventilatory units which are connected to the trachea by a system of bronchi of vary pathway length. One of the fundamental descriptors of this model is the branching ratio, that is, the ratio of the total number of branches in order to that in the next higher order. For the human airways tree this branching ratio is found to be about 1.4 on the average, whereas it is, by definition, 2 in the dichotomy model.

By counting the number of alveolar sacs, the terminal airways elements, one can estimate that, in an adult human lung, the airways must branch over approximately 23 dichotomous generations, on the average, before they eventually end in a blind sac. This means that the total number of end branch is about 2^{23} (~ $8 \cdot 10^6$). By similar arguments one finds that terminal bronchioles, the last purely conducting airways, are located in about generation 16. Beyond the 16^{th} generation all airways have alveoli in their wall and can hence participate in gas exchange. Evidently, these are average numbers; we disregard, for the time being, the fact that, in the real lung, terminal alveolar sacs may appear anywhere from about the 18^{th} to the 30^{th} generation of irregular dichotomy.

Let us now consider the reduction of airways diameters with progressive branching. In a first step we again simplify the model by “regularizing” the dichotomy, that is, we consider the mean diameter of all branches in a given generation to be the characteristic diameter d(z) for that generation. On a semi-logarithmic plot, d(z) falls approximately along a straight line following the simple law:

$$d(z) = d_0 \cdot 2^{-\frac{z}{3}} = d_0 \cdot \left[\sqrt[3]{\frac{1}{2}}\right]^z \qquad (3)$$

Where d_0 is the “ideal” diameter of the trachea. This relation shows that with each generation the airways diameter is reduced by the cube root of the branching ratio 2, a law that is well known in hydrodynamics, as it describes an optimal design of a branched system of tubes through which air or fluids can flow with a minimal loss of energy. By the way, performing this analysis on the Strahler model leads to the same result. It therefore appears that, from an engineering point of view, the airways of the lung are well designed to assure optimal conditions of air flow.

The diameters of acinar airways do not follow the law; the diameters of respiratory bronchioles and alveolar ducts change very little with each generation, as can easily verified on real specimens.

The design of the pulmonary airways system appears to be governed by strict engineering rules, striving to optimize the conditions for convective O_2 transport in the purely conducting bronchi and bronchioles, and those for diffusive O_2 transport within the acinus [8][9].

The wall thickness of conducting bronchi and bronchioles is approximately proportional to the diameter. The relationship between bronchial wall thickness and diameter may be expressed by using the T/D ratio, defined as wall thickness (T) divided by the total diameter of the bronchus (D) [10].

BRONCHI NOMENCLATURE

The bronchial nomenclature generally adopted is that described by Jackson and Huber in 1943, (Table 1) [11].

Table 1 - Bronchi Nomenclature proposed by Jackson and Huber

RIGHT LUNG		LEFT LUNG		
LOBES	SEGMENTS	LOBES		SEGMENTS
Upper	1.Apical	Upper	Upper Division	1-2.Apical-posterior
	2.Posterior			3.Anterior
	3.Anterior		Lower (Lingular) Division	4. Superior
Middle	4.Lateral			
	5.Medial			5. Inferior
Lower	6.Superior	Lower		6.Superior
	7.Medial Basal			7-8 Anterior-medial Basal
	8.Anterior Basal			
	9.Lateral Basal			9.Lateral Basal
	10.Posterior Basal			10.Posterior Basal

The total number of the airways branches is over 50,000 in the normal adult human [12], and the bronchial nomenclatures are defined to 74 proximal branches down to sub-segmental bronchi [13], [14], [15]. Currently, the most clinically important nomenclatures include 32 branches down to segmental bronchi. Peripheral bronchi that lie downstream from a segmental bronchus are usually named using the nomenclature of the parent segmental bronchi. The bronchial nomenclature is assigned according to the region of the lung to which a bronchus supplies air. There is a clear definition for the spatial division of the lung (Figure 5). Classes of lobe, segment, and sub-segment construct a hierarchic structure, and a set of all members in the same class is equal to the whole lung without overlapping. There is an exact one-to-one correspondence between a branch and the lung region supplied air by the branch, because there are no loops in the airways tree. Therefore, the bronchial nomenclatures are based upon the regional nomenclatures: lobar bronchus, segmental bronchus, and so on.

The most common way to mathematically describe the airways tree is by a graph representation using a rooted tree. However, for the purpose of bronchial nomenclature, a tree representation can lead to confusion, because the hierarchy of the rooted tree does not correspond to the nomenclature hierarchy. Figure 6 shows a standard branching pattern of the human bronchial tree [13], where thick lines indicate bronchi having anatomical nomenclatures. In this branching pattern, levels of segmental bronchi across from 3rd to 7th. Furthermore, as shown in Figure 7, there are differences in branching patterns even across normal subjects. It is obvious that the same nomenclature does not mean the same level in the tree representations of different branching patterns.

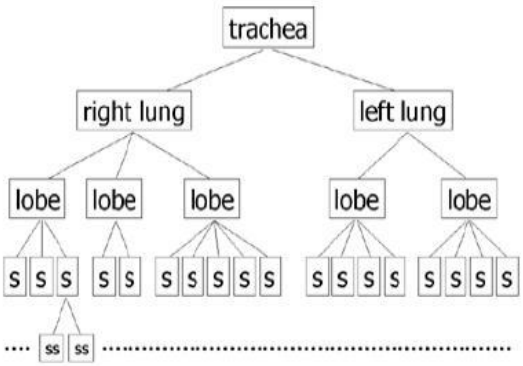

Figure 5 - Hierarchy of space division of the lung. s: lung segment. ss: sub-segment [16].

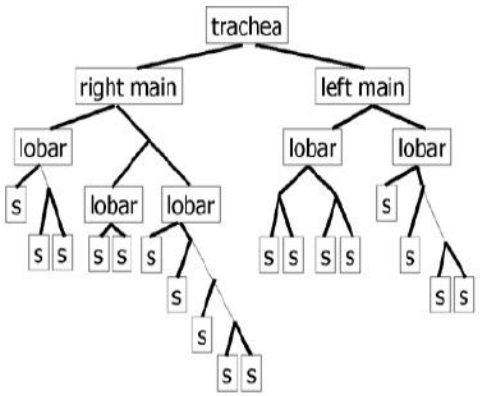

Figure 6 - A typical example of the human bronchial tree. s: segmental bronchus [16].

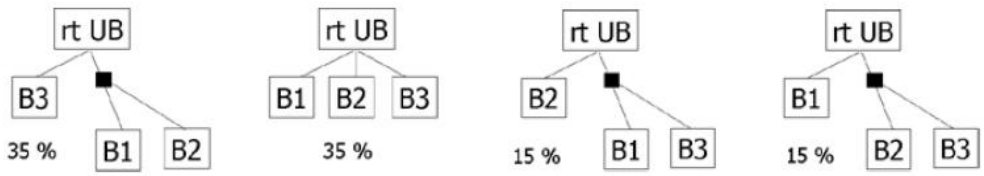

Figure 7 - Branching patterns of segmental bronchi arising from the right upper lobar bronchus (UB). Frequencies for respective branching patterns are according to [13]

Since there are only five lobar bronchi and there is little variation in the branching pattern, nomenclatures for lobar bronchi are not difficult. On the other hand, determining nomenclatures for segmental bronchi are much more difficult because of a large variety of branching patterns.

There are ten lung segments in the right lung and eight segments in the left lung. The names of lung segments describe their locations within the lung. For example, there are apical, lateral, and anterior segments of the right upper lobe. For simplicity, numbers from 1 to 10 are used for distinguishing locations. Both the right and left lower lobes sometimes have accessory segments called sub-superior segments, which are often located below the superior segmental bronchus (B6). They are usually expressed as the symbol of asterisk (*) instead of number [13], [14], [15]. Since branchpoints in the bronchial tree have only one upward branch, it is reasonable to assign bronchial nomenclatures to branchpoints, (Figure 8).

Each segmental bronchus is located neither upstream nor downstream from other segmental bronchi, since their supplying regions are independent of each other. In addition, the segmental bronchi are always located distal to their parent lobar bronchi regardless of the branching order, because each lobe is comprised of its member segments.

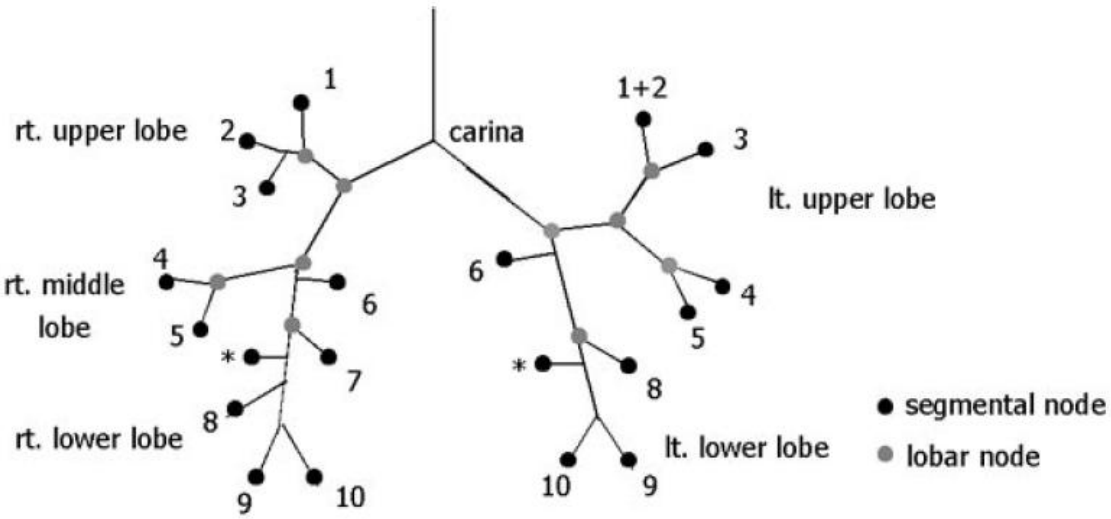

Figure 8 - Scheme of the bronchial nomenclatures. Each segmental node is connected upward to the segmental bronchi [16].

THE PROBLEM OF AUTOMATED AIRWAYS LABELING

Volume data acquisition for medical imaging is now rapidly spreading in clinical use due to the technological progress in multi-detector CT scanners. 3D image processing techniques have enabled precise structural analysis of living organs. Anatomical nomenclature is an important step in sharing a common understanding of organ structure. Inter-individual and intra-individual comparisons are meaningful only when accurate nomenclatures are applied to the structures. Accuracy of nomenclature is also critical for diagnosis and surgical planning. However, anatomical knowledge used for establishing the nomenclature of biological structure is challenging when seeking to construct robust computational algorithms, because of the nature of biologic complexity and diversity.

Discrepancy of anatomical nomenclature even between experts is not uncommon. The human airways tree is a typical example of the difficulty of nomenclature and labeling because of its hierarchical properties and the considerable variations of branching pattern.

By the use of modern multi detector CT scanners, more than a hundred bronchial branches can be extracted. The increase in the number of branches identified increases the complexity of establishing a robust labeling scheme [16].

1.2 - CT FEATURES OF THE NORMAL LUNG

1.2.1 – Lung arteries and bronchi

Within the lung parenchyma, the bronchi and pulmonary artery branches are closely associated and branch in parallel. The large pulmonary arteries normally appear as rounded or elliptic opacities on CT when imaged at an angle to their longitudinal axis and roughly cylindrical when imaged along their axis (Figure 9). These arteries are accompanied by thin-walled bronchi whose shape is also defined by the angle between the scan plane and the axis of the bronchi [10][17].

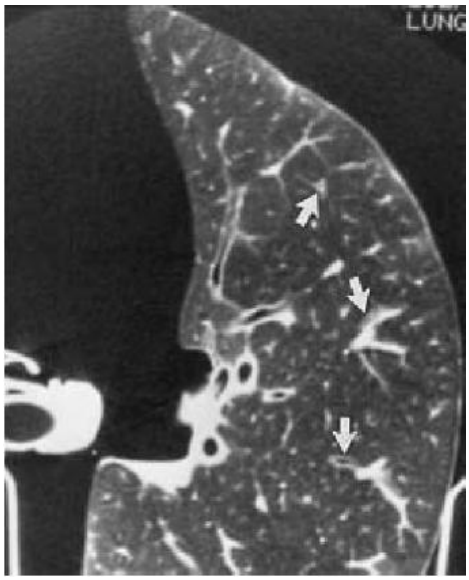

Figure 9 - Normal appearances of large bronchi and arteries. In an isolated inflated lung, the smallest bronchi visible (arrows) measure 2 to 3 mm in diameter. Bronchi and bronchioles are not visible within the peripheral 1 cm of lung in this preparation, although the artery branches in the peripheral lung are sharply seen [12].

In most normal subjects, the bronchi and adjacent pulmonary arteries are similar in diameter [18]. Their diameters may be compared by using the so-called broncho-arterial (B/A) ratio, defined as the internal diameter (i.e. luminal diameter) of the bronchus divided by the diameter of the adjacent pulmonary artery. A B/A ratio >1 is usually believed to indicate bronchiectsis, although this may be seen in some normal subjects (Figure 10).

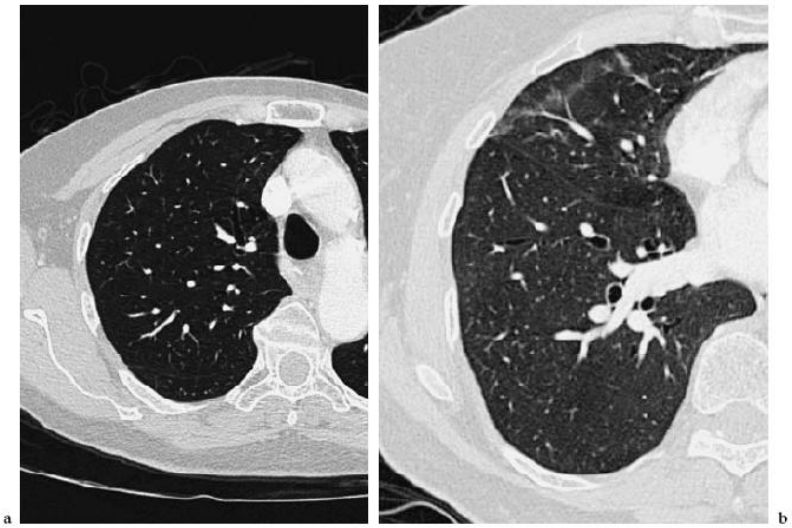

Figure 10 - HRCT of the normal lung at suspended deep inspiration. In a note that the vessels are slightly larger in the dependent areas than in the non-dependent areas, while in b some bronchi appear larger than their adjacent arteries because the scan traverses the bronchus just before it branches. So to compare their diameters the broncho-arterial (B/A) ratio is used [10].

Whether a normal airways is visible or not on a CT scan depends on its size and on the CT technique that is used. About the size, as a general rule, airways less than 2 mm in diameter or closer than 1–2 cm to the pleural surface are below the resolution of even HRCT images [19][20].

1.2.2 - Secondary pulmonary lobule

Secondary lobules (Figure 11) are separated by interlobular septa, that are not normally visible on HRCT, except as an occasional very thin line at the extreme periphery of the lung, usually at the lung apices or bases, often in gravity-dependent areas. This is due to the thicker and better defined septa of the peripherical lobules, that tend to be relatively uniform in appearance with a cuboidal or pyramidal shape [21]. Within the centre of the lobule, the centrilobular arteriole presents as a dot-like, linear or branching opacity. Between the septa and the centrilobular arteriole may be visible, as small dots or branching lines, some smaller intralobular vascular branches [10].

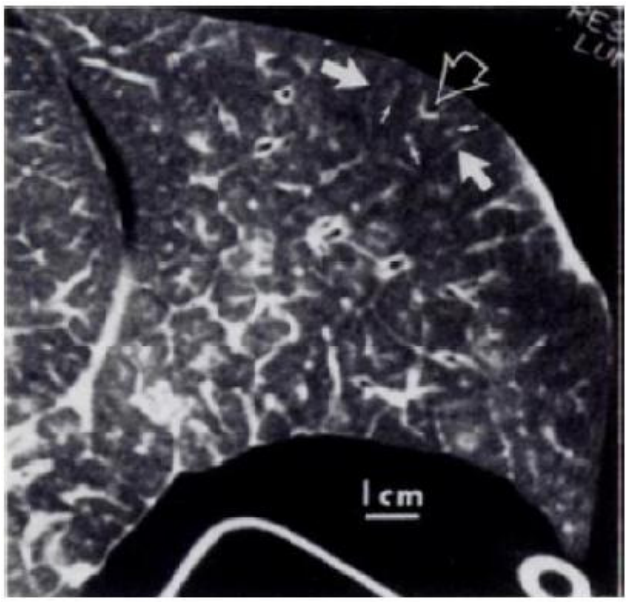

Figure 11 - The septa (large arrows) bordering a well defined lobule are partially visible. A Y-shaped branching artery (open arrow) in the lobular core, and several other lobular vessels (small arrows) are also seen. Lobular bronchioles are not visible.[12]

The substance of the secondary lobule, which surrounds the centrilobular region and is contained within the interlobular septa, consists of functioning lung parenchyma [17]. On thin-section CT scans, small intralobular vascular branches are often visible within secondary lobules, but little else is visible in healthy subjects [10]. Lung acini are not normally visible on thin-section CT scans [22].

1.2.3 - Lung parenchyma

The density of the lung parenchyma is determined by three components: lung tissue, blood in small vessels beyond the resolution of CT and air. [17]

These components are not homogeneously distributed over the lung and the relative proportion is continuously changing in function of normal physiological events [17].
Lung density decreases when lung volume is increased. However, this decrease, due to gravitational effects, is not uniform (Figure 12): lung density is higher in the gravity-dependent areas. This difference decreases as lung volume increases, and the density difference between gravity-dependent and non dependent regions becomes very small near total lung capacity [17].

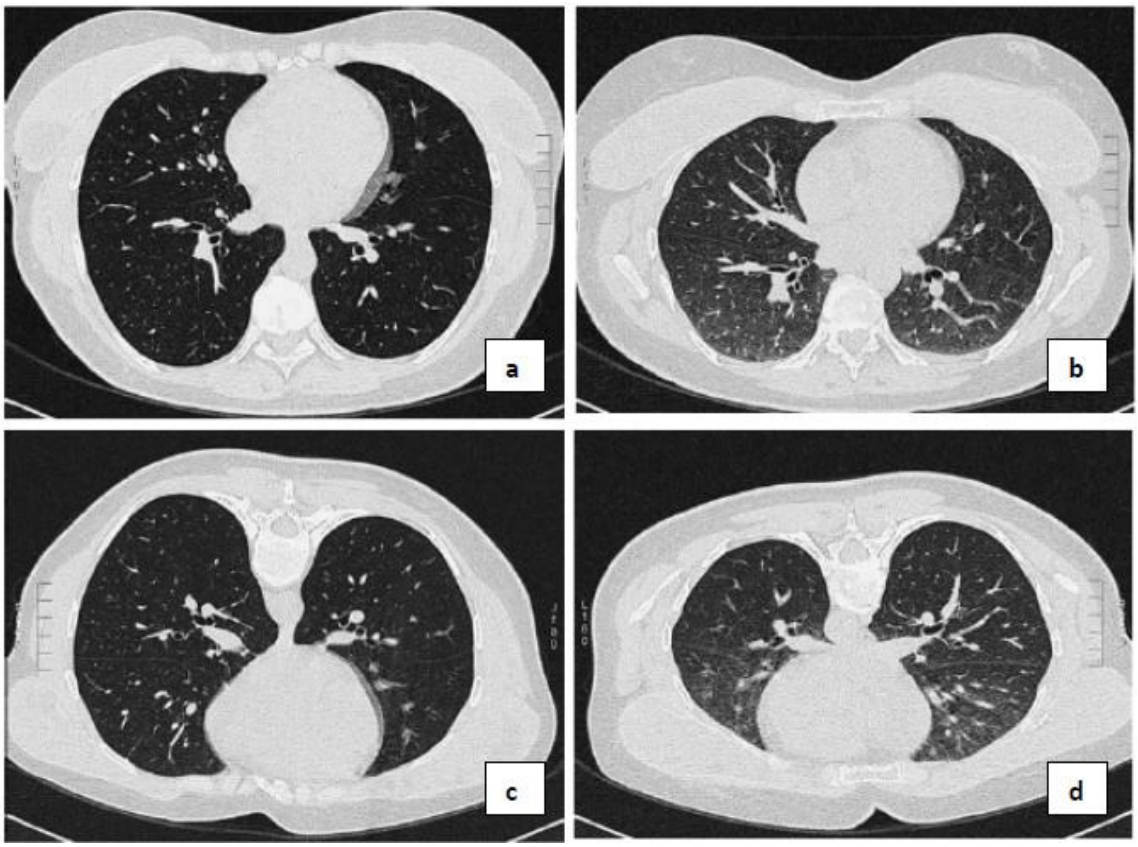

Figure 12 - HRCT of normal lung in supine (a, b) and in prone body position (c, d). a, c in suspended deep inspiration; b, d at the same level, in suspended deep expiration. Note the density gradient between the gravity-dependent and the gravity-nondependent lung which is larger on expiratory scans than on inspiratory scans [17].

1.2.4. – The airways tree extraction from CT images

Segmentation of large airways on CT images is easy because their lumen, which is filled with air, appears as a very dark area, surrounded by brighter structures, which are bronchial walls and pulmonary arteries. Intensity in a CT image is determined by the absorption of X-rays by the tissue

(that is, by tissue density). It is expressed in terms of Hounsfield units, which constitute a measure of tissue density: air corresponds to -1000 HU, water to 0 HU, blood to 45 HU, dense bone to 1000 HU. Typically, soft tissue, such as those situated in the mediastinum, are situated in the range of -100 to 200 HU, airways lumen is below -950 HU, airways walls are above -775 HU [23].

If mixtures of different tissue types comprise a voxel, intermediate gray-level values are the result (partial volume effect).

Partial volume effects cause smaller airways to have a weaker contrast respect to other structures, thus their identification is more difficult. The appearance of an airways depends not only on its diameter, but also on its orientation respect to the plane of the slice. In fact, if the airways runs parallel to the image plane, it will not no more appear dark, because of partial volume averaging of air and airways wall. The ability to perform airways segmentation depends also on the image quality inherent to CT image acquisition, which is improved utilizing thin slices and high

spatial reconstruction algorithm. The presence of thin or stenosed airways may result in discontinuities, because of the size of the voxel, as well as respiratory secretions inside the airways lumen may stop the reconstruction process.

Moreover, the image can present CT artefacts like beam hardening and X-ray scattering, noise due to low radiation doses and high body mass indexes, motion artefacts (due to hearth beating and breathing during the CT scan), which can complicate the image processing operations [24].

The reconstruction of the airways tree can be performed manually by an image analyst, but this operation is tedious and time-consuming. More over, if CT slice thickness is low, the CT dataset consists of hundreds of slices, therefore a manual analysis becomes simply impracticable.

1.3 – VIRTUAL BRONCHOSCOPY

The application field of automated airways labeling is wide and goes from clinical to fundamental imaging investigation. One of the last clinical application field is the virtual bronchoscopy.. Several research groups have been working on the development of bronchoscopic navigation systems that utilize pre-operative labeled CT images as maps.

Virtual bronchoscopy is the descriptive term given to representations of the bronchial tree and surrounding structures created from spatial information derived from imaging sources other than the bronchoscope itself. Initially applied to the two-dimensional and later three-dimensional representations of the bronchial tree obtained from X-ray computed tomography (CT) [25], the term equally applies to similar images derived from magnetic resonance imaging (MRI), from ultrasound imaging, and from image-processing techniques applied to the standard two-dimensional modern bronchoscope image [26]. X-ray CT of the lung produces two-dimensional images (a cross-section of the thorax at the slice point) with the minimal x,y resolution in this image referred to as a “pixel” and the depth of the slice adding a z direction to that pixel; this volumetric minimal resolution image is referred to as a “voxel.” Over the last 10 to 15 yr, the x,y and z resolutions of the CT scans have dramatically improved along with improved scan acquisition times. Current CT scanners (64 multi-row detector CT devices [MDCT]) now produce x,y and z resolutions of the order of 0.6 mm. If these two-dimensional x,y slices are stacked one on top of the other, maintaining their alignment, then it becomes very clear that a high-resolution three-dimensional image of the thorax can be obtained. This three-dimensional image contains all of the structures within the thorax, including the airways (where there is natural contrast between tissue and air), the mediastinal blood vessels (where, with contrast injection, there is discrimination between blood vessels and other soft tissue structures), and the mediastinal lymph nodes (where there is often significant contrast differences between the lymph node and surrounding mediastinal fat).

The three-dimensional image of the thorax obtained through MDCT is a digital image, with each voxel having a defined spatial dimension and gray-scale characteristics. As with any digital dataset, the three-dimensional image of the thorax can be analyzed, digitally stored and retrieved, and displayed as an image-based informational structure.

Similar structures within the three-dimensional image dataset can be digitally removed from the remainder of the image for later visualization and analysis. Using these principles of digital technology it is reasonable to expect that the bronchial tree (and the surrounding structures if needed) can be identified, then removed from the larger image structure and evaluated in three-dimensional digital space. This is the basis of CT-based virtual bronchoscopy and similar to the virtual bronchoscopy views derived from other digital image sources.

Most of the major CT manufacturers now offer virtual bronchoscopy software with their machines, and there are several smaller companies offering virtual bronchoscopy software.

The accuracy of virtual bronchoscopy techniques with real bronchoscopy findings is high [27][28], and this will improve further as CT scanning protocols improve. This is particularly useful for those conditions where there may be multiple stenoses (see the Figure 13), such as Wegener's granulomatosis [29], or secondary cancers where the traditional bronchoscope cannot visualize past the first obstructing segment.

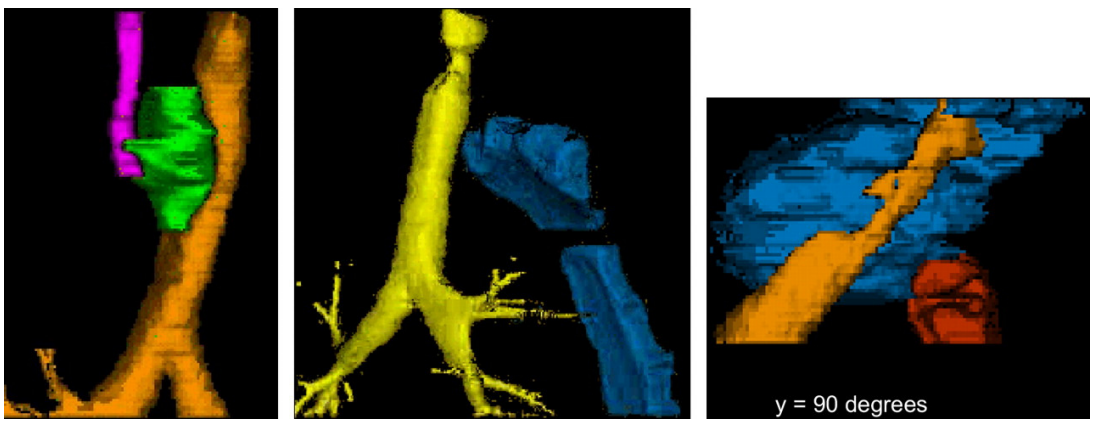

Figure 13 - *Left panel*: the relationships between the trachea, a paratracheal abscess, and the carotid artery. *Center panel*: a patient with severe subglottic stenosis from Wegener's granulomatosis, with the manubrium sterni in correct position, showing there is room for a tracheostomy. *Right panel*: lateral view of a large thyroid goiter, displacing and compressing the trachea, with no room for a tracheostomy above the manubrium sterni [30].

1.3.1 – The virtual bronchoscopy applications

The first application virtual bronchoscopy procedures examined here uses the data contained within the complex three dimensional image for procedure guidance within the mediastinum and hilar structures [31][32]. A simple example is under standing where a mediastinal lymph node is in relationship to the bronchial tree. In traditional bronchoscopy, only the air way lumen is visualized, although the bronchoscopist knows that somewhere on the other side of that non-transparent bronchial epithelium is the lymph node that is the target for a transbronchial needle aspiration or core biopsy. Using the virtual bronchoscopy information obtained from the three-dimensional MDCT dataset, a virtual bronchoscope (placing a visualization tool where the real bronchoscope might be within the lumen) can show precisely the same image as the real bronchoscope does, with gray-scale rendering rather than the colour rendering from the real bronchoscope image. With these two images side by side (the virtual bronchoscopic visualization and the real bronchoscope visualization of the same region), the next step is to make the virtual bronchoscope bronchial wall transparent.

In this manner, as with manipulation of many digital images in this current era, the structures through the bronchial wall can now be visualized. Using the extraordinary power of the human brain for image processing, or an associated computer script, the lymph node in question, now visible on the virtual bronchoscope images, can be transferred to overlay the real bronchoscopic images. The bronchoscopy operator can, with a great degree of confidence, know where the target lymph node is (see the Figure 14). This process can be simplified before the real bronchoscopic procedure in a preplanning step where the target region, be it lymph node or some other structure, can be rendered as a region of interest and displayed as a colour object in both the virtual bronchoscopic and later the real bronchoscopic images. There are several computer programs that have been developed for this application, with early results suggesting satisfactory ease of use and improvement in the biopsy return.

Early results suggest a greater than 90% success rate for mediastinal and hilar lymph node biopsies. Clearly, these early successes open the possibility of sampling mediastinal structures precisely and reliably. This also opens up the possibility of localized application of nonspecific or specific therapies.

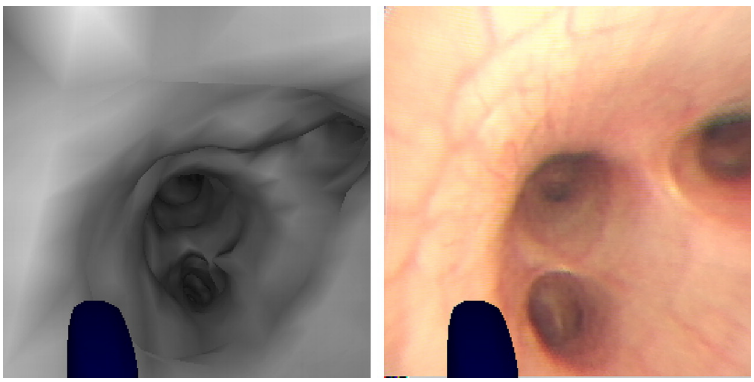

Figure 14 - Example of transbronchial lymph node biopsy using multidetector computed tomographic (CT) information. On the *left panel* is the computer-rendered virtual bronchoscopy view, with the lymph node region of interest shown through the wall as a dark blue-black. On the *right panel*, the lymph node region of interest is transposed to the real bronchoscopic view. The point to place the transbronchial needle is now easily identified [30].

A second advanced virtual bronchoscopic application is that of path-finding to a peripheral region of interest within the lung [33]. Given the respiratory motion that occurs during breathing, transcutaneous approaches to the moving lung may not be satisfactory. By approaching the peripheral lung through the bronchial tree, movement is not an issue because the parenchymal lung lesions move synchronously with the airways and with any device that is within the airways. With the significant improvement in MDCT scanners, seven or eight generations of airways can now be automatically extracted and evaluated. The simple application here is that if the trachea is the beginning point and if a pulmonary parenchymal abnormality (pulmonary nodule or region of pulmonary emphysema) is the targeted end point, then appropriate software can interrogate the three-dimensional image dataset and provide a pathway through the airways to the lesion. This pathway can then be followed by the bronchoscopist during a real bronchoscopy procedure and the correct airways pathway to the lesion quickly cannulated using a Teflon-coated tube that is very similar to the internal coating of the standard bronchoscopic instrument channel.

Once the Teflon access tube is in place, then multiple probes can be placed either to brush or biopsy or optically or by ultrasound sample the lesion of interest. Ultrathin bronchoscopes can be used in a similar manner [34]. Using these sorts of approaches in early studies, 80% of peripheral lung lesions can be easily and satisfactorily sampled. These pulmonary path-finding applications are in clinical studies and are being developed by a number of companies for medical application. They may have a synergistic role also when coupled with magnetic tracking devices.

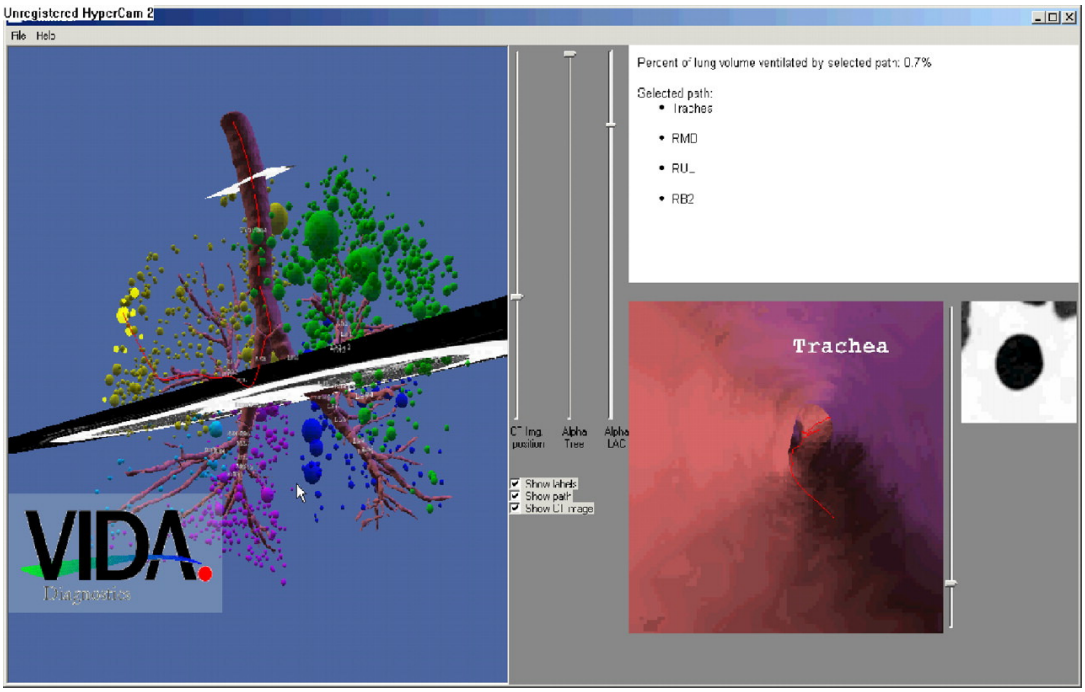

Figure 15 - Screen shot of a pulmonary path-finding program using virtual bronchoscopy advanced applications. On the *left panel* is shown the extracted bronchial tree, with the balloon shapes quantitatively showing pulmonary emphysema. There is a path-finding tool, which connects the emphysema regions through their subtending airwayss to the trachea, to allow for both sampling to be performed bronchoscopically and planning for bronchoscopic lung volume–reduction surgery. The *right panel* is the virtual bronchoscopy fly-through at the level of the *small white square* shown through the trachea at this time [30].

The third advanced virtual bronchoscopy application involves the targeting of the peripheral lung for endo-bronchial valve-type procedures in the management of pulmonary emphysema, so-called endo-bronchial lung volume reduction surgery [35]. Here, the information that is required is the state of the lung parenchyma and the extent of emphysema in each segmental region together with the anatomic configuration and size of the subtending airways segments. There are several companies now with hardware solutions for the endo-bronchial management of emphysema and most of them are in human clinical studies. To shorten procedure times, to improve accuracy of device placement, to reduce medical error, and to educate the patient and families, application of advanced virtual bronchoscopy techniques is an obvious solution. For instance, if the right upper lobe is being targeted (in some studies, this is through human read of the CT scan; in others, it is by computer read) it is unclear to the operating interventional pulmonologist how many segments might require a device to be placed and whether the segment lengths are adequate for the valve placement. Such planning including valve sizing should be performed where possible before the procedure by the management team. In the immediate future, rather than targeting lobar airways with therapeutic devices, it is likely that segmental airways devices will be placed in those airways that subtend areas of severe emphysema. In the lobar-only approach, regions of the lobe that may not have much emphysema are treated unnecessarily. Segmental airways targeting will certainly require computer assistance and procedure planning to improve accuracy of device placement (see the Figure 15).

CHAPTER 2

Materials and Methods

2.1 – STATE OF ART

Automatic and semi-automatic methods for anatomical labeling of bronchial branches published up to now rely on two relevant strategy: *association graph* and *machine learning and combination optimization*. Both methods start from a skeletonization of the segmented airways tree.

2.1.1 – Association graph

The technique proposed by Kitaoka [16] and Tschirren [36] uses a method based on an association graph.

They start from a skeletonization method proposed by Palagyi [37]. The skeletonization is performed by a sequential three-dimensional thinning algorithm. Thinning is an iterative object reduction technique for producing a reasonable approximation to the skeleton in a topology preserving way. This type of skeletonization can easily generate circuits and false branches that must manually be corrected.

The labeling algorithm is a weighted maximum clique search of an association graph between a reference tree and an object tree. The adjacency between nodes in the association graph is defined so as to reflect the consistency between the bronchial name in the reference tree and the node connectivity in the object tree. Nodes in the association graph are weighted according to the similarity between two tree nodes in the respective trees.

Automated bronchial nomenclature and labeling can be viewed as a tree matching problem between an object tree and a standard airways tree. The nomenclature labeling is then applied to give the same name to a node in the object tree as that of its corresponding node in the reference tree. The algorithm is based on a weighted tree matching method proposed by Pelillo et al. [38].

Their method seeks the maximum weight clique in a tree association graph (TAG), equivalent to the maximum similarity sub-tree isomorphism between two trees. We modify the definition of adjacency of TAG nodes and construct a similarity measure between a reference tree and an object tree according to the property of the bronchial nomenclature.

To perform this method is required a pruning of spurious branches introduced by segmentation and subsequently by the skeletonization.

2.1.2 - Machine learning and combination optimization

The method proposed by Mori [39] and Ota [40] is based on machine learning and combination optimization.

They start from a skeletonization method proposed by Kitasaka [41]. The skeletonization is performed during the segmentation. The centres of gravity are extracted from the bounding boxes that contain the branches just emerged through the segmentation. In a second step these centres are linked.

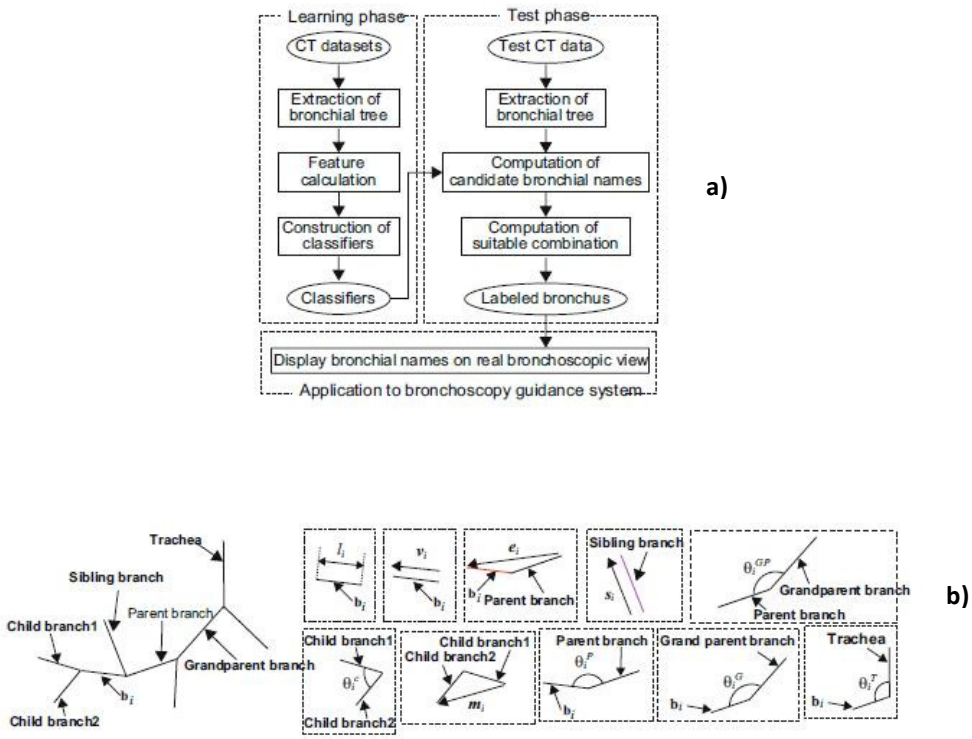

Figure 16 – Flowchart a) and ten feature extracted b) in method proposed by Mori [39]

The labeling method is based on classifiers that output bronchial branch name candidates with likelihoods using learning datasets. A machine learning approach is utilized here. In the anatomical labeling process, is compute the feature values of bronchial branches extracted from CT images. Then is compute the bronchial branch name candidates with the likelihoods for each bronchial branch using the classifiers. Finally, the anatomical names for each branch by a combination optimization technique is determined.

LEARNING PHASE

Learning datasets is prepared by computing 10 (5 in the Ota method) feature values (visible in Figure 16-b) of the bronchial branches extracted from the CT images. It is also manually assign anatomical names to each bronchial branch.

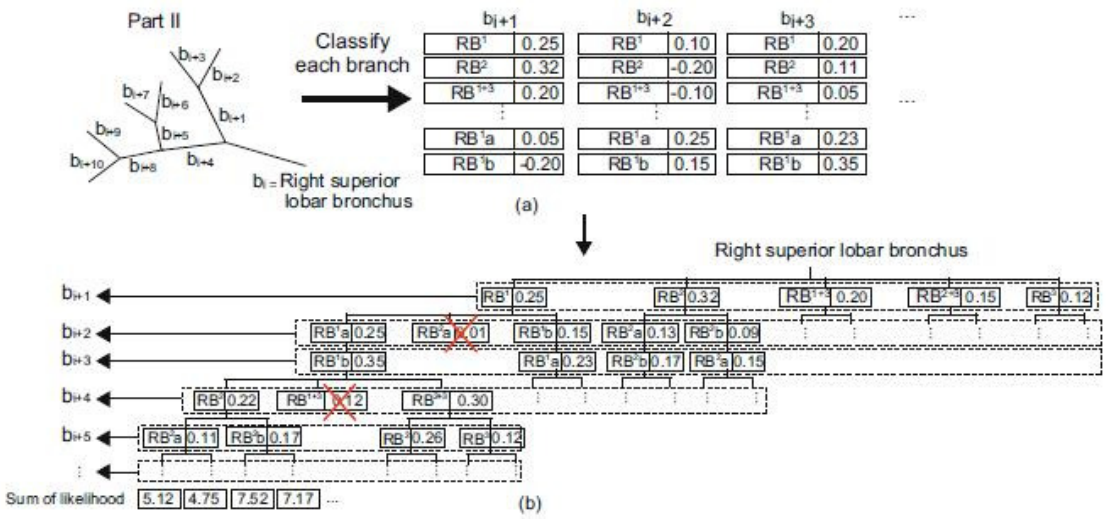

Figure 17 - Illustration of procedures for anatomical labeling of bronchial branches using a combinatorial optimization approach: (a) Example for classifying branches; (b) Example for constructing a combination tree [39].

Classifiers that output bronchial branch name candidates with likelihoods is construct (Figure 17-a). These classifiers are constructed using a multi-class AdaBoost technique [42].

TEST PHASE

From an unknown airways tree is generated, by the classifiers, a list of bronchial branch name candidates with the respective likelihoods. Subsequently a combination tree T is generated that enumerates the multiple pairs of a bronchial branch name candidate and its likelihood as nodes (Figure 17-b).

Anatomical labeling is finally performed by finding path L showing the maximum of the sum of the likelihoods along with it in T.

The next table (Table 2) shows advantages and disadvantages of the two methods just discussed: association graph and machine learning and combination optimization method.

Table 2 – Advantages and disadvantages of the association graph and machine learning and combination optimization methods.

PRINCIPLE	ADVANTAGES	DISADVANTAGES
Association graph	Use a robust three-dimensional mathematical model. It is not necessary an ample thoracic CT data-set.	Skeletonization is required (can introduce artefacts). Manual pruning is required. Labeling is based only on the tree nodes position.
Machine learning and combination optimization	More relative and absolute branch features are exploited. Pruning it is not required.	Skeletonization is required (can introduce artefacts). Human intervention is required in learning phase to label test trees branches. An ample thoracic CT data-set is required.

2.2 – METHODS

2.2.1 – Main steps

The method developed in this work to obtain an automated labeling of the tracheo-bronchial tree, is schematically described in the following block diagram (Figure 18) which shows the main steps of the complete algorithm.

2.2.2 – Airways segmentation form thoracic CT

THORACIC CT

Thoracic CT data used for the present work belong to a database of 10 healthy volunteers (3 males/7 females, age 44 ±6 years, weight 67±5 Kg, height 178±32 cm) with no history of smoking or lung disease and normal spirometric values were used for the analysis.

The Institutional Review Board of Washington University of St. Louis approved the protocol for healthy humans and informed written consent was obtained from each healthy subject.

CT scans were performed using the same scanner model (Somatom Definition Dual Source CT, DSCT; Siemens, Forchheim, Germany). CT images were reconstructed using 1 mm slice thickness and scanner settings were: tube voltage, 120 kV; tube current, 110 mA; matrix 512x512.

Subjects were scanned during suspended end-inspiration at total lung capacity (TLC) and during suspended end-expiration or near residual volume (RV).

AIRWAYS SEGMENTATION

Input data of the algorithm were the segmented airways of each subject at two different lung volume as obtained from the thoracic CT images by three-dimensional region-growing technique developed in a previous thesis work [43].

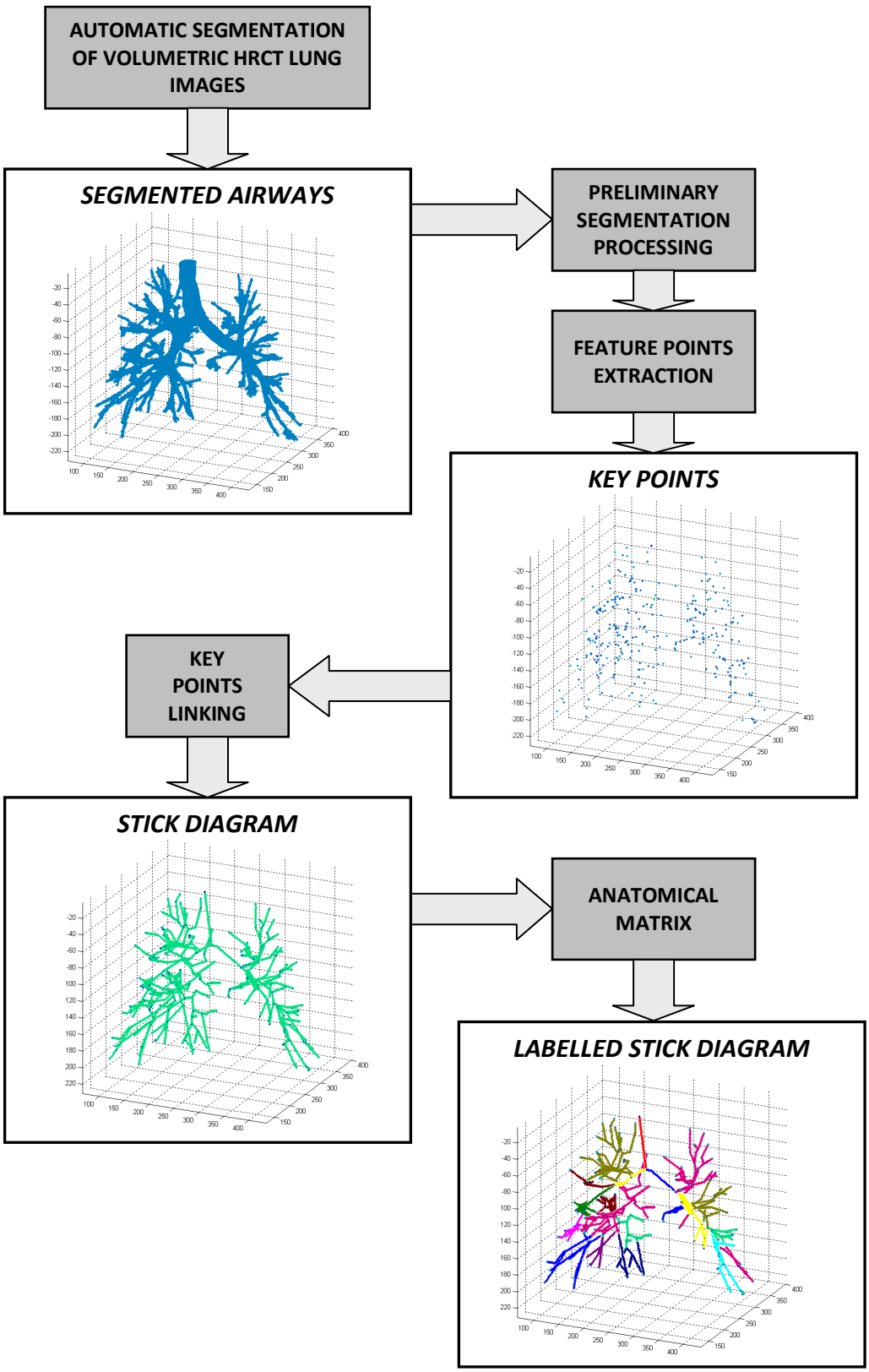

Figure 18 – Automated labeling of the tracheo-bronchial tree block diagram.

2.2.3 – Preliminary segmentation processing

A pre-processing of the segmented images of the airways tree is required before to perform the extraction of the feature points. Two main operations are necessary: *closing* and a *carina de-masking*.

CLOSING OPERATION

Closing morphology operator is applied on two-dimensional slices representing the section of the airways branches to connect all the pixels belonging to the same anatomical region. An example is showed in Figure 19.

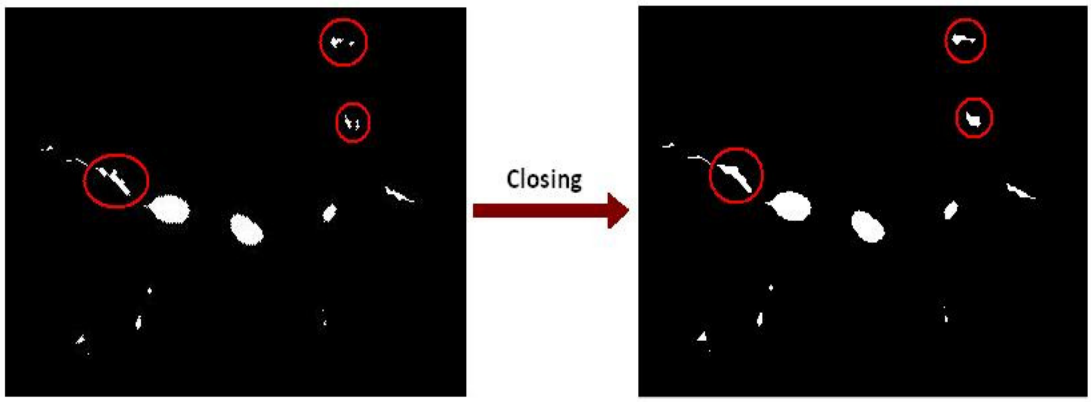

Figure 19 – Example of closing operation on a segmentation slice. Red circles shows zones where the changes introduced by the closing are most visible.

The morphological close operation is a dilation followed by an erosion, using the same structuring element for both operations. Dilation adds pixels to the boundaries of objects in an image, while erosion removes pixels on object boundaries. The number of pixels added or removed from the objects in an image depends on the size and shape of the structuring element used to process the image. In the morphological dilation and erosion operations, the state of any given pixel in the output image is determined by applying a rule to the corresponding pixel and its neighbours in the input image.

CARINA DEMASKING

The closing operation can produce misleading bifurcation in the airways tree. This can be a problem for the identification of the carina, the main bifurcation of the trachea in the two main bronchi, right and left.

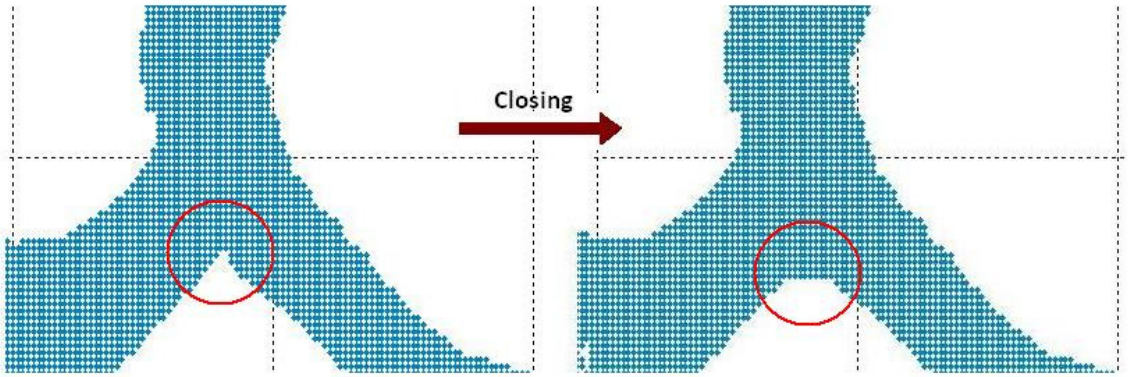

Figure 20 – Example of carina de-masking. Red circle shows voxels deleted to restore the original carina position.

Through an area analysis of the regions that constitute the trachea (see Carina Move flow-chart in Appendix 2) it is possible to identify, with good approximation, the original main bronchi division, the carina, removing all the voxels added by closing operation. In Figure 20 an example is reported.

2.2.4 – Key points extraction

First step of the proposed method is to extract a system of feature points, called "*key points"*, from the segmented tracheo-bronchial tree. Connecting all these points is possible to obtain a schematic representation of the airways tree. This is not a result of a classic skeletonization because lines that link two points not represent the medial axis of the airways. This schematic representation is called *"stick diagram of the tracheo-bronchial tree"*.

Each segment of the stick diagram is labelled coherently to the airways branch which follow. The idea is to get a guide to overlap to the original segmentation in order to help the labelling of the principal branches.

In the next paragraphs is described how it is possible extrapolate key points from the airways segmentation and what are the feature points needed for the construction of the stick diagram.

SLICE ANALYSIS

Key points extraction starts from a bi-dimensional analysis of airways segmentation slices. The segmented images of the airways tree (Figure 21) are binary images in which all the pixels of the airways are equal to 1. Thus, segmented tracheo-bronchial tree is constituted from the contour in each slice of the segmented airways at each Z level in cranio-caudal direction.

It is possible to construct a 3D matrix with the three coordinates X, Y, Z of each point. The reference system is oriented in this way:

- ***Axis X***, in ventral-dorsal direction;
- ***Axis Y***, from right to left bronchus;
- ***Axis Z***, in cranio-caudal direction.

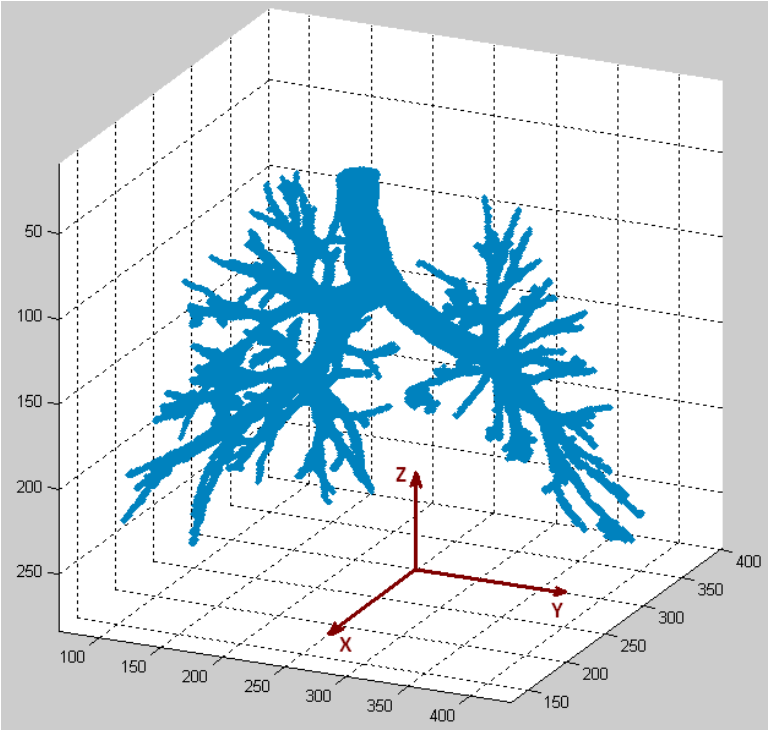

Figure 21 – Example of tracheo-bronchial tree segmentation. Image shows segmentation matrix with orientation axises X-Y-Z.

Considering the matrix at fixed Z it is possible analyse a single slice of the segmented tracheo-bronchial tree.

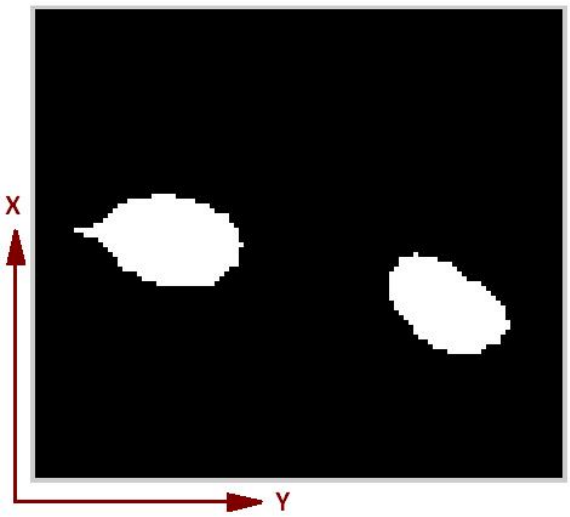

Figure 22 – Single slice at fixed Z extracted from an airways segmentation. In this particular slice are visible the sections of main bronchus.

On a single slice pixel regions with value “1” which represent a section of the airways tree at a fixed Z are visible (Figure 22).

Looking at a particular slice, the region which represents the section of the airway followed is called “*target region*”. Its projection on the above and on the below slice is considered. The projection or shadow cone can intersect one or more different region on the other slices. An example, of intersection between target region and regions of the upstairs slice, is showed in Figure 23.

If a single intersection is found, it means that the branch followed continues without ramifications, instead if a multiple intersection is found, it means a bifurcation of the tree. If no intersection is found, it means that the end of a branch has been reached.

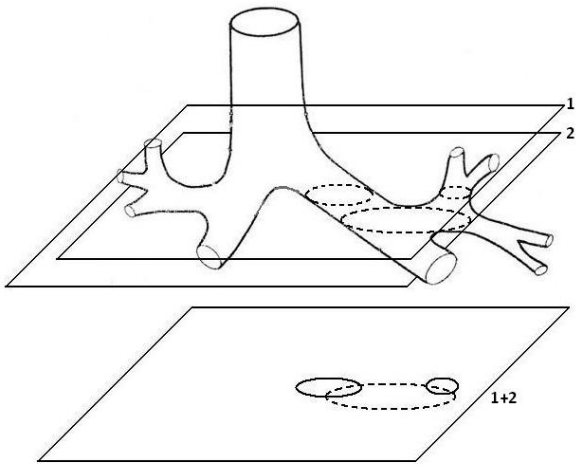

Figure 23 – Two consecutive slices of an airways tree segmentation. On slice number 2 there is target region that intersects two regions on the upstairs slice number 1.

Starting from Z=1, the first section of the trachea is individuated as the biggest region on the first slice: this is the first target region. On the central slice of three consecutive slices group, a single target region is identified. Then the intersection between the projection of the target region and the contiguous slices is considered. If a single intersection is found, the single region intersected is the new target region. If more intersections are found, one of this is selected and it will be the new target region, the other regions will be stored and recovered when the end of a branch has been reached. The mechanism is schematically showed in Figure 24.

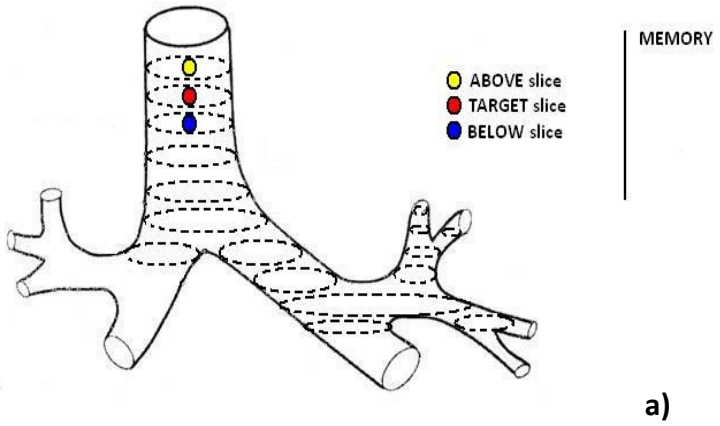
ABOVE slice
TARGET slice
BELOW slice
MEMORY

a)

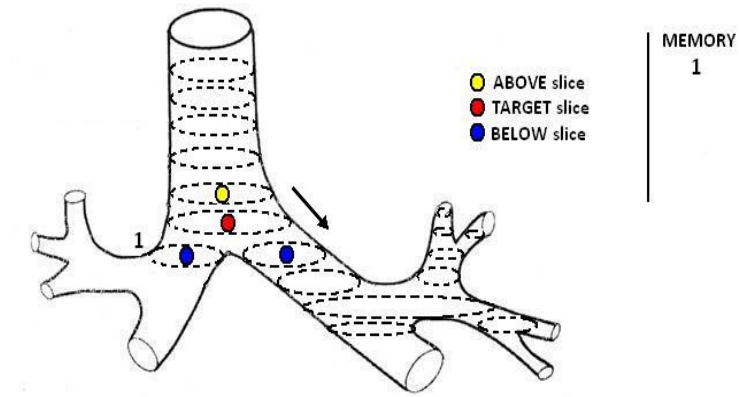
ABOVE slice
TARGET slice
BELOW slice
MEMORY
1
1

b)

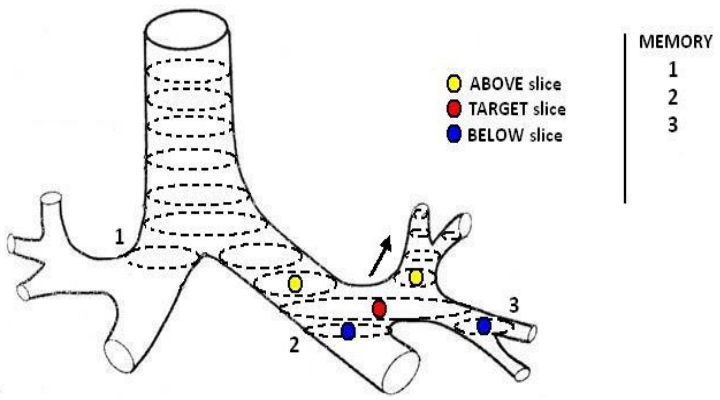
ABOVE slice
TARGET slice
BELOW slice
MEMORY
1
2
3
1
2
3

c)

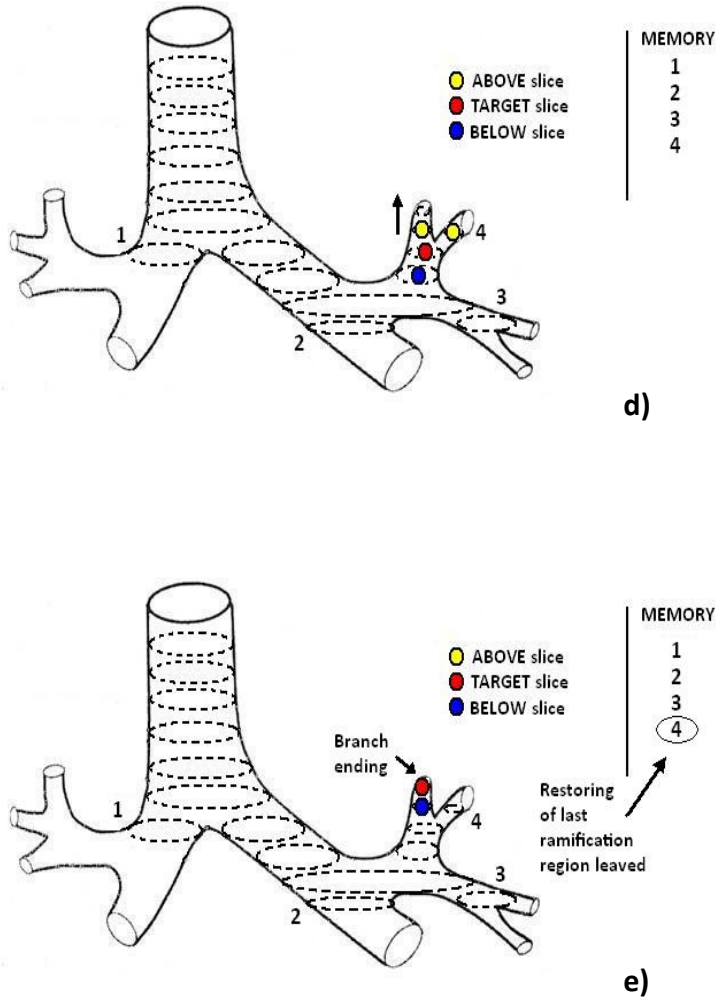

Figure 24 – Five significant steps of branch recognition mechanism. In every step the region intersected in ramification points are numerated. The branch followed is indicated by a row and the first region of the other branches is stored in the memory showed on the right top of the Figure.

In this way the algorithm is able to:

- Identify uniquely the regions.
- Identify the branches of the airways tree which have already followed.
- Store and recover the bifurcation point of the airways tree.

CENTROIDS MATRIX

The centroids of the pixel regions are used to identify uniquely the sections of the airways visible on the slices. The coordinates of centroid of a finite sets of point are computed as (1):

$$C_X = \frac{x_1 + x_2 + ... + x_n}{n} \qquad C_Y = \frac{y_1 + y_2 + ... + y_n}{n} \qquad (1)$$

C_X and C_Y are respectively the coordinates x and y of the centroid of a n points set in two-dimensional space. In a matrix the coordinates of the points are discrete and the coordinates of the centroids are approximated to the most near integer number. An example is showed in Figure 25.

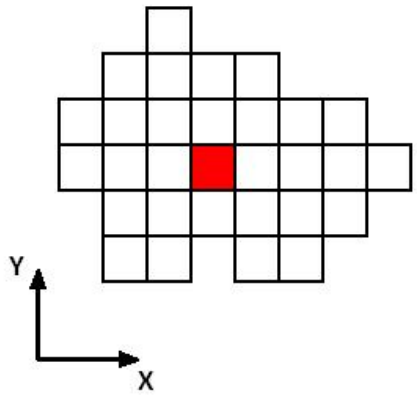

Figure 25 – Example of centroids (pixel in red) of a group of connected pixels.

The computation of the centroid is useful for two principal reasons:

- Every region is identified by a unique couple of coordinates.
- The position of the centroid is approximately in the center of the region which is crossed by the central axis of the airway.

These centroids will be the key points of the stick diagram. Thanks to the central position of the centroids, the line of the diagram represents approximately the branches axis.
This can happen with good precision for the ascending and descending branches, instead, for the branches with the axis perpendicular to the axis Z of the three-dimensional matrix, is different (see Figure 26). This is one of the reasons for which the stick diagram will not represent the anatomical morphology of the tracheo-bronchial tree.

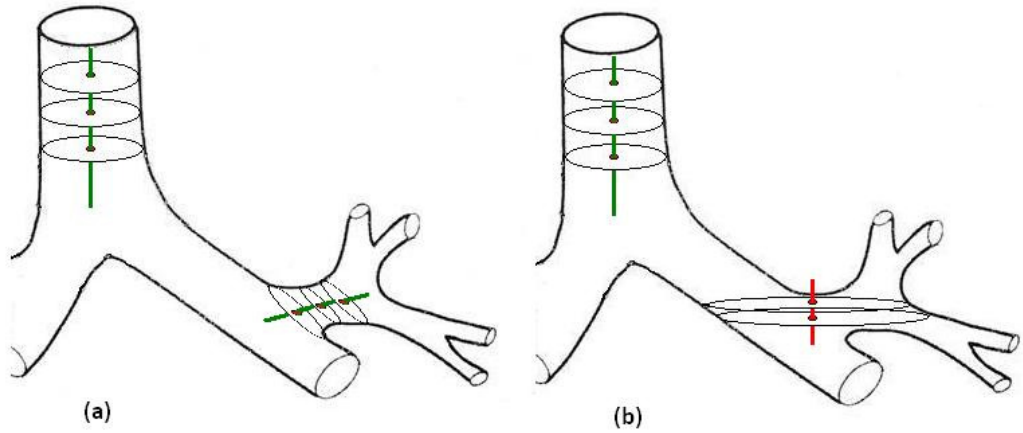

Figure 26 – The figure shows how the regions centroids linking track the real central axis for branches like trachea. In branches like left upper lobe bronchus central axis follows a different line showed in green in figure 26-a. The centroids linking is showed in red in figure 26-b.

The objective of the diagram it is not to faithfully represent the anatomy of the airways like a classical skeletonization. The idea is to get a guide to overlap to the original segmentation to help the labeling of the principal branches.

Sometimes can happen that the computed centroid falls out of the region. This is acceptable from a purely geometric point of view, but in order to assimilate it to a point of the central axis of the airways, it is necessary to correct its position. Thus, the position of the centroid is moved to the nearest pixel belong to the region (see Figure 27).

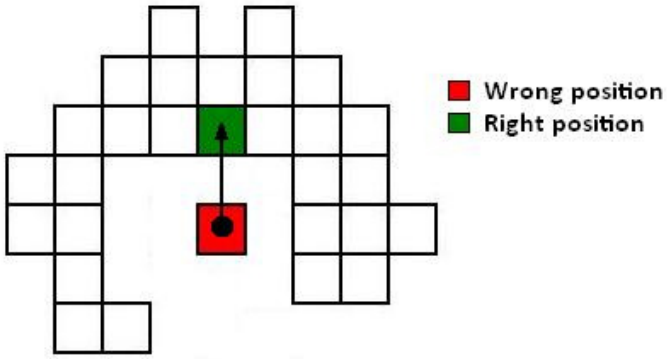

Figure 27 – Example of centroid moving. Computed centroid in red does not correspond to any region pixels. Its position is corrected on green pixel.

The first step of the algorithm is to create a matrix called "*centroids matrix*" in which all the regions of the segmented airways tree are classified. Centroids matrix columns are showed in Table 3.

Table 3 – Columns composition of centroids matrix.

X	Y	Z	CODE	C	S	AREA	ECCENTRICITY

- **X, Y, Z**: are the coordinates of the centroids.
- **CODE**: is a tag associated to a region which contains information about the branch that has given origin to the region (see next paragraph).
- **C**: bit of checking region.
- **S**: bit of tracking region.
- **AREA**: region area.
- **ECCENTRYCITY**: region eccentricity.

Bit C is set when a region is found and is encoded. **Bit S** is set when a region is a part of a tracking branch.

AREA contains the number of pixels that constitute the region. This number is important to avoid false ramification (see ramification flow-chart in Appendix 1) and to individuate the carina from the masking due to the preliminary closing operation (see closing operation and carina de-masking paragraph).

ECCENTRICITY is a scalar that specifies the eccentricity of the ellipse that has the same second-moments as the region. The eccentricity is the ratio of the distance between the foci of the ellipse and its major axis length. The value is between 0 and 1. (0 and 1 are degenerate cases: an ellipse whose eccentricity is 0 is actually a circle, while an ellipse whose eccentricity is 1 is a line segment.). This number is not used in this version of the algorithm but can be useful for future development.

CENTROIDS CODE

Centroids code is a tag assigned to the region which contains information about all the branches that have given origin to the region. The suffix of each tag is the trachea ID “1” because each branch is originated by the trachea. Every time a ramification is found a prefix, that indicate the order number of ramification, is added to the tag. Ramification order number grow up with Y grow up: order number for the right main bronchus is 1 and for the left main bronchus is 2. In this way, reading the code of a branch after the first number, it is possible to go back to the branch from which has been generated.

The code is utilized coupled with bit C and S during the tracking and classification of the branches of the tracheo-bronchial tree and, in the next phase, is used to link correctly the key points.

BRANCH RECOGNITION

The analysis starts from the trachea. If none ramification is found the code of centroids is the ID of the followed branch ("1" for trachea), bits C and S of each centroids are set. When a ramification is found the code of each branch is the same of the branch that have generated the ramification (father branch) with a prefix that indicate the order number. Bit C of all the coded branch is set. At this point only one branch will be followed, only bit S of the followed centroid is set. When an end of a branch is reached the last ramification leaved is recovered. The analysis proceeds with the search of a possible "brother" of the end branch. Looking between checked centroids, but don't followed (C=1,S=0), it is necessary to found a code with the same suffix but a different order number as a prefix. If a brother-branch is found the analysis restart from it. If no brother-branch is found the analysis continues looking for an "uncle-branch": ID equal to the end branch code ,except that for the first two numbers, not yet followed (C=1,S=0).

In Figure 28 an example is showed.

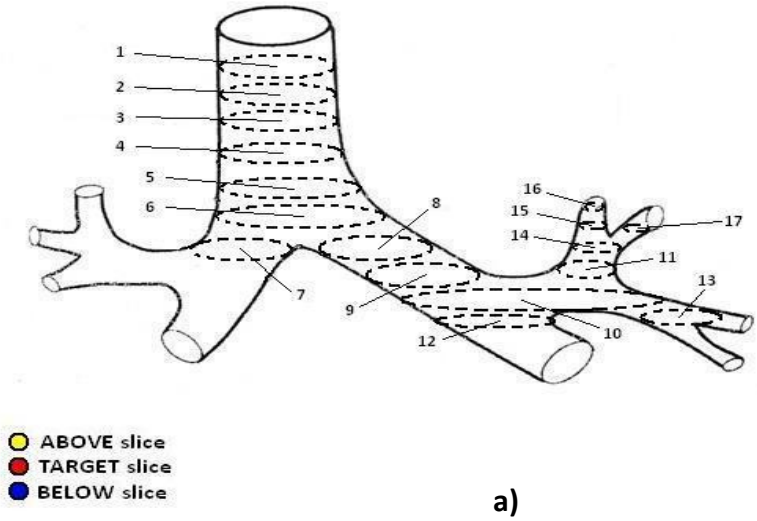

a)

Centroids Matrix

X Y Z	ID	C	S
1	1	0	0
2	1	0	0
3	1	0	0
4	1	0	0
5	1	0	0
6	1	0	0
7	1	0	0
8	1	0	0
9	1	0	0
10	1	0	0
11	1	0	0
12	1	0	0
13	1	0	0
14	1	0	0
15	1	0	0
16	1	0	0
17	1	0	0
.	1	0	0
.	1	0	0
.	1	0	0

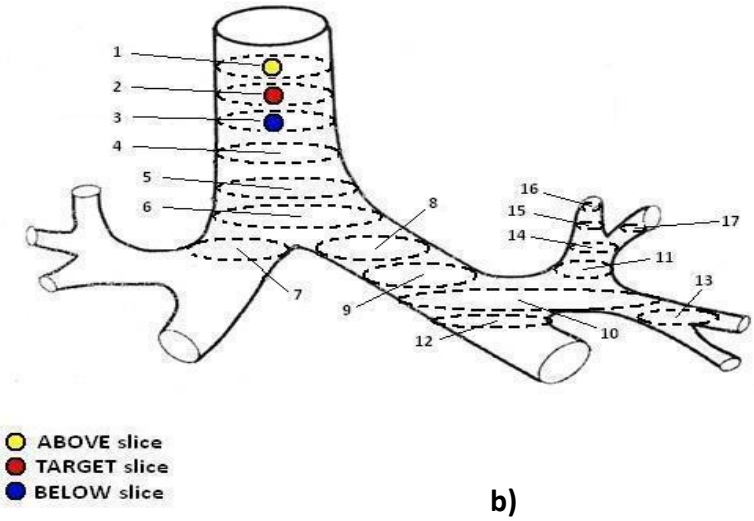

b)

Centroids Matrix

X Y Z	ID	C	S
1	1	1	1
2	1	1	1
3	1	1	0
4	1	0	0
5	1	0	0
6	1	0	0
7	1	0	0
8	1	0	0
9	1	0	0
10	1	0	0
11	1	0	0
12	1	0	0
13	1	0	0
14	1	0	0
15	1	0	0
16	1	0	0
17	1	0	0
.	1	0	0
.	1	0	0
.	1	0	0

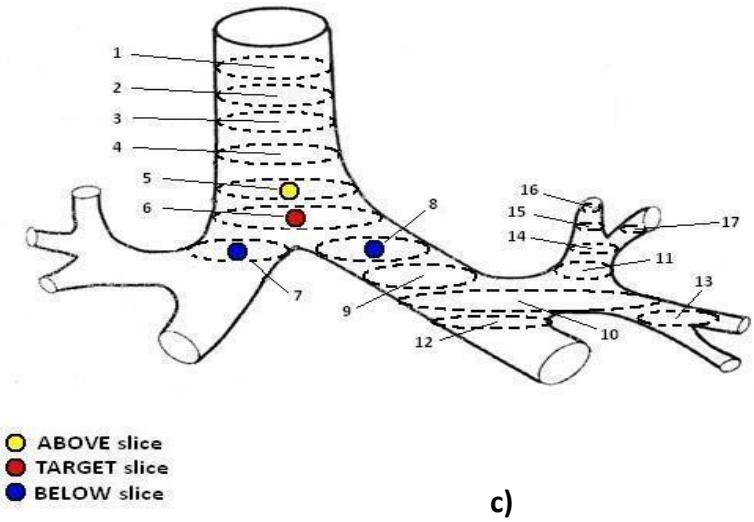

c)

Centroids Matrix

X Y Z	ID	C	S
1	1	1	1
2	1	1	1
3	1	1	1
4	1	1	1
5	1	1	1
6	1	1	1
7	11	1	0
8	21	1	0
9	1	0	0
10	1	0	0
11	1	0	0
12	1	0	0
13	1	0	0
14	1	0	0
15	1	0	0
16	1	0	0
17	1	0	0
.	1	0	0
.	1	0	0
.	1	0	0

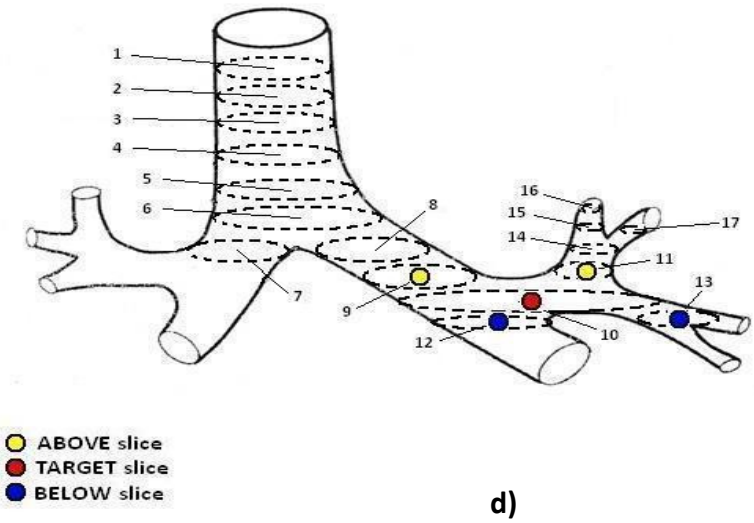

d)

Centroids Matrix

X Y Z	ID	C	S
1	1	1	1
2	1	1	1
3	1	1	1
4	1	1	1
5	1	1	1
6	1	1	1
7	11	1	0
8	21	1	1
9	21	1	1
10	21	1	1
11	321	1	0
12	121	1	0
13	221	1	0
14	1	0	0
15	1	0	0
16	1	0	0
17	1	0	0
.	1	0	0
.	1	0	0
.	1	0	0

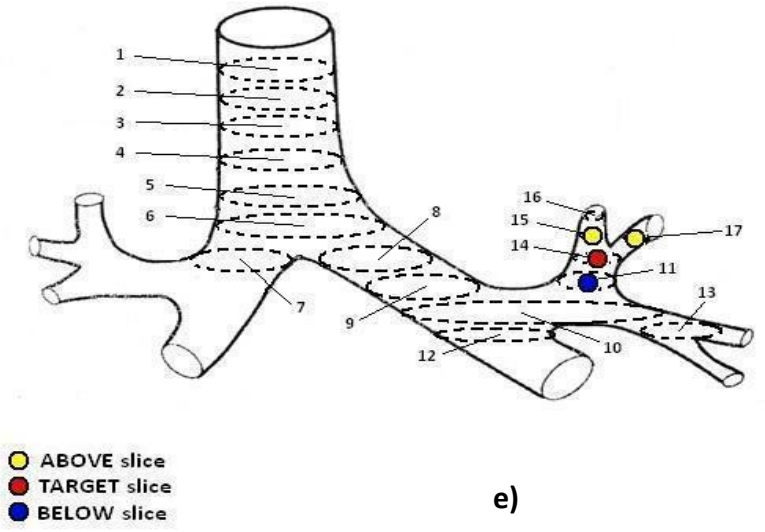

e)

Centroids Matrix

X Y Z	ID	C	S
1	1	1	1
2	1	1	1
3	1	1	1
4	1	1	1
5	1	1	1
6	1	1	1
7	11	1	0
8	21	1	1
9	21	1	1
10	21	1	1
11	321	1	1
12	121	1	0
13	221	1	0
14	321	1	1
15	1321	1	0
16	1	0	0
17	2321	1	0
.	1	0	0
.	1	0	0
.	1	0	0

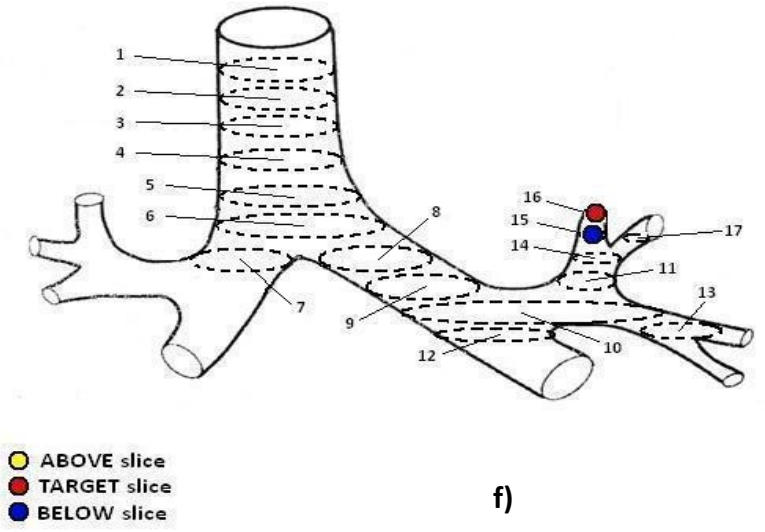

f)

Centroids Matrix

X Y Z	ID	C	S
1	1	1	1
2	1	1	1
3	1	1	1
4	1	1	1
5	1	1	1
6	1	1	1
7	11	1	0
8	21	1	1
9	21	1	1
10	21	1	1
11	321	1	1
12	121	1	0
13	221	1	0
14	321	1	1
15	1321	1	1
16	1321	1	1
17	2321	1	0
.	1	0	0
.	1	0	0
.	1	0	0

Figure 28 – Example of tags assignment and bit C and S utilization. In the first step (28-a) all the regions are catalogued in centroids matrix with tag “1”. In centroids matrix XYZ of the target region is indicated in blue and ID, C and S of intersected regions that change are indicated in red. In the last step (28-f) the row of brother branch found is in yellow.

KEY POINTS

The key points searched in the segmentation are:

- First region of the trachea.
- Carina.
- First region of left main bronchus.
- First region of right main bronchus.
- Ramification points.
- First regions of a ramification branch.
- Branches ending.

First region of the trachea: is the region with the biggest area in the first slice of segmentation. This is start point of the airways analysis.

Carina: is the first ramification point found in trachea

First region of left and right bronchus: the first regions which start from carina. The discrimination between left and right is possible by the analysis of coordinate Y of centroids that represent the regions: if Y growth are in presence of left bronchus instead if Y decrease right bronchus is found.

Ramification points: every times a ramification is found (except for the carina) the centroid of the region which generates the ramification is classified as ramification point.

First regions of a ramification branch: is the centroid of a region directly connected to a ramification region (except for the left and right main bronchus).

Branches ending: each centroid of a last region of a branch.

Key points are stored in a matrix called “key points matrix”. This is composed as follow:

Table 4 – Columns division of key points matrix.

X	Y	Z	CODE	KEY POINT	AUX

X,Y,Z: contain the coordinates of centroids classified as a key points.

CODE: is the ID of the centroids classified as a key points.

KEY POINT: is the key point ID

- 1 → First region of the trachea.
- 2 → Carina.
- 7 → First region of left and right main bronchus.
- 3 → Ramification points.
- 4 → First regions of a ramification branch.
- 5 → Branches ending.

AUX: is used for ramifications points. It contains the order numbers of the ramifications branches which start from the ramifications point. These auxiliary numbers are necessary because from two ramification point with the same ID (CODE) could start different branches. When key points must be linked it is necessary to have all information about the relations between the feature points.

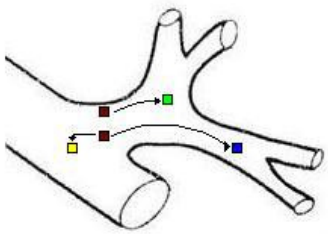

ID	KEY POINT	AUX	
21	3	3	
21	3	1	2
121	4		
221	4		
321	4		

Figure 29 – Example of AUX useful. The two regions indicated with red square have the same ID but they are generation point of different ramifications (indicated by yellow, blue and green square). In the table on the right is visible the AUX value equal to the ramification order number (in red).

Only with the code of centroids, classified as ramification point, it is impossible to know the right branch which starts from them. The ID does not contain information about the order number of son branches the but only about the son branches name. The name is equal for each branch generated. For an useful AUX example see Figure 29.

2.2.5 – Stick diagram

The next paragraphs describe in detail each step of the key points linking operation.

SHORT TERMINATION BRANCHES ELIMINATION

This step is performed preliminary on the entire key points matrix. The link segment between branch ending key points and the respective ramification points represent, in the final stick diagram, a termination branch. Computing the distance between this two key points is possible to determine, with good approximation, the length of the termination branch that they represent. It is possible to eliminate from the key points matrix a couple of point that represent a termination branch under a "*termination branch length threshold"* chosen previously. In this way, short false branches derived from segmentation, and branches that are not necessary to label, are eliminated from the stick diagram. After this processing the stick diagram will result more clean and realize the successive analysis will be more simple.

KEY POINTS LINKING RULES

The key points extracted from the segmentation are linked knowing the rapports of connection. From the key points matrix are extracted: CODE, KEY POINTS NUMBER and AUX NUMBER. The result of the key points linking is the stick diagram.

These are the key points linking rules and represent how the key points must be linked among them:

1 **-** First region of the trachea (1) - Carina (2).

2 **-** Carina (2) - First region of left main bronchus (7, CODE: 21).

3 **-** Carina (2) - First region of right main bronchus (7, CODE: 11).

4 **-** Ramification point (3) - First region of a ramification branch (4) - Ramification point (3).

5 **-** Ramification point (3) - First region of a ramification branch (4) - Branch ending (5).

6 **-** Ramification point (3) with the same code.

The first three rules are obvious and are however showed in the linking scheme.

Rule n° 4: the link between two ramification point is found through the branch which starts from the first ramification point. The order number in the CODE prefix of ramification branch must be found in the AUX of the first ramification point and the CODE suffix of ramification branch must be equal to the entire CODE of the first ramification point. The CODE of the second ramification point will be equal to the CODE of the ramification branch. At this point is possible to link correctly the two ramification point. An example in showed in Figure 30.

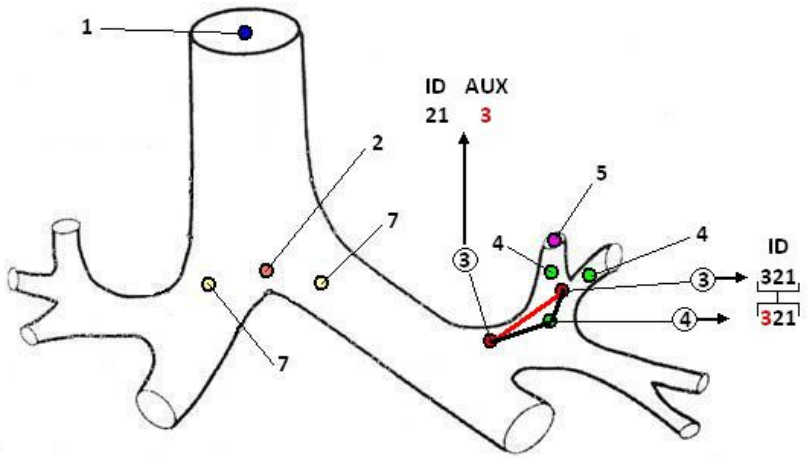

Figure 30 – Example of linking rule 4 application. Key points interested in the linking are inside a circle.

Rule n° 5: the same method of the rule n° 4 is followed, but with a branch ending instead of the second ramification point. See Figure 31 for an example of rule 5 application.

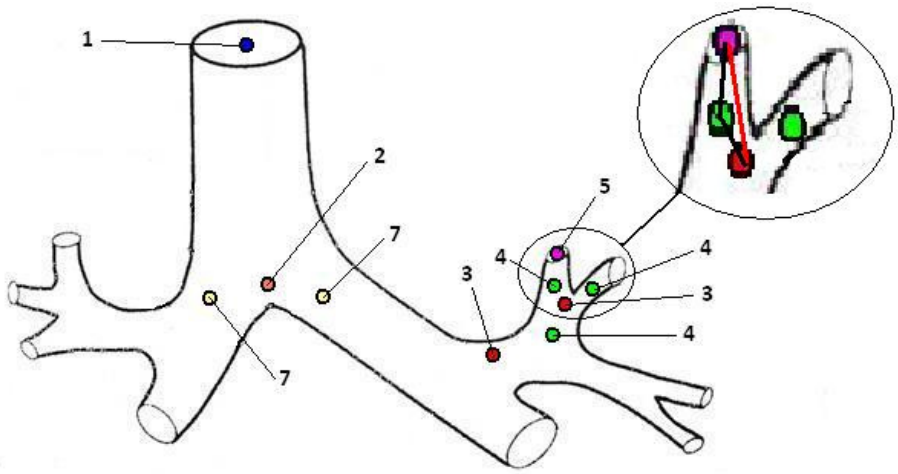

Figure 31 – Example of linking rule 5 application.

Rule n° 6: in the key points matrix there are some ramification point with the same CODE. These represent different ramification points of the same branch. The most clear example is the right upper lobar bronchus (see Figure 32). These points are connected and the linking order is established by the first number of AUX. The ramification point with the same CODE of the first point of the left main bronchus and with 1 between the AUX numbers is linked to the first point of the left main bronchus. The same is done for the right main bronchus.

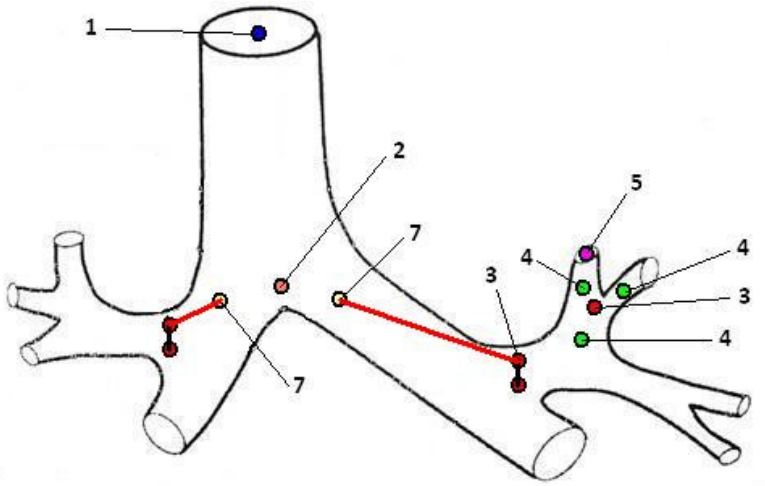

Figure 32 – Example of linking rule 6 application.

In some situation is possible to have the same centroid classified as ramification branch and ramification point. These cases are individuated preliminary on the entire key points matrix: centroid recognized as a ramification point is divided in two different new points with the same coordinate X-Y of the correspondent ramification branch. It is possible to individuate in this way the presence of two (or more) different branch just from the first ramification point.

KEY POINTS MATRIX CLASSIFICATION

The key points linking algorithm works iteratively on couple of feature points. It is necessary to create some different small matrixes from the entire big key points matrix to join the points that must be linked divided by category.

Four matrixes from key points matrix are created:

- **Trachea-carina-bronchus matrix**: contains the couples of points that generate trachea and its first ramification.
- **Ramification points to ramification points matrix**: contains the couples of ramification points that must be linked among them.
- **Ramification points to branches ending matrix**: contains the couples of points that generate termination branches by their linking.
- **Ramification point with the same code matrix**: contains the couples of ramification points with the same code sorted by the branch order number that generate.

Linking algorithm provide to connect the key points couple by couple, in four phases showed in Figure 33.

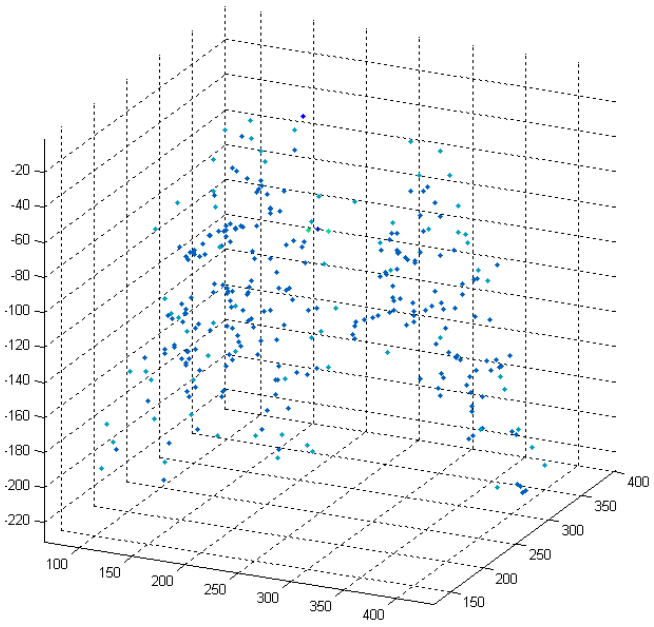

a)

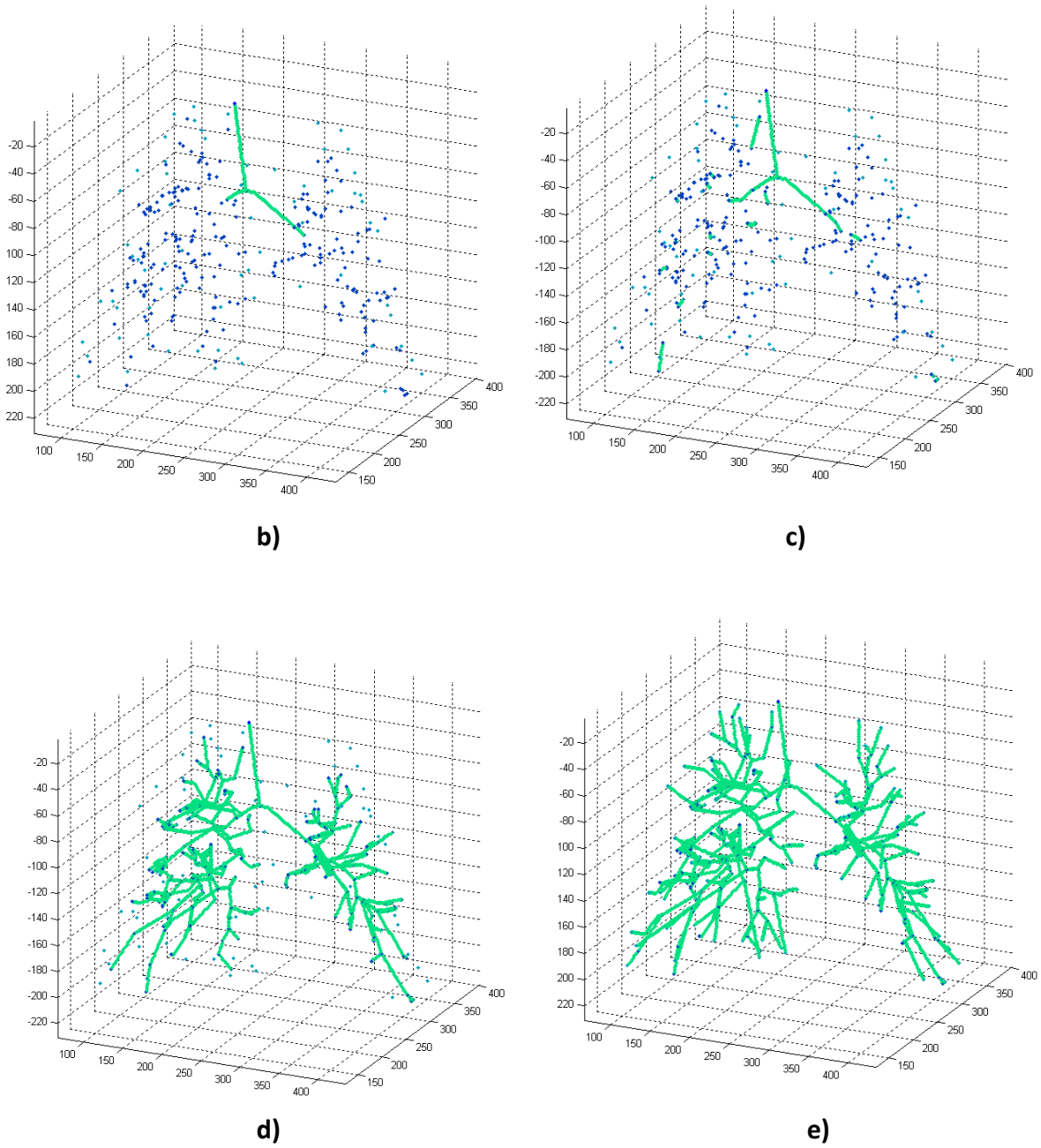

Figure 33 – The four step of stick diagram creation. 33-a shows key points placement. In figure 18-b there are trachea-bronchus linking. 33-c,d,e show respectively ramification points with same ID linking, ramification points linking and ramification points-branches ending linking.

LINKING ALGORITHM

By the linking algorithm is possible to connect a couple of points with a segment avoiding possible collisions.

Computing of the ideal trace

The first step is to compute the ideal segment that linked the two points. With the term "*line rasterization*" is indicated the problem of approximation of a segment, in a continuous space, in a system of connected pixels (2D) or voxels (3D) in a discrete space. For a 2D example see Figure 34. To compute the ideal trace that connect a couple of points in three-dimensional discrete space Bresenham's rasterization line algorithm [44] is used. This method uses only integer addition, subtraction and bit shifting, all of which are very cheap operations in standard computer architectures.

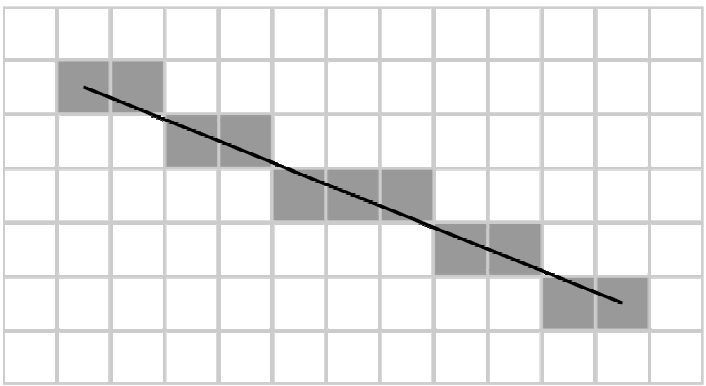

Figure 34 – Example of 2D line rasterization. The line in black is approximated by connected gray pixels.

The voxels coordinates that compose the ideal trace are stored in a matrix called "*ideal trace matrix*".

Collision prevention

It is necessary to avoid the collision between the segments that are traced and the segments that are already on the matrix. The problem is the generation of false ramifications. The voxels are added to the trace one by one. Every time a list of candidate voxels for the trace is generated.

Are excluded from the list all the voxels that have one or more neighbourhood that touch another voxel on the matrix off the points of the segment that is traced now.

To individuate the nearness is created a collision sensitivity matrix called "*ghost matrix*". The ghost matrix have the same size of the matrix that will contain the stick diagram. It includes all the voxels that the trace does not have to touch:

- All key points except the two points that must be linked and their neighbourhoods.
- All the traces that are already on the matrix.
- All the voxels of the present trace except the last three traced.

If between the candidate voxels there are no one voxel belonging to the ideal trace then there is an obstacle on the ideal trace. From this point up to the end of the linking the voxel nearest to the stop voxel is chosen from the candidate list.

The Figure 35 shows the mechanism in a two-dimensional space.

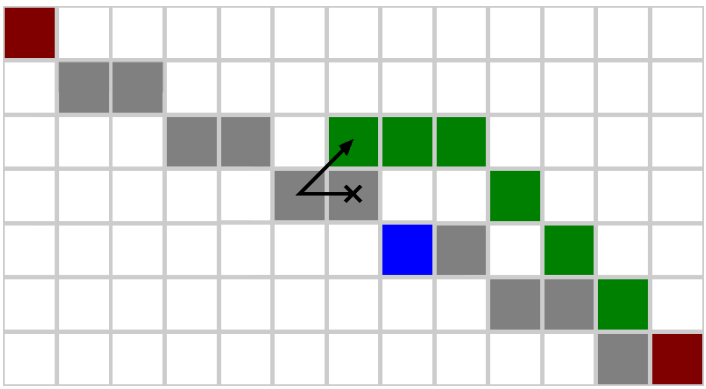

Figure 35 – A two-dimensional example of collision avoidance. On ideal trace in gray for red points linking there is an obstacle represented by the pixel in blue. Algorithm exit from the ideal trace and follow minimisation distance principle (green line).

The traces created in case of collision follow very bad the ideal trace especially in the last part (see Figure 36).

If the key points are linked from the center to surround of the airways tree, the segment maintains the same starting direction of the branch that represents.

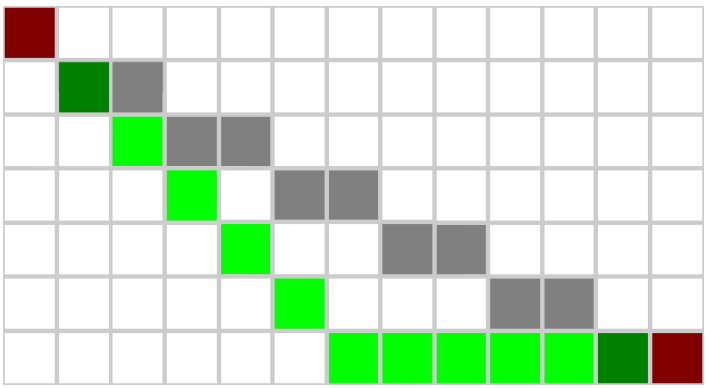

Figure 36 – The difference, in a two-dimensional space, between a track that follows rasterization line principle and a track that follows minimization distance principle, adopted ,from the obstacle point, in case of collision.

When the number of the trace voxels overcomes a threshold called "*watch-dog*" the stop voxel and all the segments traced are cancelled because the stop voxel is too difficult to reach.

To avoid the cancellation of part of the airways tree that must be labelled and to obtain the most clear and clean stick diagram as possible, the key points are sorted preliminary form the center to the surrounding of the tracheo-bronchial tree.

STICK DIAGRAM

The final result of the key points linking is the stick diagram (Figure 37).

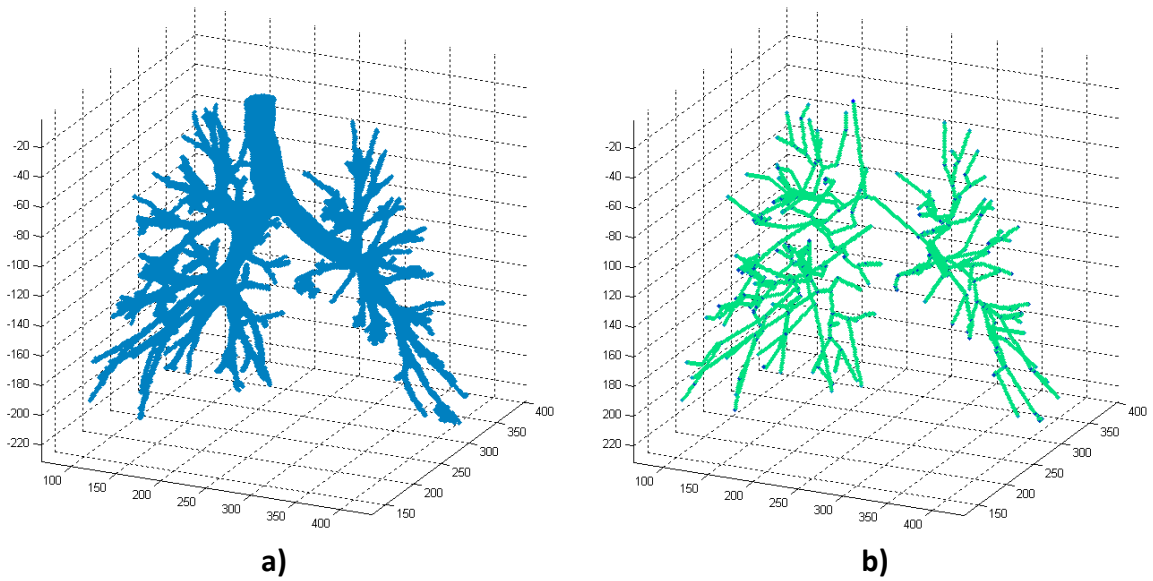

Figure 37 – The stick diagram (37-b) obtained from an airways segmentation (37-a).

Each segment represents a schematization of an airways tree branch. The line starts from the generation point already with the characteristic direction of the branch that represents. It is possible now to reassume all the differences between a classical skeletonization and the stick diagram.

1. For the branches perpendicular to the axis Z of the three-dimensional matrix the centroid linking does not follow the real branch central axis (Figure 38).
2. The branches generated from a branch parallel to the X-Y plane are represented as distinct lines that start from the false father-branch central axis (Figure 38).
3. The rasterized segment approximating the anatomical pattern of the branches.
4. The traces created in case of collision, in the second part, follow with very bad approximation the anatomical pattern of the branches (Figure 36).

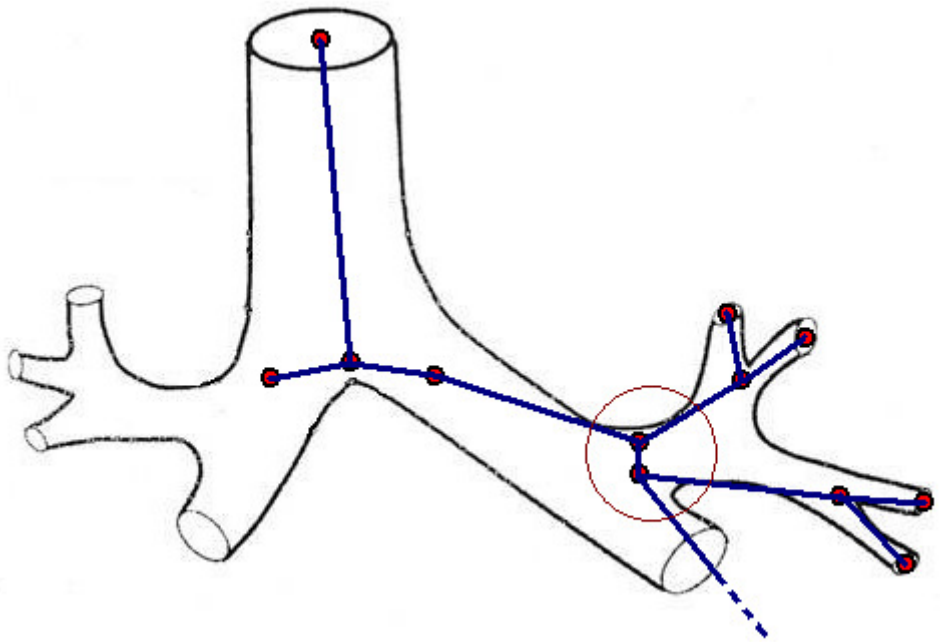

Figure 38 – Stick diagram of the left upper lobe bronchus. This is a typical example of the first two mentioned difference between a classical skeletonization and the stick diagram.

2.2.6 – Labeling

The purpose of the stick diagram is to track, with a straight line, all the branches of the original segmented airways. The result is a kind of translation or interpretation of the segmentation.

The diagram lines start from the generation points already with the characteristic direction of the branches that represent. The objective is to label the segment that represent the principal branches of the airways tree.

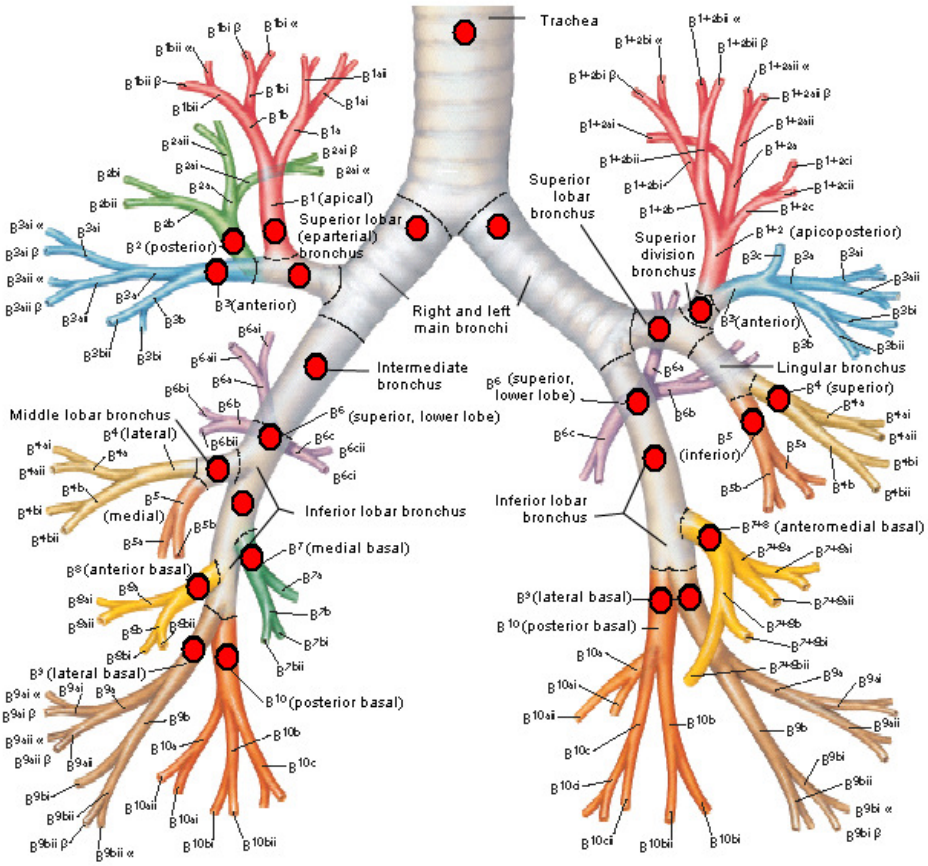

Figure 39 – The airways tree extracted from Netter Atlas of Anatomy [45]. The red spots indicate branches to label.

The objective is to label at least up to the segmental bronchi indicate in Figure 39 with a red circle. The branches of deeper generations than the 24 branches to label will assume the same label of the father-branches. The idea is to label an unknown branch knowing its direction and the name of the branch that generate it.

ANATOMICAL MATRIX

A matrix called "*anatomical matrix"* is created to associate the right name to an unknown branch that starts with a known direction from a ramification point of a known branch.

Table 5 – The anatomical matrix column division.

	SON DIRECTION			
FATHER LABEL	*DX*	*DY*	*DZ*	**SON LABEL**

- ***FATHER LABEL***: is the known name of the analyzed branch.
- ***SON DIRECTION*** (*DX, DY, DZ*): are the components of the vector that represents the direction of the unknown branch. These are obtained from the subtraction between the coordinates of the first voxel of the unknown branch and the coordinates of ramification voxel.
- ***SON LABEL***: is the name to associate to the unknown branch.

In order to create the anatomical matrix each sector is considered as a voxel surrounded by its 26 neighbourhoods. Each neighbourhood is considered as a possible direction of ramification.

A different cube for each sectors, divided in 27 more little cubes, has been created with a three-dimensional CAD (Rhinoceros version 4.0 ® Robert McNeel & Associates). The central cube is the present voxel of the reference sector and the other cubes represent the possible development of ramifications from the sector. At each neighbour of the central voxel of the cube is assigned the name of the possible branch in particular, Figure 25, shows the cube used to classify trachea.

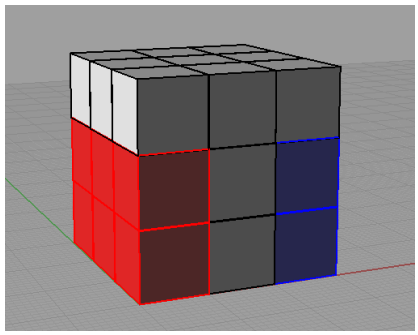

Figure 40 – Example of cube for possible ramifications development classification from a target sector. In this case target sector is trachea and possible ramification are right main bronchus (in red) and left main bronchus (in blue).

The red cubes represent the possible development directions of the right main bronchus, the blue cubes represent the possible development directions of the left main bronchus.

STICK DIAGRAM ANALYSIS

The segments of the stick diagram are tracked, by the labelling algorithm, starting from the trachea. When a bifurcation voxel is found the ramification voxel are analyzed one by one. The direction of each generated branch is associated to the label of the father-branch. At each couple *son-direction + father-label* corresponds the label of the unknown branch (son-label). The labeling mechanism and the anatomical matrix use are showed in Figure 41.

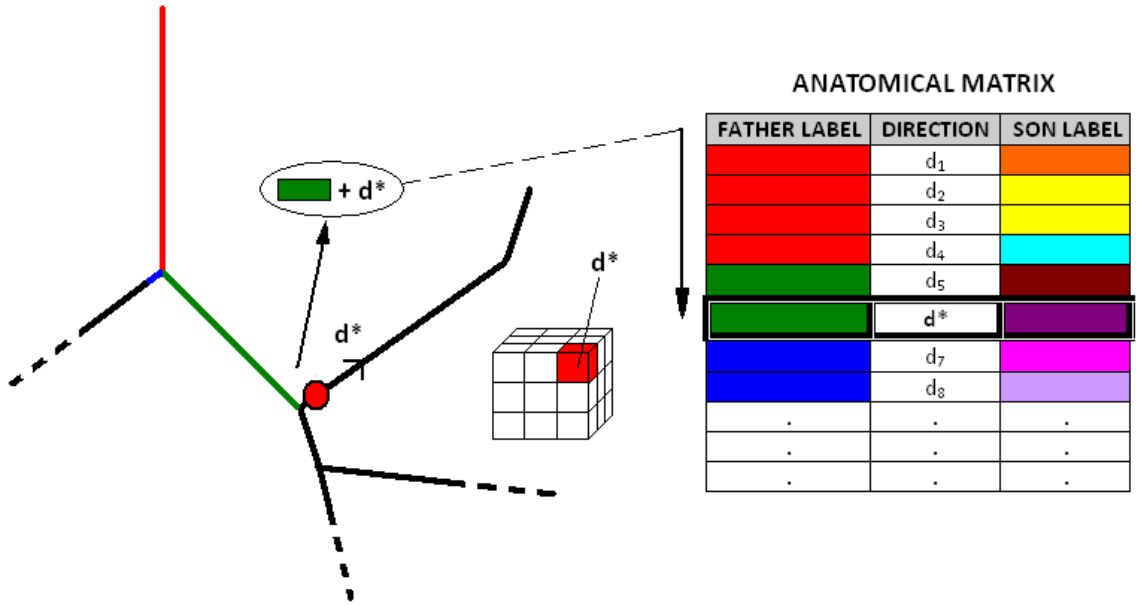

Figure 41 – Example of labeling mechanism. From the green sector a branch with direction d* is found. In anatomical matrix at the couple green-d* correspond violet label. The cube in the middle shows in red 3D direction d* respect to the green sector represented by the central cube.

If there are, in the anatomical matrix, more than one single label associated to a couple *son-direction + father-label*, the user intervention is required. Two or more alternative label are proposed and the stick diagram with a red spot on the first unknown branch voxel is showed. The user will select the right label using his experience and the information given by the software.

Only one of the branches generated by the ramification is followed, the other are stored in a LIFO (last input, first output) stack and are recovered when the end of a branch is reached.

NEIGHBOURHOODS THEFT: the ramification branch to be followed for first is chosen as follow. Ramification branch start voxels are sorted by the number of their unknown neighbourhoods. The branch with the start voxel with less neighbourhood is chosen. This is the procedure to avoid the phenomena of "*neighbourhoods theft*".

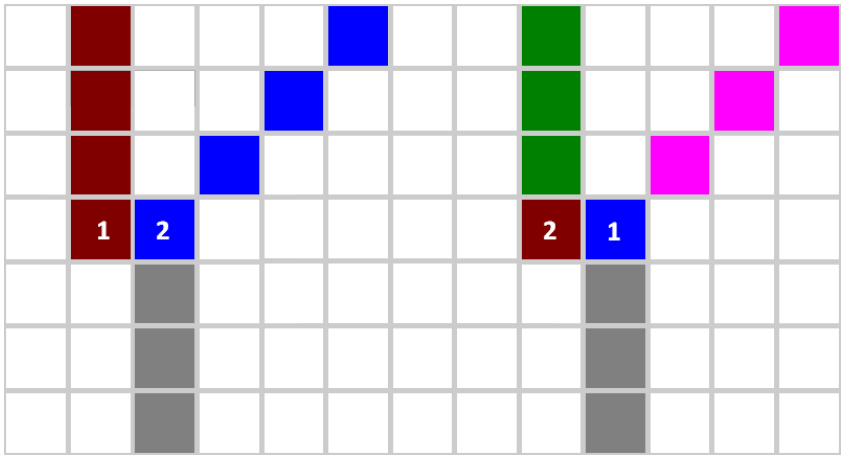

Figure 42 – Example of correct 2D ramification classification (42-a) that avoid the neighbourhood theft phenomena. Figure 42-b shows a wrong classification that move ramification point and close the real branch starting point indicated by the red pixel.

Figure 42-a shows the right tracking of ramification branches. When ramification point is reached start voxels of the branches generated are labelled. The branch with the first voxel with less unknown neighbourhood is followed for first (red). In this way the voxels which follow on the branch (red) inherit the label of the first. When the end of the branch is reached voxel number 2 is recovered from the stack and also the second ramification branch (blue) is tracked.

Figure 42-b shows an incorrect procedure. The first branch followed is the other one (blue). Another ramification point is immediately found and the only one unknown neighbourhood of the red voxel is stolen. Consequently the red voxel is isolated and the branch is incorrectly labelled because the direction and father label extracted are different.

BRANCHES NAME CODES

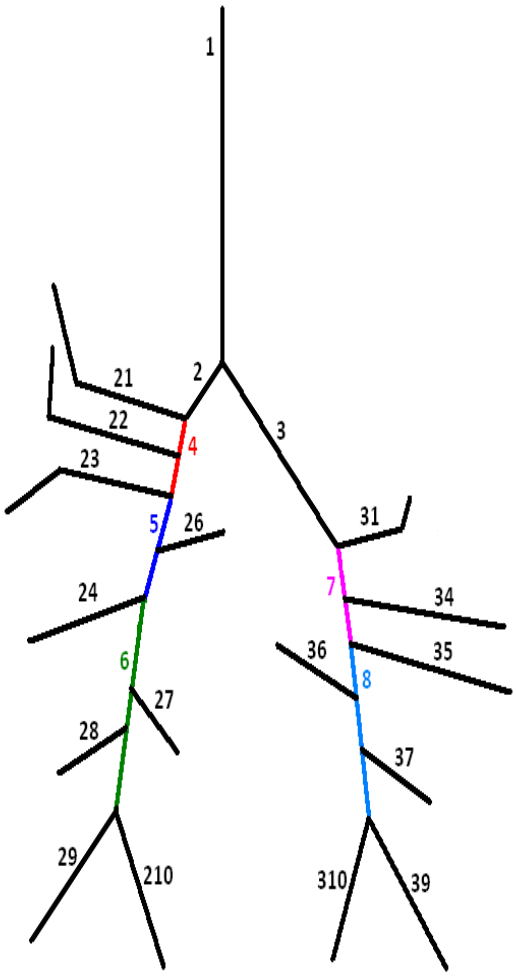

NAME	SYMBOL	CODE
Trachea	-	1
Right		
Main bronchus	-	2
Upper lobe bronchus	-	4
Apical	B^{1}	21
Posterior	B^{2}	22
Anterior	B^{3}	23
Intermediate bronchus	-	5
Superior, lower lobe	B^{6}	26
Lower lobe bronchus	-	6
Middle lobe bronchus	B^{4+5}	24
Medial basal	B^{7}	27
Anterior basal	B^{8}	28
Lateral basal	B^{9}	29
Posterior basal	B^{10}	210
Left		
Main bronchus	-	3
Upper lobe bronchus	-	7
Superior division bronchus	B^{1+2+3}	31
Superior	B^{4}	34
Inferior	B^{5}	35
Lower lobe bronchus	-	8
Superior lower lobe	B^{6}	36
Anteromedial basal	B^{7+8}	37
Lateral basal	B^{9}	39
Posterior basal	B^{10}	310

Figure 43 – The complete stick diagram with the correct label on every branch.
The table on the right shows the codification of the anatomical branches name adopted.

In the Figure 43 is showed a stick diagram with all the necessary segments labelled in the right way.

Each anatomical label is encoded by a symbolic number. The Table on the Figure 43 right side shows the correspondences.

The main bronchus are divided in 7 sectors. Respectively 4 sectors for the right main bronchus with codes 2,4,5,6 and 3 sectors for the left main bronchus with codes 3,7,8. There is an approximate correspondence between the anatomy and this sectors. Each sector generates its characteristic branches.

UPPER LOBE LIMITS: a statistical analysis is performed on all the data-set segmentations to found the limits of sectors 4 and 7. Z values of the first and last start point of the segments representing a segmental branches of the upper lobe has been analyzed (see Table 6 and 8). Subtracting the two Z values it is possible to found the extension of the upper lobe of each airways tree. This operation is performed for the right and left upper lobe of each segmented airways tree both at TLC and RV volume. The final output is the maximum upper lobe extension.

Table 6 – Characteristic Z value extracted from database stick diagrams at TLC volume useful to obtain a common right and left upper lobe extension.

TLC	**UPPER LOBE BRONCHUS**		**B6**	**UPPER LOBE EXT**
SUBJECT NUM (branch length limit)	***FIRST BRANCH***	***LAST BRANCH***	***FIRST BRANCH***	
		DX		
1 (bl8)	82	94	115	12
2 (bl8)	58	58	97	0
3 (bl8)	72	77	99	5
4 (bl8)	88	88	113	0
5 (bl8)	80	82	114	2
6 (bl8)	72	80	120	8
7 (bl8)	53	61	80	8
8 (bl8)	67	67	98	0
9 (bl8)	77	82	110	5
10 (bl8)	74	80	110	6
				max + 1: 13
		SX		
1 (bl8)	102	109	114	7
2 (bl8)	78	85	91	7
3 (bl8)	93	93	102	0
4 (bl8)	99	106	108	7
5 (bl8)	101	108	113	7
6 (bl8)	95	100	109	5
7 (bl8)	67	74	78	7
8 (bl8)	84	88	97	4
9 (bl8)	89	98	100	9
10 (bl8)	88	96	97	8
				max + 1: 10

Table 7 – The stick diagrams at TLC volume with the left or right upper lobe extension out of the range calculated as typical from the data of Table 6 (red square).

UPPER LOBE *LAST BRANCH*	B6 *FIRST BRANCH*	UPPER LOBE FIRST BRANCH + MAX+1 (UPPER LOBE EXT)	
DX			
94	115	95	
58	97	70	
77	99	84	
88	113	100	
82	114	92	
80	120	84	
61	80	65	
67	98	79	
82	110	89	
80	110	86	
SX			
109	114	112	
85	91	88	
93	102	103	
106	108	109	
108	113	111	
100	109	105	
74	78	77	
88	97	94	
98	100	99	
96	97	98	

At TLC for the right bronchus (sector 4) adding the maximum upper lobe extension plus one to the Z value of the first ramification in the main bronchus, during the stick diagram analysis, is possible to predict the inferior limits of the upper lobe and in this way the extension of sector 4 .

At TLC for the left bronchus (sector 7) there are three cases out of the limit found for the left upper lobe (red squares in Table 7). For the left upper lobe is not possible to predict a limit at TLC: during the labelling procedure will be required the user intervention to establish the limit of the left upper lobe bronchus. For the exactly values see the Table 7.

Table 8 – Characteristic Z value extracted from database stick diagrams at RV volume useful to obtain the right and left upper lobe extension.

RV	UPPER LOBE BRONCHUS		B6	UPPER LOBE EXT
SUBJECT NUM (branch length limit)	*FIRST BRANCH*	*LAST BRANCH*	*FIRST BRANCH*	
	DX			
1 (bl3)	52	66	77	14
2 (bl3)	87	90	115	3
3 (bl3)	56	63	78	7
4 (bl3)	66	70	85	4
5 (bl3)	53	61	78	8
6 (bl3)	50	54	70	4
7 (bl3)	39	48	69	9
8 (bl3)	38	38	63	0
9 (bl0)	48	54	73	6
10 (bl0)	43	48	64	5
				max + 1: 15
	SX			
1 (bl3)	68	68	75	0
2 (bl3)	106	106	108	0
3 (bl3)	75	75	81	0
4 (bl3)	77	83	103	6
5 (bl3)	71	71	74	0
6 (bl3)	63	70	91	7
7 (bl3)	49	54	60	5
8 (bl3)	54	61	63	7
9 (bl0)	55	60	61	5
10 (bl0)	56	56	60	0
				max + 1: 8

Table 9 – The stick diagrams at RV volume with the left or right upper lobe extension out of the range calculated as typical from the data of Table 7 (red square).

UPPER LOBE *LAST BRANCH*	B6 *FIRST BRANCH*	UPPER LOBE FIRST BRANCH + MAX+1 (UPPER LOBE EXT)	
DX			
66	77	67	
90	115	102	
63	78	71	
70	85	81	
61	78	68	
54	70	65	
48	69	54	
38	63	53	
54	73	63	
48	64	58	
SX			
68	75	76	
106	108	114	
75	81	83	
83	103	85	
71	74	79	
70	91	71	
54	60	57	
61	63	62	
60	61	63	
56	60	98	

At RV for the right bronchus it is possible to establish the extension of sector 4 real time by the extraction of the Z value of the first upper lobe ramification.

At RV for the left bronchus there are six cases out of range (red square in Table 9). In the majority of the cases (6/10) there is a very few space on Z axis between the last ramification of the upper lobe and the first manifestation of the lower lobe first branch (B6). For the exactly values see Table 9.

TOPOLOGIC RULES: in some cases when a bifurcation is found one of the two ramifications is correlated to the other. This correlation is due to the topology of the stick diagram deriving from the airway anatomy. It is possible to extrapolate two rules:

- The second bifurcation branch cannot have the same label of the first.
- Univocal correspondence between particular couples of branches (Table 10): if the first branch label found is in a row of the first column the second ramification branch have the label indicate in the second column at the same row.

Table 10 – Univocal correspondence between particular couples of branches.

FIRST DETERMINED BRANCH LABEL	SECOND BRANCH LABEL
21	4
22	4
23	4
24	5
24	6
26	5
25	6
27	6
28	6
36	8
37	8
29	210
210	29
39	310
310	39

CANDIDATE LABEL REDUCTION: the number of label candidate to be the correct label for an unknown branch is reduced following some topologic rule coming from the observation of the stick diagram label pattern due to the anatomy structure of the tracheo-bronchial tree:

- When a right middle lobe bronchus (24) has been found it is not possible to have among the candidates a right B6 (26) label.
- When a right B8 (28) or B9 (29) or B10 (210) have been found it is not possible to have among the potential candidates a right B7 (27) label.
- When a right B9 (29) or B10 (210) have been found it is not possible to have among the potential candidates a right B8 (28) label.
- When a left B7+8 (37) or B9 (39) or B10 (310) have been found it is not possible to have among the potential candidates a left B6 (36) label.
- When a left B9 (39) or B10 (310) have been found it is not possible to have among the potential candidates a left B7+8 (37) label.

The candidate label vector is checked and cleaned from the "*impossible label*" before the correct label choice by the user or by the software. In this way the autonomy of the software increases and in case of user intervention the number of proposed labels decrease.

ANATOMICAL MATRIX REAL TIME UPDATE: during the labelling algorithm runtime is possible to update the anatomical matrix. When among the label proposed to the user there is not the correct label for an unknown branch or when there is not any candidate is possible to indicate arbitrarily the exact label. The new correspondence will be stored in a new updated anatomical matrix. At the end of labelling software running is possible to maintain the old version of anatomical matrix or to use the update version for the next analysis.

BRANCHES MATRIX: at the end of stick diagram analysis the algorithm returns an auxiliary matrix called "*branches matrix*". This matrix is composed as follow:

Table 11 – The branches matrix column composition.

ID NUMBER	COORDINATES	LABEL	DIRECTION

ID NUMBER: can assume value of 1 or 2. 1 identifies a ramification point voxel and 2 identifies the first ramification voxel.

COORDINATES: are the coordinates X Y Z of the stored voxel.

***LABEL*:** is the label assigned to the voxel by the algorithm.

DIRECTION: is null in case of ramification point (ID number = 1). In case of first ramification voxel it contains the direction of ramification respect to the ramification point.

This matrix is very useful to find the right and wrong label assignment on the stick diagram labelled by the algorithm.

2.2.7 – Statistical analysis

A t-test was performed to evaluate the influence of the lung volume on the percentage of labeled branches for each subject. For each branch, the relation between the percentage of recognized branches, the levels of the branches and lung volume was evaluated by means of a Two Way Analysis of Variance (Holm-Sidak method).

Statistic was performed by SigmaStat software (version 11.0, San Jose, California, USA). P values less than 0.05 were considered to indicate significant differences.

CHAPTER 3

Results

3.1 – EXPERIMENTAL PROTOCOL

DATABASE

The thoracic CT data used for the present work belong to a database of 10 healthy volunteers with no history of smoking or lung disease and normal spirometric values were used for the analysis. Subjects were scanned during suspended end-inspiration at total lung capacity (TLC) and during suspended end-expiration or near residual volume (RV).

The total database available for the algorithm running is composed by 20 airways tree (10 at TLC and 10 at RV volume) extracted from thoracic CT with a segmentation region growing algorithm [43]

The extraction of stick diagrams is performed on the complete 20 airways tree database, but only 16 are used for the labelling because of the complexity of the segmented airways tree reconstruction. In the two excluded cases the density of the key points cloud was too high and the present version of the algorithm failed.

ANATOMICAL MATRIX

The anatomical matrix used for the labeling is created analyzing the direction of the sticks on 3 full complete stick diagrams obtained at TLC.

Each sector, contained in the matrix, has been completed with other possible branch development direction, combined to the correct label extracted from an accurate anatomical analysis of the human airways tree from the Atlas of Anatomy by Netter [45].

During the running of the labeling algorithm the anatomical matrix is updated by the user observations on the other 10 stick diagrams. For the particular anatomical matrix updating interventions, on each single stick diagram labeling see Appendix 2.

3.2 – REPRESENTATIVE AUTOMATED AIRWAYS LABELING

In this paragraph one of the 16 airways tree labeling is presented step by step. This is the labeling performed on a tracheo-bronchial tree which contain all the 24 branches to label. The result of the automatic nomenclature is representative of the average algorithm performance.

This is a good example useful to understand how the software works and, particularly, when is necessary the intervention of the user to choose the correct label.

In the Figures 44-a, 44-b, 44-c are showed the first three step on the thoracic CT image to perform the automated airways labeling. The Figure 44-a shows the segmented airways tree, the Figure 44-b shows the key points extracted from the segmentation and the Figure 44-c shows the feature points linking to realise the stick diagram.

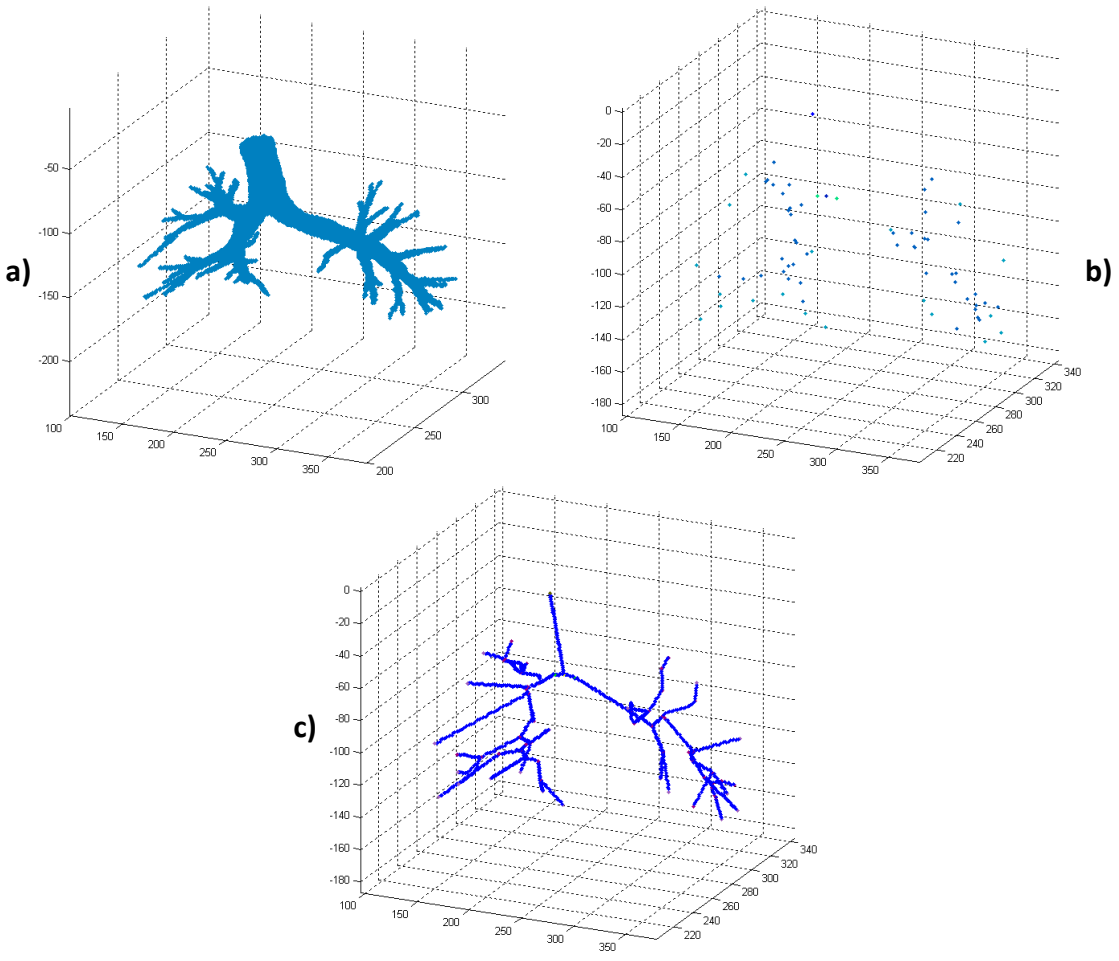

Figure 44 – Segmented airways tree (Figure 44-a), key points extracted from the segmentation (Figure 44-b), stick diagram from feature points linking (Figure 44-c).

The Figure from 45-a to 45-u show the labeling algorithm work, step by step, on the stick diagram.

How to read the labeling steps:

- ***Black arrow***: follows the directions of target branches.
- ***Green arrow***: follows the ramification branches labelled automatically by the algorithm.
- ***Red arrow***: follows the ramification branches labelled by the user.
- ***Orange arrow***: follows the ramification branches waiting for the user intervention.
- ***Red spot***: indicates a bifurcation processed during the current labeling step.

Each labelled branch is linked to a box with the label by a black slim line.

When the intervention of the user is required, a window, with the possible actions appears on the screen. An eye icon appears in correspondence of the user selection when the label is arbitrarily chosen.

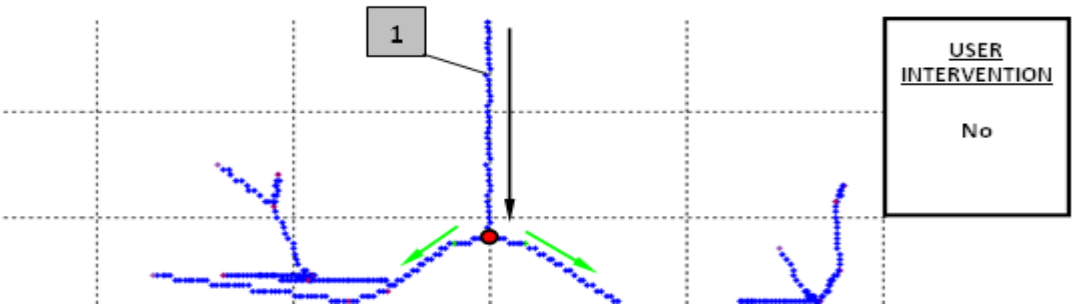

a)

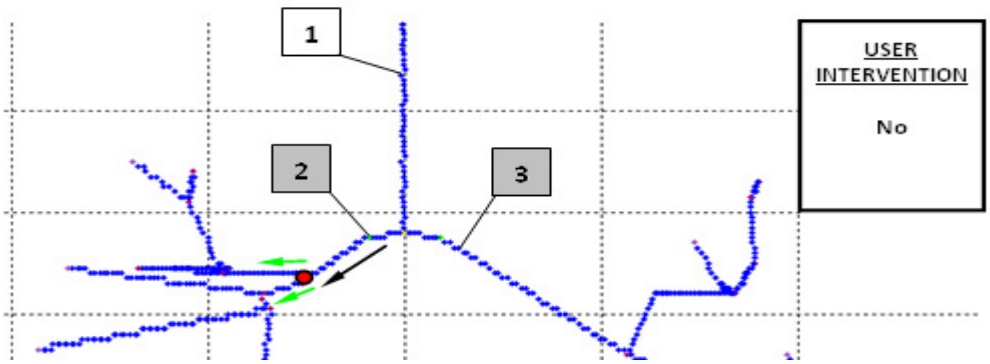

b)

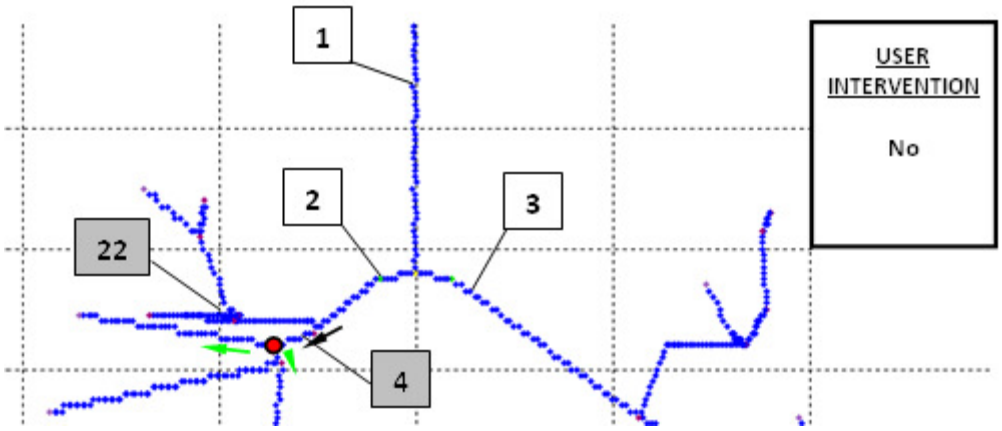
1
2
3
22
4
USER
INTERVENTION
No

c)

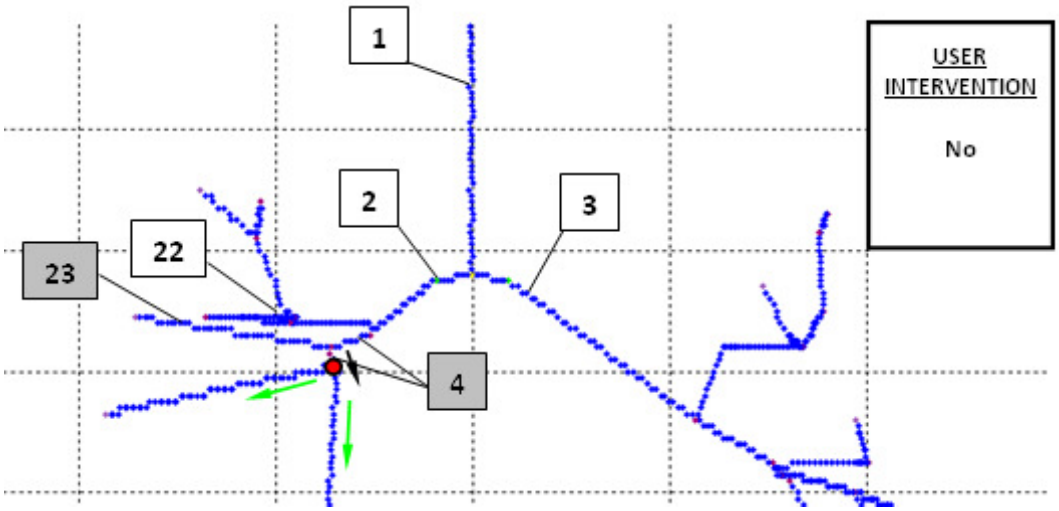
1
2
3
22
23
4
USER
INTERVENTION
No

d)

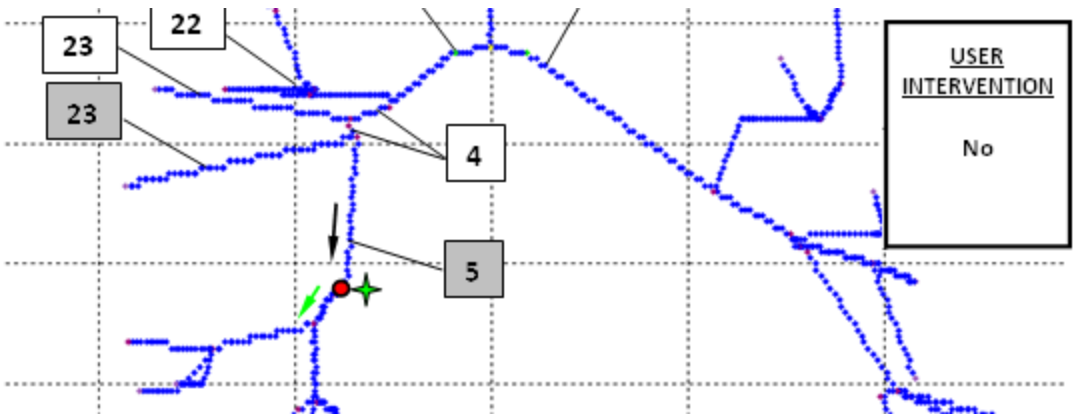
22
23
23
4
5
USER
INTERVENTION
No

e)

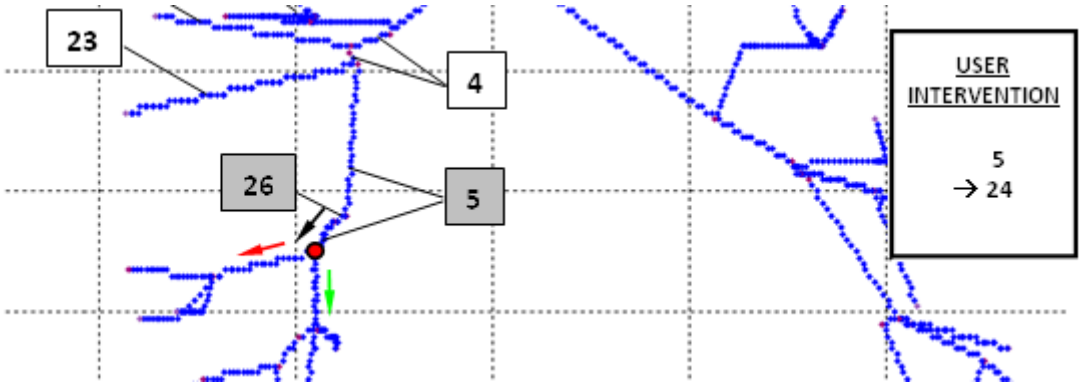
23
4
26
5
USER
INTERVENTION
5
→ 24

f)

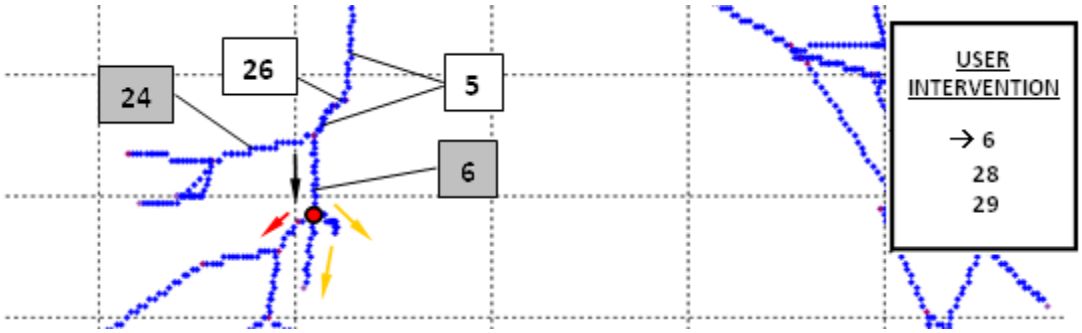
24
26
5
6
USER
INTERVENTION
→ 6
28
29

g)

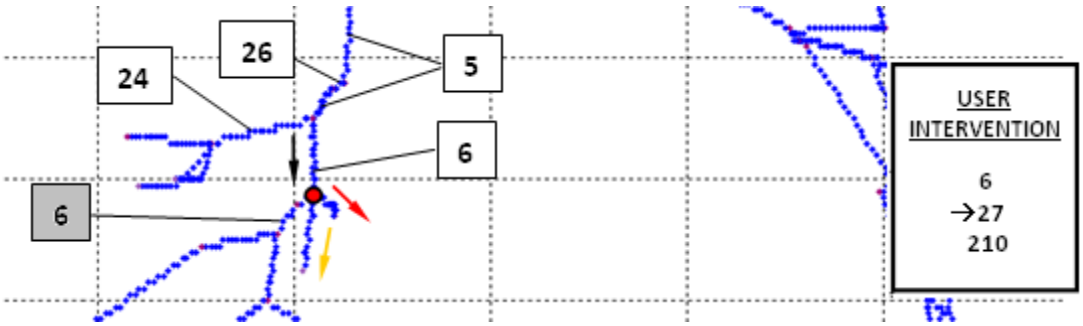
24
26
5
6
6
USER
INTERVENTION
6
→27
210

h)

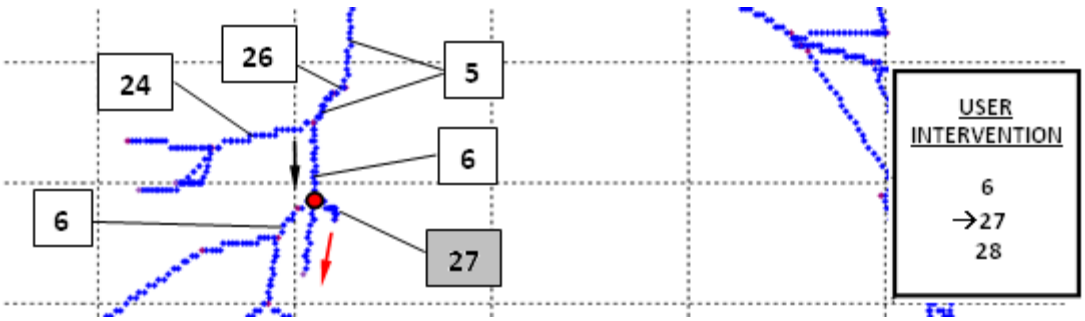
24
26
5
6
6
27
USER
INTERVENTION
6
→27
28

i)

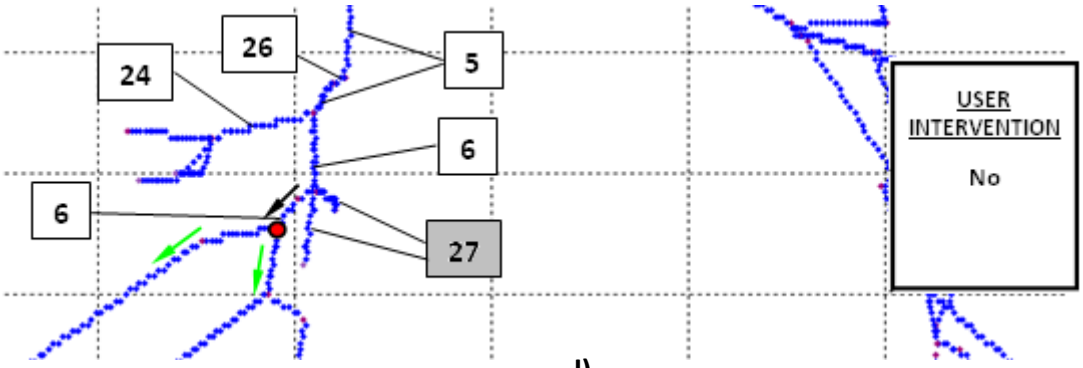
26
24
5
6
6
27
USER
INTERVENTION
No

l)

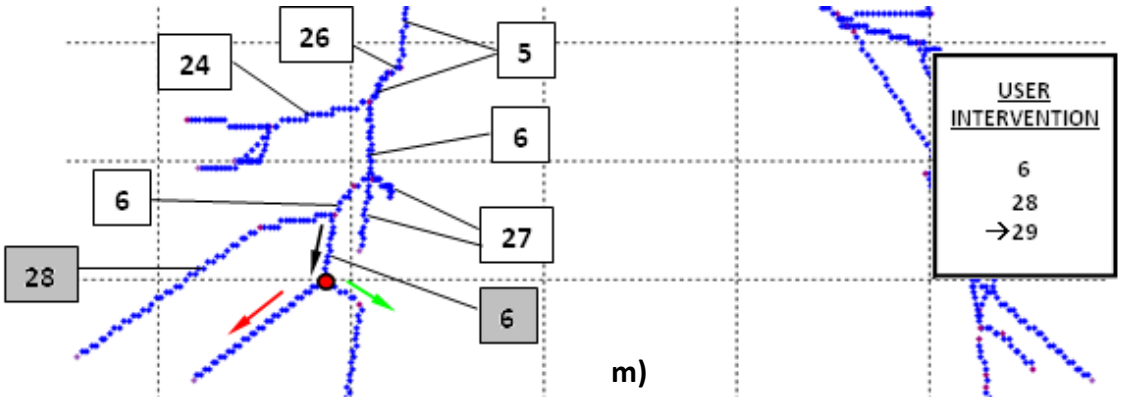
26
24
5
6
6
27
28
6
USER
INTERVENTION
6
28
→29

m)

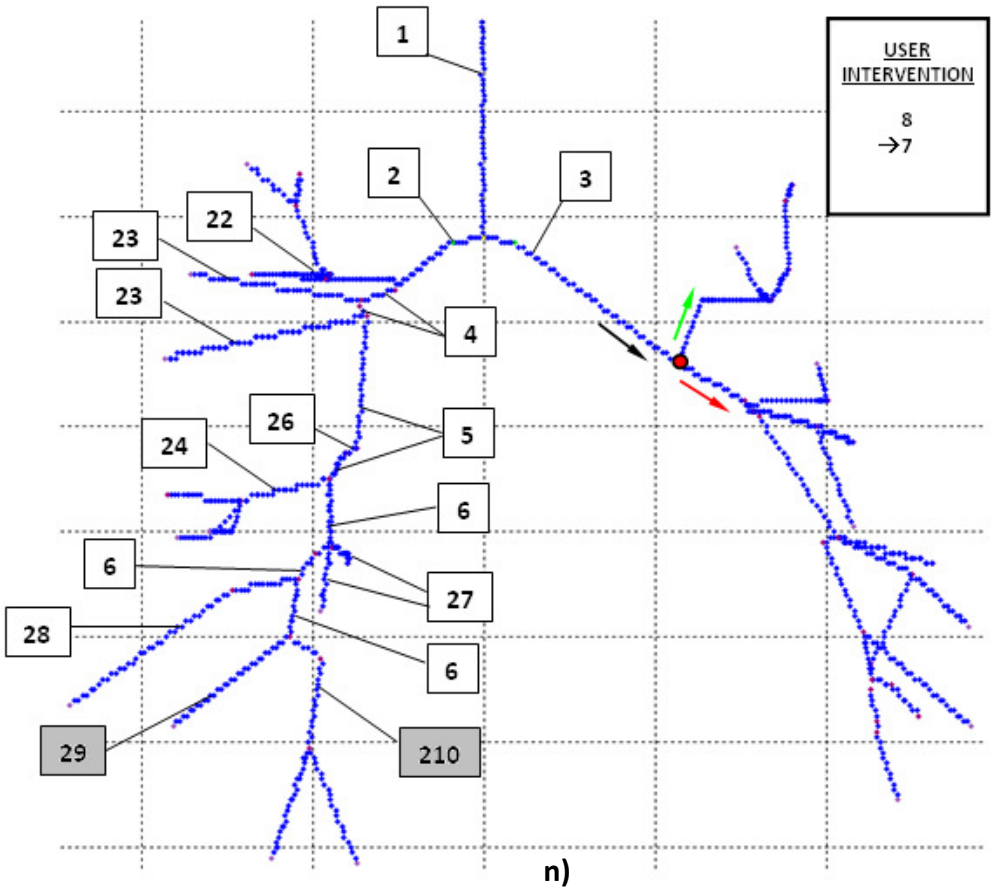
1
2
3
22
23
23
4
26
24
5
6
6
27
28
6
29
210
USER
INTERVENTION
8
→7

n)

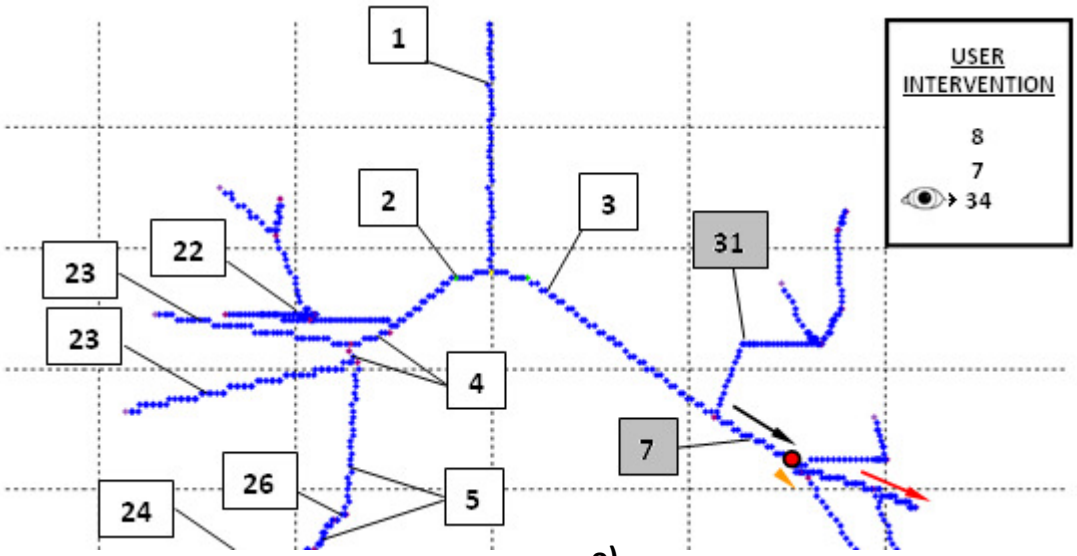
1
2
3
22
23
23
31
4
7
26
5
24
USER
INTERVENTION
8
7
34

o)

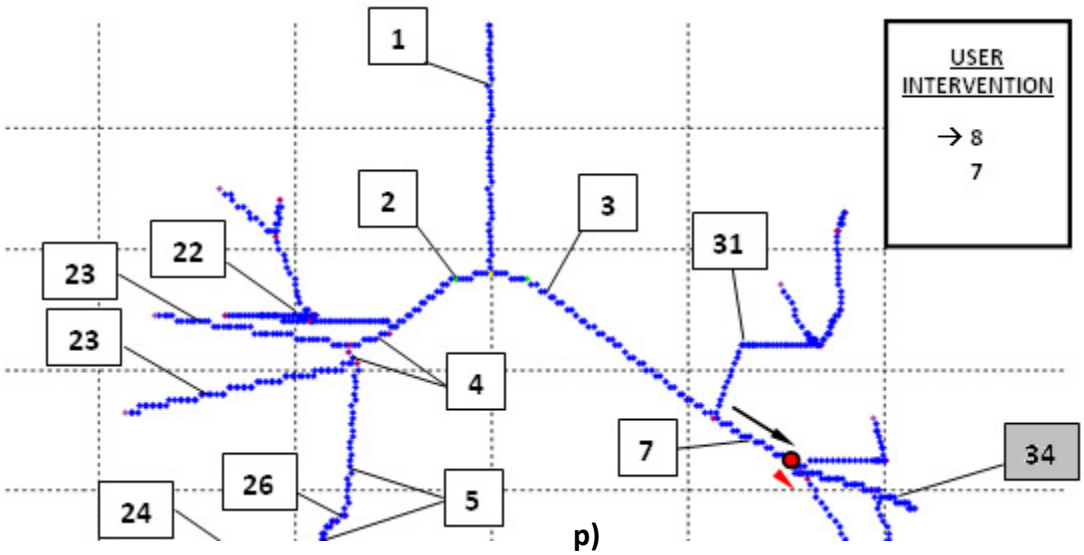
1
2
3
22
23
23
31
4
7
34
26
5
24
USER
INTERVENTION
8
7

p)

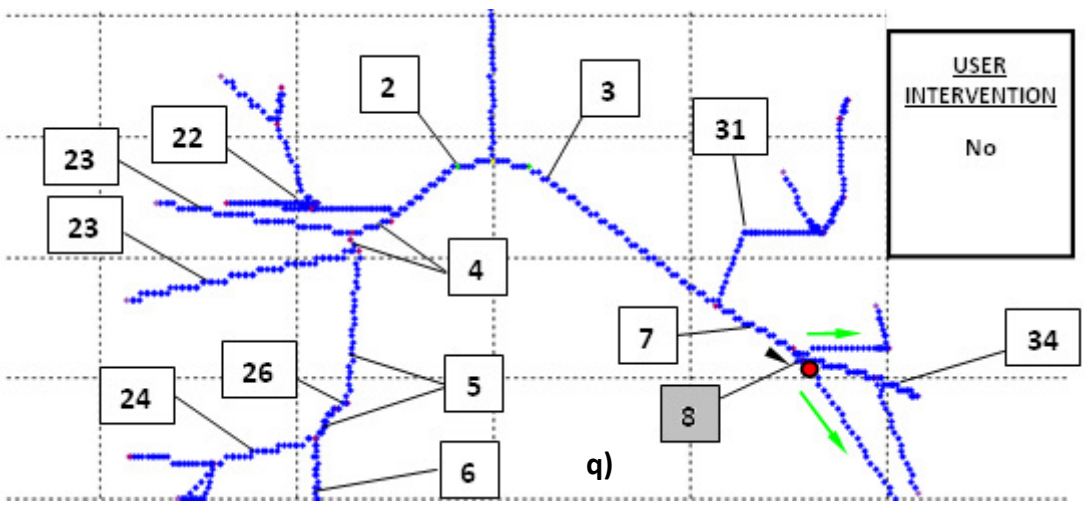
2
3
22
23
23
31
4
7
34
26
5
24
8
6
USER
INTERVENTION
No

q)

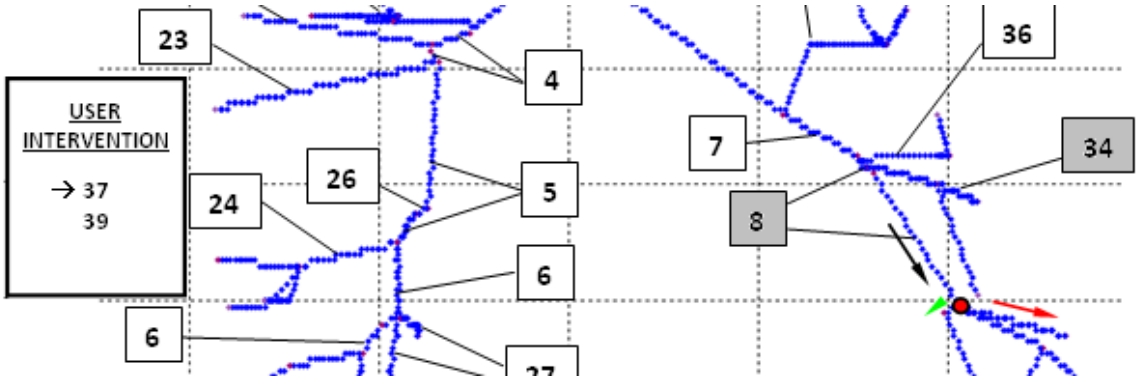
23
4
USER
INTERVENTION
→ 37
39
24
26
5
6
6
36
7
34
8

r)

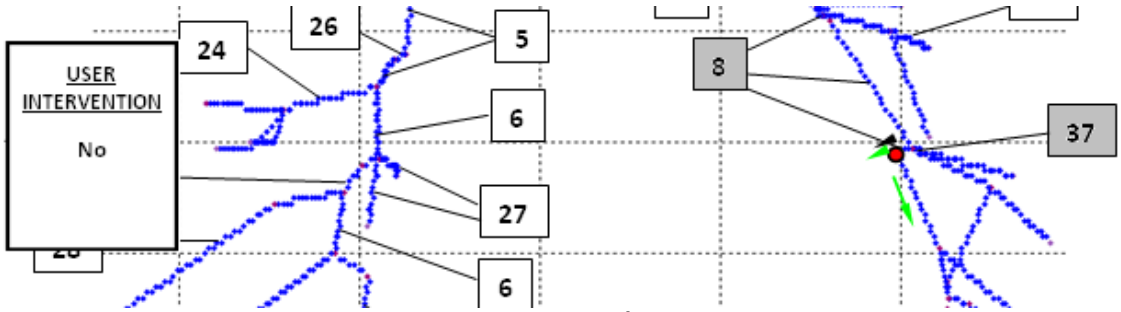
24
26
5
USER
INTERVENTION
No
6
27
6
8
37

s)

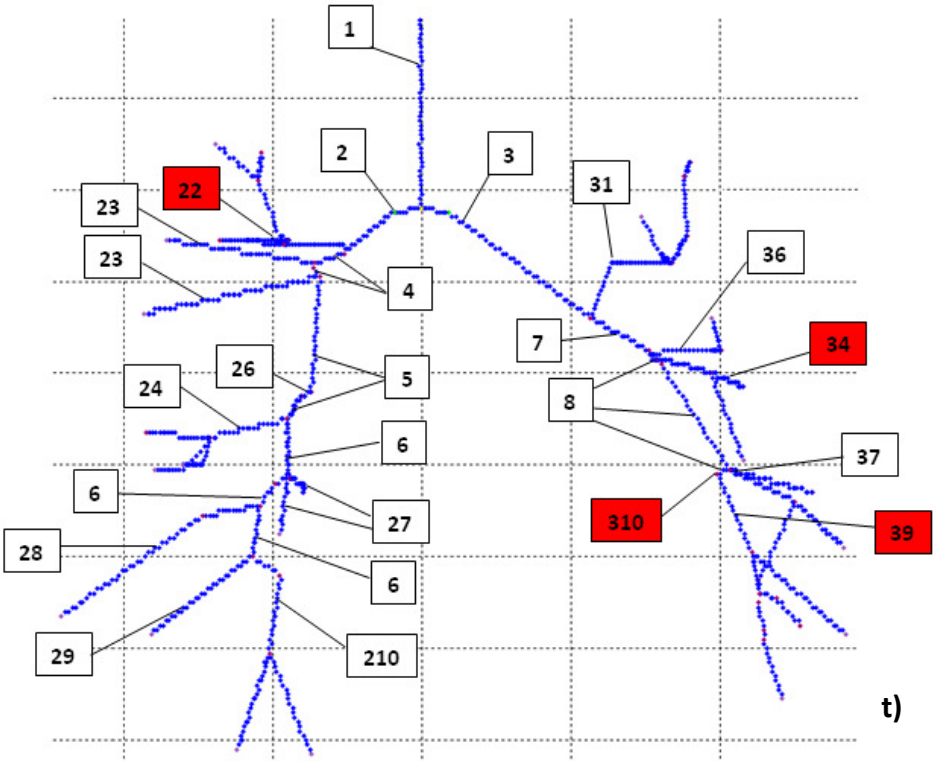

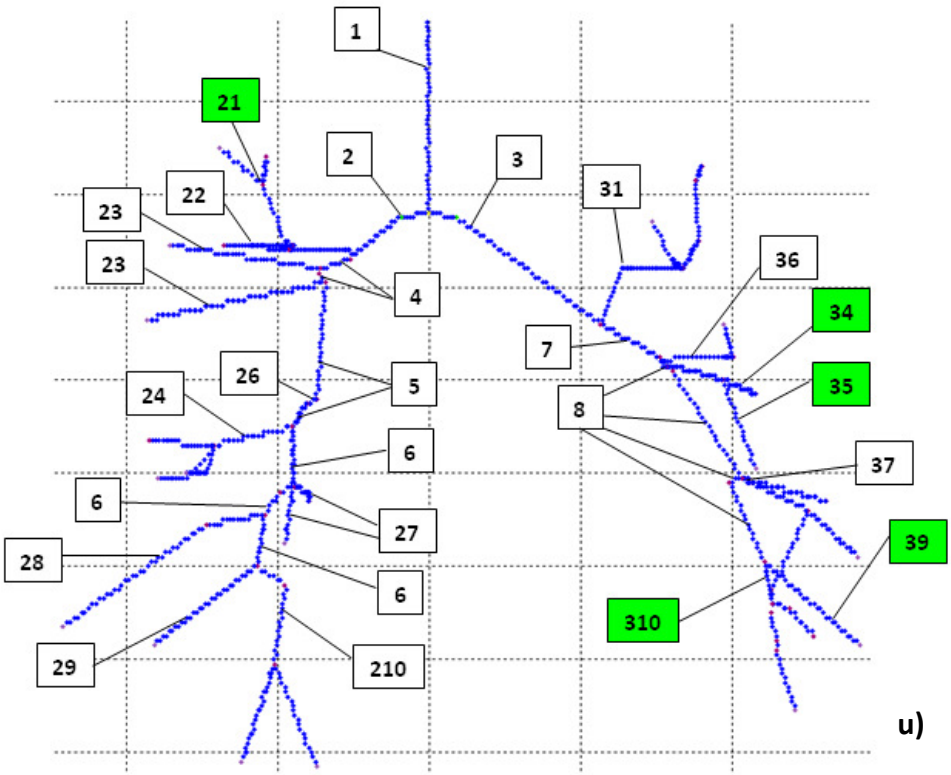

Figure 45 – Steps of a representative case of automated airways labeling. The label of the branch labelled at each step is indicated by grey rectangles. The Figure 45-t shows the airways tree totally labelled with the error indicated by red rectangles. The Figure 45-u shows the airways tree totally labelled with the corrections indicated by green rectangles. The meaning of the different coloured arrows is reported in the text

In the Figure 45-t the wrong labels are showed in red and in the Figure 45-u the corrected labels are represented in green.

The example shown in Figure 45 is representative of the mistakes that frequently occur, particularly in the apical segmental bronchus (B1) and posterior segmental bronchus (B2) segments of the right upper lobe, the lingular segments (B4, B5) of the lower lobe and the basal segments (B9, B10) of the left lower lobe. More in detail:

- ***In the right upper lobe apical segmental bronchus (B1) is labelled as posterior segmental bronchus (B2)***: as previously reported in the literature [35], about in 1 case out of 3 in the right upper lobe bronchus B2 is generated by B1. In the stick diagram this anatomical variation manifest it as a unique segment which starts from right main bronchus in sector 4. As consequence this segment is whole erroneously labelled as B1 or B2 (see Figure 45-c).
- ***In the left upper lobes inferior segmental bronchus (B5) is labelled as superior segmental bronchus (B4)***: in some cases, in the left upper lobe, inferior lingular bronchus, B5, arises from the superior lingular bronchus, B4. As consequence, in the stick diagram, the unique segment which starts from left main bronchus in sector 7, is whole erroneously labelled as B4 (see Figure 45-p).
- ***In the left lower lobe bronchus ramification lateral basal - posterior basal segmental bronchus (B9-B10) is anticipated***: the algorithm classifies a single voxel as a first ramification voxel. This happen when there is a voxel not lined up on the segment which link a couple of key point (see Figure 45-t)

3.3 – RESULTS

In Table 12 and Table 13 the results of the labeling for each subject (from S1 to S8) are reported at two different lung volume (TLC and RV). For each branch of the tracheo-bronchial tree, for right and left lung, the branches manifestations number correctly labelled on the total branches manifestations number, are showed.

The first row reports the percentage of reconstruction of the airways tree from HRCT lung images. The last five rows report:

- **Branch ok**: total number of branches manifestations correctly labelled respect to the entire branches manifestations number.
- **%ok/tot**: percent of branches manifestations correctly labelled respect to the totality of branches manifestations.
- **Br. Auto**: branches manifestations automatically named by the algorithm respect to the total branches manifestations.
- **%auto/tot**: percent of branches manifestations automatically named by the algorithm respect to the total branches manifestations.
- **%ok/auto**: percent of branches manifestations automatically recognized by the algorithm respect to the total branches manifestations.

In Table 14 the total performances are reported at TLC, RV and on the entire database. In the last column P value of the statistical analysis are summarized, to evaluate the influence of the volume on the performances.

Table 12 – The results of the labeling for each subjects at TLC volume.

TLC	S1		S2		S3		S4		S5		S6		S7		S8	
Reco. %	87,5		87,5		95,8		91,6		95,8		91,6		100		100	
	Ok	*Tot*	*Ok*	*Tot*	*Ok*	*Tot*	*Ok*	*Tot*	*Ok*	*Tot*	*Ok*	*Tot*	*Ok*	*Tot*	*Ok*	*Tot*
Trachea	1	1	1	1	1	1	1	1	1	1	1	1	1	1	1	1
RIGHT																
Main b.	1	1	1	1	1	1	1	1	1	1	1	1	1	1	1	1
Up Lobe	1	1	0	0	4	4	2	2	2	2	0	0	1	3	2	2
B1	1	1	1	1	0	1	1	1	1	1	2	2	1	1	0	1
B2	0	1	0	1	1	1	0	1	1	1	0	1	1	3	1	1
B3	2	2	0	3	3	4	1	1	1	1	0	1	0	2	2	2
Inter. b.	4	4	2	2	2	2	1	1	3	3	1	1	0	2	2	2
B6	3	3	1	1	2	2	0	0	2	2	0	0	0	1	1	1
Low Lobe	5	5	3	3	7	7	4	4	4	4	5	5	0	3	3	3
Mid. L. b.	1	1	1	2	1	1	1	1	1	1	3	3	0	1	1	1
B7	2	2	0	0	1	1	1	1	1	1	0	1	0	1	2	2
B8	1	1	0	0	2	2	0	0	2	2	1	1	0	1	1	1
B9	1	2	1	1	1	1	1	1	2	2	0	1	0	1	1	1
B10	1	1	0	1	1	1	1	1	2	2	1	1	0	1	1	1
LEFT																
Main b.	1	1	1	1	1	1	1	1	1	1	1	1	1	1	1	1
Up Lobe	0	0	1	1	1	1	1	1	2	2	3	3	2	2	1	1
Sup div. b.	1	1	1	1	1	1	1	1	1	1	1	1	1	1	1	1
B4	0	0	1	1	0	0	1	1	1	1	1	1	3	3	1	1
B5	0	0	1	1	1	1	0	1	1	1	0	1	1	1	0	1
Low Lobe	2	2	3	3	6	6	4	4	5	5	2	2	2	2	3	4
B6	1	1	1	1	2	2	2	2	2	2	1	1	2	2	1	1
B7	1	1	1	1	2	2	1	1	0	0	1	1	0	1	2	2
B9	1	2	1	1	2	2	0	1	2	2	1	1	0	3	1	1
B10	1	1	1	1	1	2	0	1	1	1	1	1	1	1	0	1
TOT																
Branch ok	32	35	41	43	44	47	26	30	40	40	27	32	18	39	30	34
%ok/tot	91,4		95,3		93,6		86,6		100		84,4		46,2		88,2	
Br. auto	21	35	25	43	29	47	20	30	18	40	14	32	31	39	25	34
%auto/tot	60		58,1		61,7		66,7		45		43,7		79,5		73,5	
%ok/aut	85,7		92		89,7		80		100		64,3		32,3		84	

Table 13 – The results of the labeling for each subjects at RV volume.

RV	S1		S2		S3		S4		S5		S6		S7		S8	
Reco. %	83,3		70,8		79,2		87,5		79,2		70,8		83,3		87,5	
	Ok	*Tot*	*Ok*	*Tot*	*Ok*	*Tot*	*Ok*	*Tot*	*Ok*	*Tot*	*Ok*	*Tot*	*Ok*	*Tot*	*Ok*	*Tot*
Trachea	1	1	1	1	1	1	1	1	1	1	1	1	1	1	1	1
RIGHT																
Main b.	1	1	1	1	1	1	1	1	1	1	1	1	1	1	1	1
Up Lobe	1	1	2	2	2	2	1	1	2	2	1	1	2	2	0	4
B1	1	1	1	1	1	1	0	0	1	1	1	1	0	1	1	1
B2	0	1	1	1	1	2	1	1	1	1	0	0	0	1	0	2
B3	1	1	1	1	1	1	1	1	1	1	1	1	1	1	0	3
Inter. b.	3	3	2	2	2	2	2	2	1	1	3	3	2	2	0	2
B6	2	2	1	1	1	1	1	1	0	0	1	1	2	3	0	1
Low Lobe	0	2	1	1	2	2	1	1	1	3	1	1	3	3	0	4
Mid. L. b.	3	3	1	1	1	1	1	1	1	1	1	3	1	1	0	1
B7	0	1	0	0	1	1	1	1	0	1	0	0	1	1	0	1
B8	0	1	0	0	2	2	0	0	0	1	0	0	1	1	0	1
B9	0	1	1	1	0	0	1	1	0	0	0	0	0	0	0	1
B10	0	0	1	1	0	1	1	1	0	0	0	0	0	0	0	1
LEFT																
Main b.	1	1	1	1	1	1	1	1	1	1	1	1	1	1	1	1
Up Lobe	0	0	0	0	0	0	2	2	1	1	1	1	1	1	0	0
Sup div. b.	1	1	1	1	1	1	1	1	1	1	1	1	1	1	1	1
B4	0	0	0	0	0	0	1	1	0	0	1	1	0	1	0	0
B5	0	0	0	0	0	0	1	1	1	1	0	0	0	0	0	0
Low Lobe	3	3	3	3	2	2	2	2	3	3	3	3	3	3	4	4
B6	1	1	1	1	1	1	0	0	1	1	2	2	1	1	2	2
B7	1	1	1	1	0	1	1	1	1	1	0	0	0	0	2	2
B9	1	1	0	0	1	1	1	1	0	0	1	1	1	1	1	1
B10	1	1	0	0	0	1	1	1	0	1	1	1	1	1	1	1
TOT																
Branch ok	22	28	20	20	21	25	24	24	18	23	21	23	24	28	15	36
ok/tot%	78,6		100		84		100		78,3		91,3		85,7		41,7	
Br. auto	20	28	10		13	25	10	24	15	23	15	23	12	28	29	36
auto/tot%	71,4		50		52		41,7		65,2		65,2		42,9		80,6	
ok/auto%	70		100		69,2		100		66,7		86,7		66,7		27,6	

Table 14 – The total results of the labeling at TLC, RV and on the entire database. In the last column P values of the statistical analysis are summarized to evaluate the influence of the volume.

TOT	TLC	RV	TOT	P value
ok/tot%	84,2	79,7	82,3	0,442
auto/tot%	61,8	59,9	61	0,724
ok/auto%	74,4	66,1	71	0,721

The results in Table 12 and 13 show that the total percent of branches recognized at TLC is 84,2 % and at RV is 79,7 %. There is not a significant influence of the lung volume on the total percent of branch recognized (P= 0,442). The percent of the automatism of the software at TLC is 61,8 % and at RV is 59,9 % (P= 0,724). The total percent of branches automatically recognized by the software at TLC is 74,4 % and at RV is 66,1 % (P= 0,721).

In the Table 15, Table 16 and Table 17 the algorithm performances on the airways tree are showed zone by zone. In this paragraph, the results of the labeling, with the number of branch manifestation automatically labelled by the algorithm, are presented for each branch of the tracheo-bronchial tree, for right and left lung, at TLC (Table 15), at RV (Table 16) and on the entire database (Table 17).

The first two columns in the tables show the total manifestation number of the branch, indicated in the first column, rightly labelled (OK) and the total manifestation number (TOT). In the third column (AUTO) the total manifestation number of the branch automatically labelled by the algorithm is reported.

Table 15 – The results of the labeling with the branch manifestation number automatically labelled by the algorithm at TLC volume.

TLC	OK	TOT	AUTO	%OK/TOT	%AUTO/TOT	%OK/AUTO
Trachea	8	8	8	100	100	100
RIGHT						
Main b.	8	8	8	100	100	100
Up Lobe	12	14	13	85,7	92,9	84,6
B1	7	9	9	77,8	100	77,8
B2	4	10	10	40	100	40
B3	9	15	14	60	93,3	57,1
Inter. b.	16	17	13	94,1	76,5	92,3
B6	9	10	10	90	100	90
Low Lobe	31	34	22	91,2	64,7	86,4
Mid. L. b.	10	11	2	90,9	18,2	50
B7	8	9	5	88,9	55,6	80
B8	7	8	3	87,5	37,5	66,7
B9	7	10	5	70	50	40
B10	7	9	4	77,8	44,4	50
TOT	**135**	**164**	**118**	**82,3**	**72,0**	**75,4**
LEFT						
Main b.	8	8	8	100	100	100
Up Lobe	11	11	1	100	9,1	100
Sup div. b.	8	8	5	100	62,5	100
B4	8	8	1	100	12,5	100
B5	4	7	3	57,1	42,9	0
Low Lobe	27	28	15	96,4	53,6	93,3
B6	12	12	6	100	50	100
B7	8	9	2	88,9	22,2	50
B9	8	13	10	61,5	76,9	50
B10	6	9	6	66,7	66,7	50
TOT	**100**	**113**	**57**	**88,5**	**50,4**	**77,2**

Table 16 – The results of the labeling with the branch manifestation number automatically labelled by the algorithm at RV volume.

RV	OK	TOT	AUTO	%OK/TOT	%AUTO/TOT	%OK/AUTO
Trachea	8	8	8	100	100	100
RIGHT						
Main b.	8	8	8	100	100	100
Up Lobe	11	15	13	73,3	86,7	69,2
B1	6	7	7	85,7	100	85,7
B2	4	9	9	44,4	100	44,4
B3	7	10	10	70	100	70
Inter. b.	15	17	10	88,2	58,8	80
B6	8	10	7	80	70	71,4
Low Lobe	9	17	11	52,9	52,9	11,1
Mid. L. b.	9	12	3	75	25	0
B7	3	6	3	50	50	0
B8	3	6	4	50	66,7	25
B9	2	4	2	50	50	0
B10	2	4	3	50	75	33,3
TOT	**87**	**125**	**90**	**69,6**	**72,0**	**57,8**
LEFT						
Main b.	8	8	8	100	100	100
Up Lobe	5	5	0	100	0	0
Sup div. b.	8	8	4	100	50	100
B4	2	3	1	66,7	33,3	0
B5	2	2	0	100	0	0
Low Lobe	23	23	10	100	43,5	100
B6	9	9	3	100	33,3	100
B7	6	7	1	85,7	14,3	0
B9	6	6	2	100	33,3	100
B10	5	7	5	71,4	71,4	60
TOT	**74**	**78**	**34**	**94,9**	**43,6**	**88,2**

Table 17 – The results of the labeling with the branch manifestation number automatically labelled by the algorithm on the entire database.

TLC + RV	OK	TOT	AUTO	%OK/TOT	%AUTO/TOT	%OK/AUTO
Trachea	16	16	16	100	100	100
RIGHT						
Main b.	16	16	16	100	100	100
Up Lobe	23	29	26	79,3	89,7	76,9
B1	13	16	16	81,3	100	81,3
B2	8	19	19	42,1	100	42,1
B3	16	25	24	64	96	62,5
Inter. b.	31	34	23	91,2	67,6	87
B6	17	20	17	85	85	82,4
Low Lobe	40	51	31	78,4	60,8	64,5
Mid. L. b.	19	23	5	82,6	21,7	20
B7	11	15	8	73,3	53,3	50
B8	10	14	7	71,4	50	42,9
B9	9	14	7	64,3	50	28,6
B10	9	13	7	69,2	53,8	42,9
TOT	**222**	**289**	**206**	**76,8**	**71,3**	**67,5**
LEFT						
Main b.	16	16	16	100	100	100
Up Lobe	16	16	1	100	6,3	100
Sup div. b.	16	16	9	100	56,3	100
B4	10	11	2	90,9	18,2	50
B5	6	9	3	66,7	33,3	0
Low Lobe	50	51	25	98	49	96
B6	21	21	9	100	42,9	100
B7	14	16	3	87,5	18,8	33,3
B9	14	19	12	73,7	63,2	58,3
B10	11	16	11	68,8	68,8	54,5
TOT	**174**	**191**	**91**	**91,1**	**47,6**	**81,3**

When the percent of manifestation number of each branch correctly labelled for right lung is considered there is a significant influence of the lung volume (P=0.013). There is not a statistically significant influence (P = 0,456) for left lung.

The results of the Table 17 (entire database) are then reported in bars graphs to better highlight the algorithm performances for each branch of the tracheo-bronchial tree. The Figure 46-a and the Figure 46-b show respectively performances on the right and left part of the tree. In particular performances are showed as groups of three columns that represent %OK/TOT, %AUTO/TOT and %OK/AUTO for each branch. The last two groups report the total software performances on the right or left part of the tree (TOT R and TOT L) and on the entire tree (TOT).

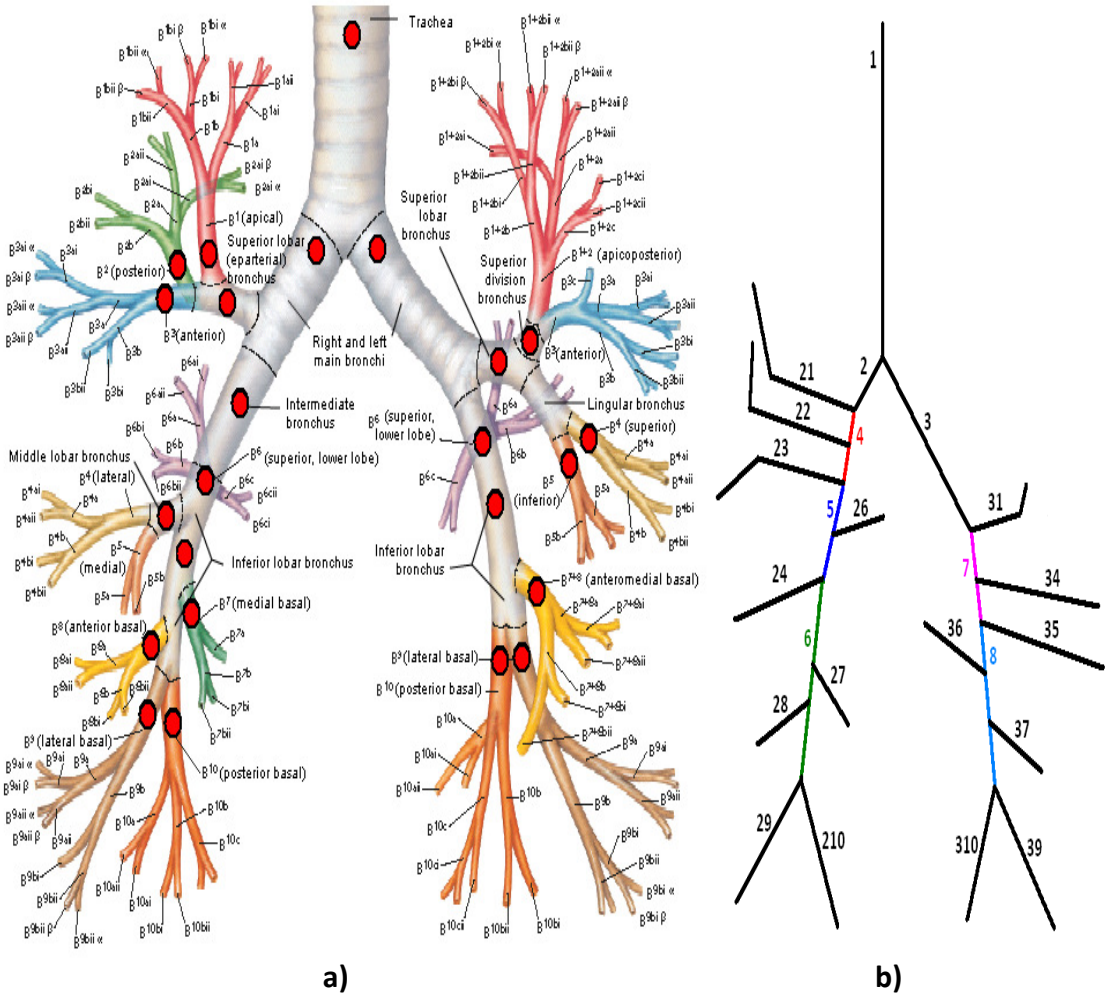

Figure 46 – The airways tree extracted from Netter Atlas of Anatomy [45] (46-a). The red spots indicate branches to label. In Figure 46-b the complete stick diagram extracted from the human tracheo-bronchial tree.

The Figure 46 is reported to help in the reading of the observations on the algorithm performances, extracted from statistical and graph analysis of the labeling results zone by zone.

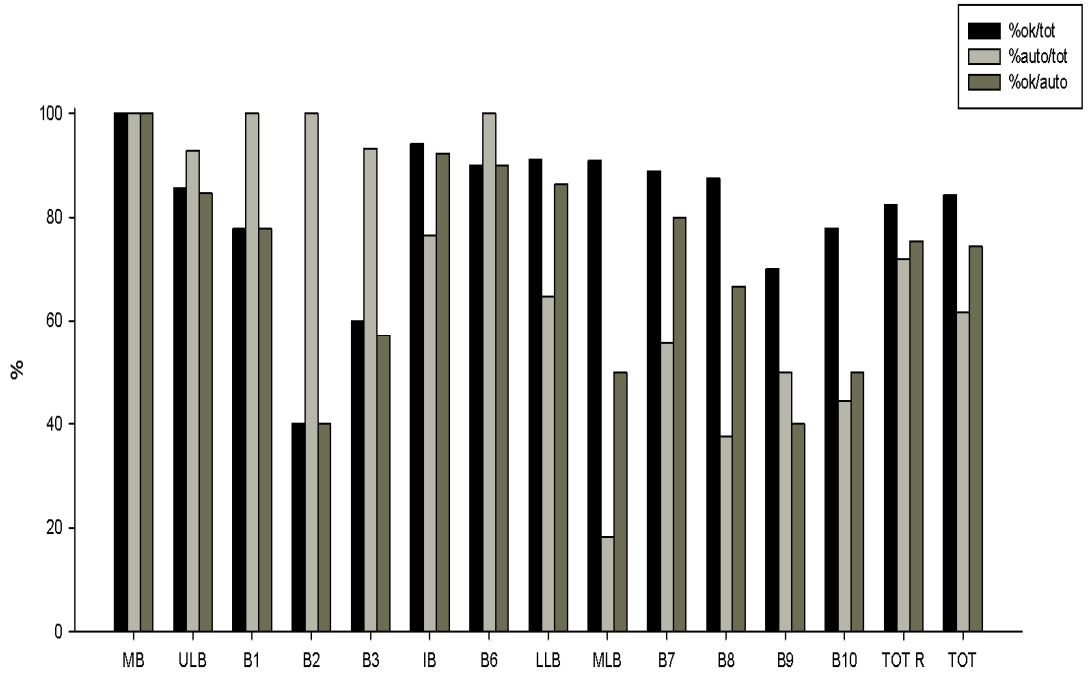

a)

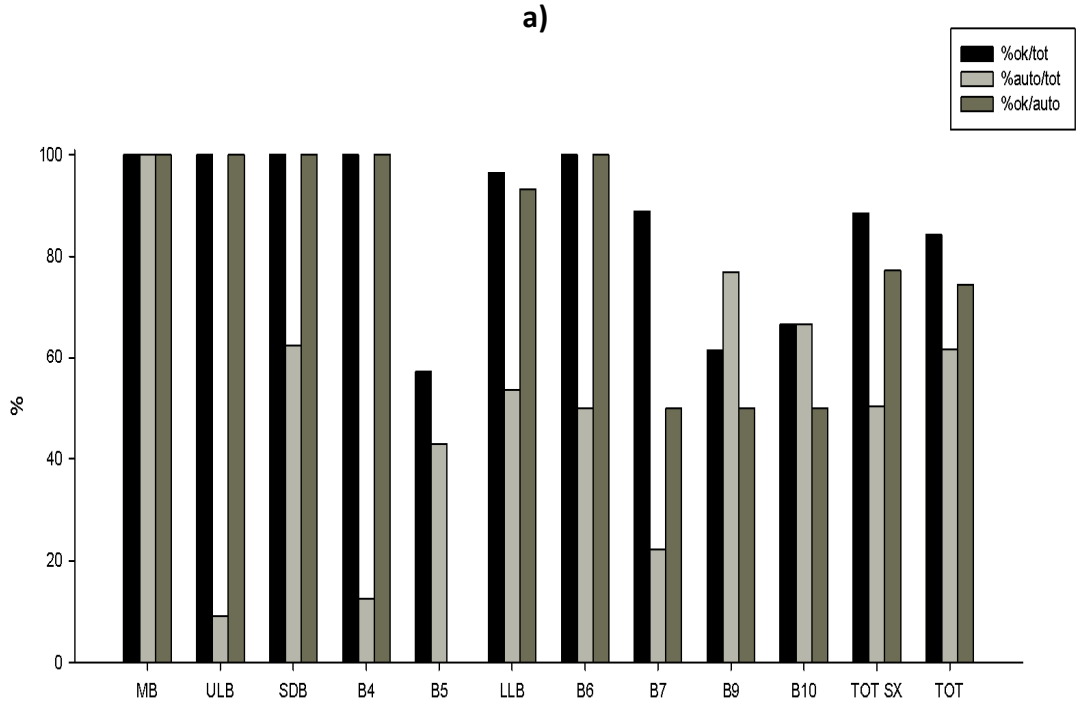

b)

Figure 47 – Bars graphs that represent the algorithm performances for each branch of the tracheo-bronchial tree. The Figure 47-a and the Figure 47-b show respectively performances on the right and left lung.

Next is showed where, for the right part of the airways tree, the algorithm gives the best performances in term of:

- **Total percent of branches recognized**: for main bronchus, intermediate bronchus, superior lower lobe (B6) and middle lobe bronchus, this performance is up to 80%. The starting directions of this group of branches are characteristic and it is simple recognize them. The generation zone of this four branches is in the right upper lobe where there is a clear separation between the segments of the stick diagram.
- **Percent of the automatism of the software**: for main bronchus, upper lobe bronchus, apical, posterior, anterior segmental bronchus (B1,B2,B3) and superior lower lobe (B6), this performance is up to 80%. Generation points of this group of branch are in the right upper lobe. The autonomy of the software in this zone is high because there is a clear separation between the segments of the stick diagram. A few number of branches starts from the sectors interested 1,2,4,5 (see the Figure 46-b) for this reason for the software is simple to proceed in autonomy in the branch directions discrimination.
- **Total percent of branches automatically recognized by the software:** for main bronchus, upper lobe bronchus, apical segmental bronchus (B1), intermediate bronchus and superior lower lobe (B6), this performance is up or near to 80%. Generation points of this group of branches are in the right upper lobe. The algorithm works good in autonomy where the stick diagram is clean. This group of branches are not interested by inter-individual anatomical variability of branches generation points.

Next is showed where, for the left part of the airways tree, the algorithm gives the best performances in term of:

- **Total percent of branches recognized**: for main bronchus, upper lobe bronchus, superior division bronchus (B1+2), lower lobe bronchus and superior lower lobe (B6) this performance is up or near to 90%. Generation points of this group of branches are in the left upper lobe where the distance between the stick diagram segments is bigger than the left lower lobe.
- **Percent of the automatism of the software**: except for main bronchus this performance in under to 70%. This is due to the software inability to recognize automatically, and real time, the end of the left upper lobe sector 4 (see paragraph 2.2.6 – upper lobe limits).
- **Total percent of branches automatically recognized by the software:** for main bronchus, upper lobe bronchus, superior division bronchus (B1+2), lower lobe bronchus and superior lower lobe (B6) this performance is near or equal to 100%. Algorithm recognize independently these zones few times but labeling them with the correct label.

In terms of ***percent of automatic labeling on the entire database (TLC and RV)*** there is a big difference between the right and the left lung: **71,3 % for the right and 47,6 % for the left**. This difference is due to the software inability to recognize automatically, and real time, the end of the left upper lobe sector (see paragraph 2.2.6 – upper lobe limits).

The airways tree zones of the right lung, where the software have the worst performances, are next reported:

- **Posterior and anterior segmental bronchus (B2 and B3):** %OK/TOT (under 65%). The problem is the inter-individual anatomical variability of branches generation points in the right upper lobe [35]. The most common errors are B2 or B3 named as B1, or B2 named as B3 and vice versa.
- **Medial basal, anterior basal, lateral basal, posterior basal segmental bronchus (B7, B8, B9, B10)**: %OK/TOT is under 75%. %AUTO/TOT and %OK/AUTO is under 55%. For the right lower lobe the segmentation is less accurate than the right upper lobe. The branches are few distinguishable and there are 5 branches to distinguish and label (see Figure 46).
- **Middle Lobe Bronchus**: the worst performance in term of %AUTO/TOT and %OK/AUTO. It is the first branch that the algorithm analyzes during the right lower lobe bronchus labeling. Its orientation is very similar to that of B8 and B9.
- **Lower Lobe Bronchus**: %AUTO/TOT and %OK/AUTO under 65%. The segmentation here is less accurate than for upper sectors. The orientation respect to the target branch with the same label is very variable.

The airways tree zones of the left lung, where the software have the worst performances, are next reported:

- **Superior and inferior segmental bronchus (B4 and B5)**: B5 has the worst %OK/TOT, %AUTO/TOT is under 35% and %OK/AUTO is 0%. %AUTO/TOT and %OK/AUTO for the superior lingular bronchus B4 are respectively 18,2% and 50%. The problem is the inter-individual anatomical variability of branches generation points in the lingular bronchus. The most common errors is B5 named as B4 and vice versa.
- **Antero-medial basal, lateral basal, posterior basal segmental bronchus (B7+8, B9, B10):** for B7 %AUTO/TOT is under 20%. This is the first branch that the algorithm analyzes during the left lower lobe bronchus labeling. Its orientation is very similar to that of B9.

  For B7, B9, B10 %OK/AUTO is under 60%. In this left lower lobe the segmentation is less accurate and so it is difficult to distinguish the branches. Respect to the right lower lobe here are generated only 3 branches and %OK/AUTO is in fact 5% point greater.
- **Upper Lobe:** %AUTO/TOT is equal to 6,3%. The problem is the software inability to recognize automatically and real time the end of the left upper lobe sector.

The Figure 48, Figure 49 and Figure 50 show the comparison between the software performances on the branches of the airways tree at TLC and RV volume. It is possible to observe if there are airways tree zones more influenced by the volume.

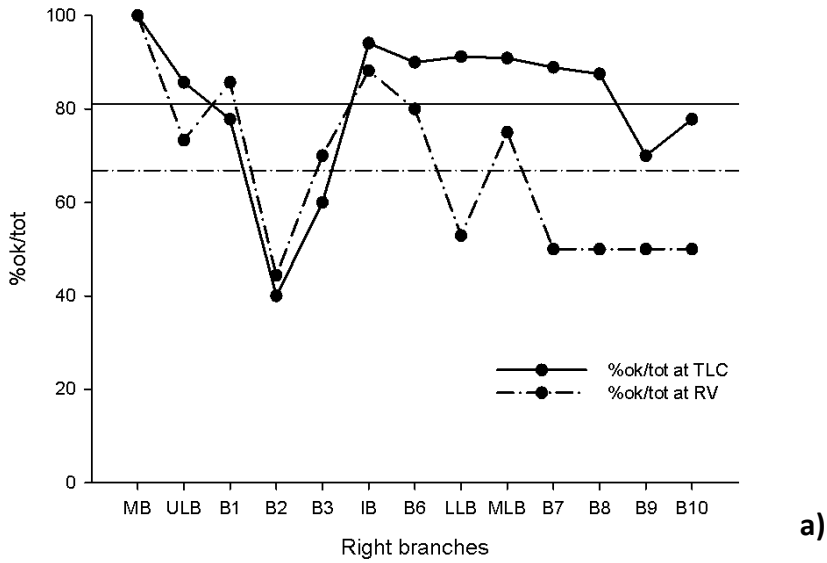

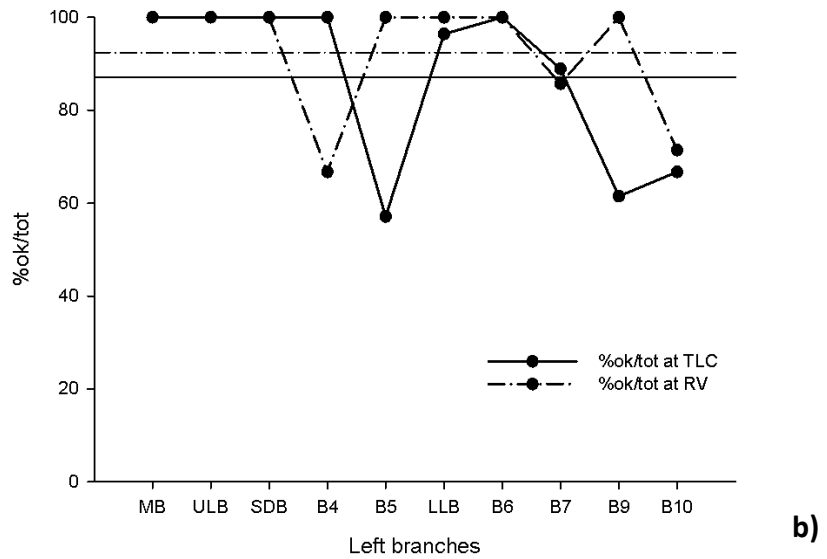

Figure 48 – Comparison between the total percent of branch recognized on the airways tree zone by zone at TLC and RV volume. In the Figure 48-a there are the branches of right lung and in the Figure 48-b there are the branches of left lung. The horizontal lines represent the mean value of the performance analyzed.

There is not a significant influence of the lung volume on the total percent of branch recognized for the right upper lobe (P=0.944). The performance analyzed is influenced by the volume in the right lower lobe (P=0.005). For the left lung there is not a variation due to the volume (P=0.476).

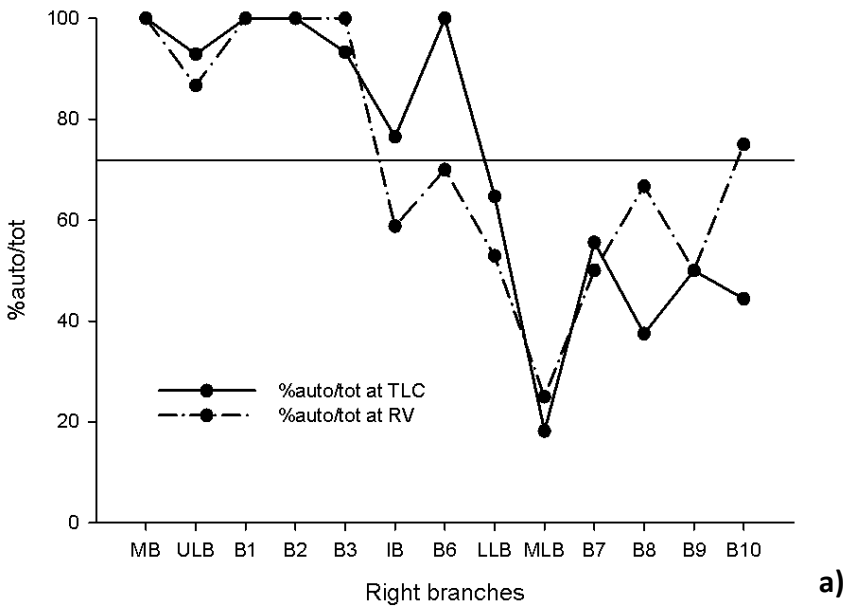

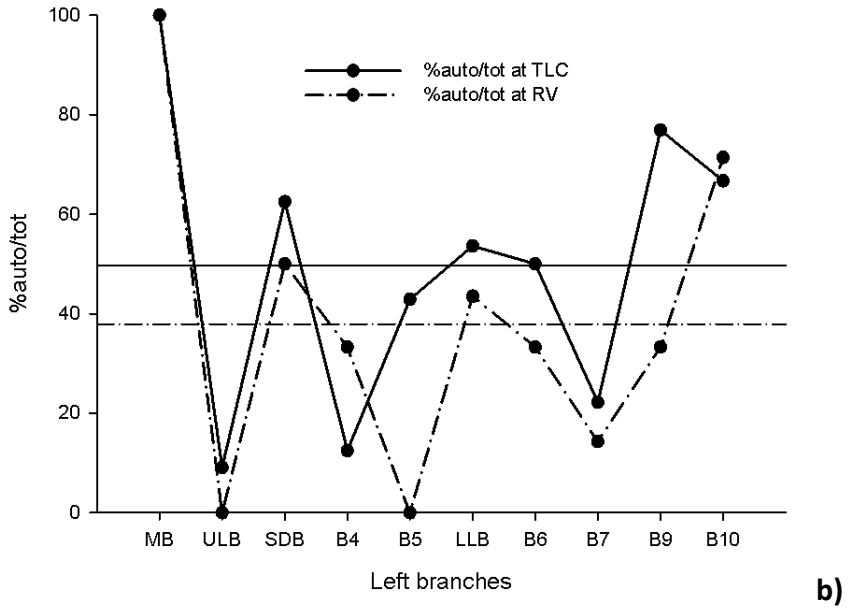

Figure 49 – Comparison between the percent of the automatism of the software on the airways tree zone by zone at TLC and RV volume. In the Figure 49-a there are the branches of right lung and in the Figure 49-b there are the branches of left lung. The horizontal lines represent the mean value of the performance analyzed.

The scatter line that represent the percent of the automatism of the software in the right and left lung at TLC, traces with good approximation the scatter line for the same performance on the same zones at RV (P=0.993 for the right lung, P=0.419 for the left lung).

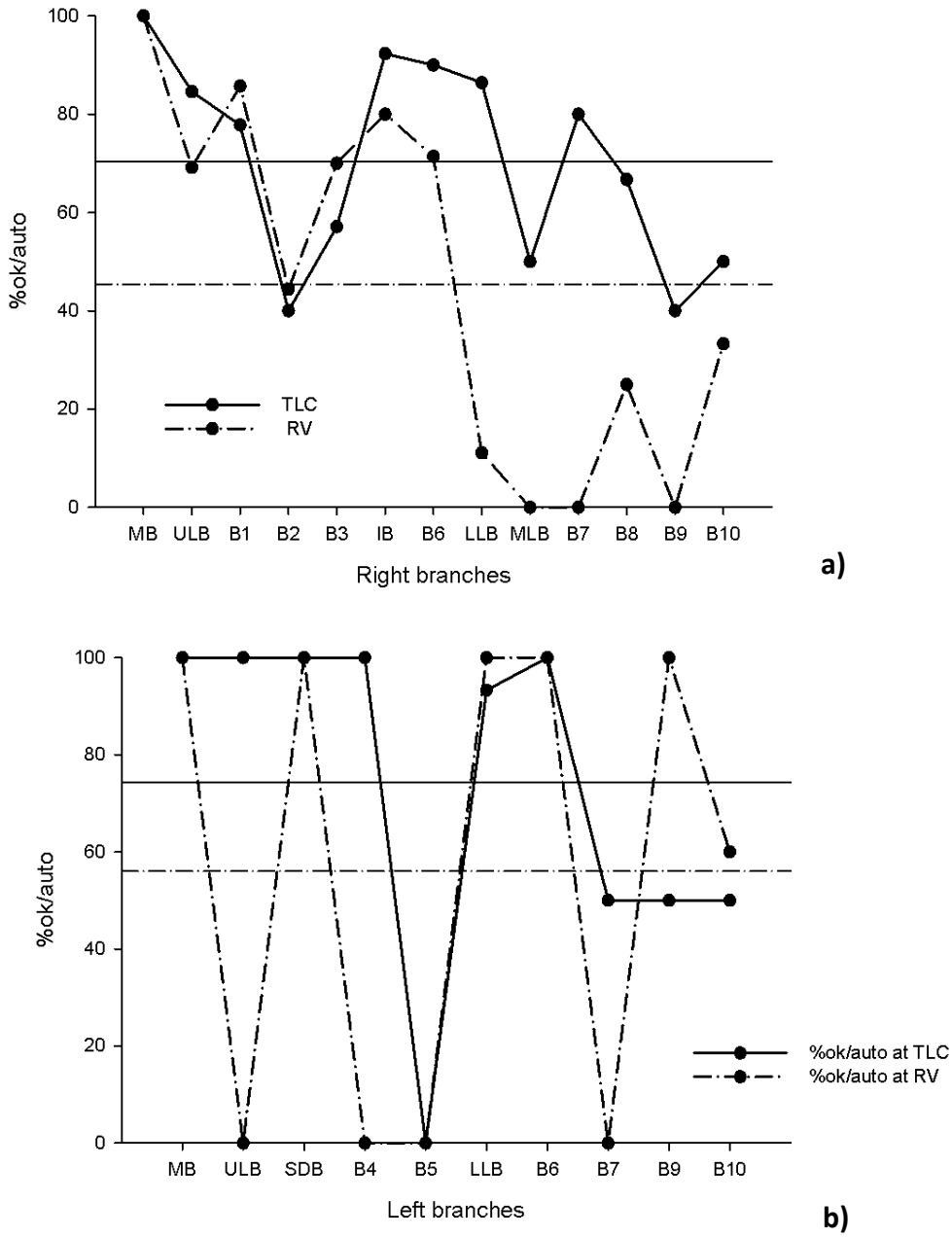

Figure 50 – Comparison between the total percent of branches automatically recognized by the software on the airways tree zone by zone at TLC and RV volume. In the Figure 50-a there are the branches of right lung and in the Figure 50-b there are the branches of left lung. The horizontal lines represent the mean value of the performance analyzed.

The total percent of branches automatically recognized by the software in the right lower lobe is influenced in a significant way by the volume ($P<0.001$). In the right upper lobe the same performance does not suffer from the volume influence ($P=0.974$). In the left lung there are not zone where, the performance analyzed, is particularly influenced by the volume ($P=0.360$).

All the performances analyzed in the left lung are not influenced in a significant way by the volume. This is due to the low autonomy of the software in this part. For the right lung the situation is different: the total percent of branch recognized and the total percent of branches automatically recognized, for the right lower lobe, are influenced by the volume. In the lower right lobe the segmentation is less accurate and so it is difficult to distinguish the branches: there is not a clear separation between the segments of the stick diagram.

Conclusions and future development

The aim of this thesis was to develop a new method for an automatic labelling and anatomical nomenclature of the tracheo-bronchial tree, from multi-detector CT 3D images of the lung.

Among all the human anatomical structures, the airway tree is a case particularly challenging, because of its hierarchical properties and the considerable variations of branching pattern.

The innovativeness of the method here proposed, and developed, is constituted by the way adopted to extract information from the segmented airways, which is different from the more traditional algorithms based on skeletonization. Through the linking of key points, extracted from the tracheo-bronchial tree, it is possible to obtain a guide to be overlapped to the original segmented airways tree. This guide is called "*stick diagram*" and it is useful to help the labeling of the branches up to the segmental bronchus.

This kind of approach introduces less artefacts than a classical skeletonization algorithm, such as those proposed by Kitaoka [16] and Tschirren [36], which use a method based on an association graph, or those proposed by Mori [39] and Ota [40], which are based on machine learning and combination optimization.

In our method, the labeling of the stick diagram is performed using information of relative orientation between a known target branch and an unknown branch to label.

Topologic information, from the airways anatomy, based on the presence of a particular branch respect to the other are used only when this particular branch has really been found on the stick diagram. In this way the lack of branches, due to a poor segmentation, does not heavily influence the labelling process.

The implemented method was applied on a set of CT images of eight healthy subjects, taken at two different lung volumes. The obtained results were highly positive. In fact, considering the overall data, the algorithm recognized 405 branch manifestation on 492 with a success percentage equal to 82,3%. The branches manifestation automatically labelled were 300 (61% of the total) with a percentage of success equal to 71%. The total percent of branches recognized at TLC is 84,2% and at RV was 79,7%. There was not a significant influence of the lung volume on the total percent of branch recognized (P= 0.442). The percent of the automatism of the software at TLC was 61,8% and at RV was 59,9% (P= 0.724). The total percent of branches automatically recognized by the software at TLC was 74,4% and at RV was 66,1% (P= 0.721). When, the percent of manifestation number of each branch correctly labelled for right lung was considered, there was a significant influence of the lung volume (P=0.013). There was not a statistically significant influence (P = 0,456) for left lung. In terms of percent of automatic labelling on the entire database (TLC and RV) there was a big difference between the right and the left airways tree: 71,3% for the right and 47,6% for the left. The total percent of branches recognized and the total percent of branches automatically recognized for the right lower lobes were influenced by the lung volume. No influence of the lung volume on the performance of the algorithm for the left lung.

At the conclusion of our work, we can affirm that the principal sources of error, that influence the algorithm performances, in its actual form, are due to the inter-individual anatomical variability of branches generation points in the right upper lobe and in the lingular bronchus, the major anatomical complexity of the airways tree in the lower lobes, so that the labeling in the lower lobes cannot be accurate as for the upper lobes and the software inability to recognize automatically, and real time, the end of the left upper lobe sector.

Therefore, future developments will be important in order to improve the algorithm performances in these critical airways tree zones and, a compromise between computational costs and the comprehension of the reconstructed stick diagram, will be necessary.

An increase of the database, moreover, should be very useful to improve the statistical power of the study.

Finally, topologic rules on ramification with more than two branches, can be introduced to reduce the number of label candidates for the user interventions and, consequently, to improve the automatism of the software.

The application fields of the present work are numerous and include virtual bronchoscopy and bronchoscopic navigation systems, with clinical applications such as pulmonary path-finding of peripheral lung lesions, mediastinal biopsies, and surgical planning of increasingly important procedures for the treatment of emphysema, such as endo-bronchial valves and airway bypass.

Appendix 1
The algorithm flow charts

In this appendix the software flow charts are showed. The flow charts are sorted following a top-down logic: from the main frame to each single functions. Near the functions visible in a main program there is the page number of the correspondent flow chart.

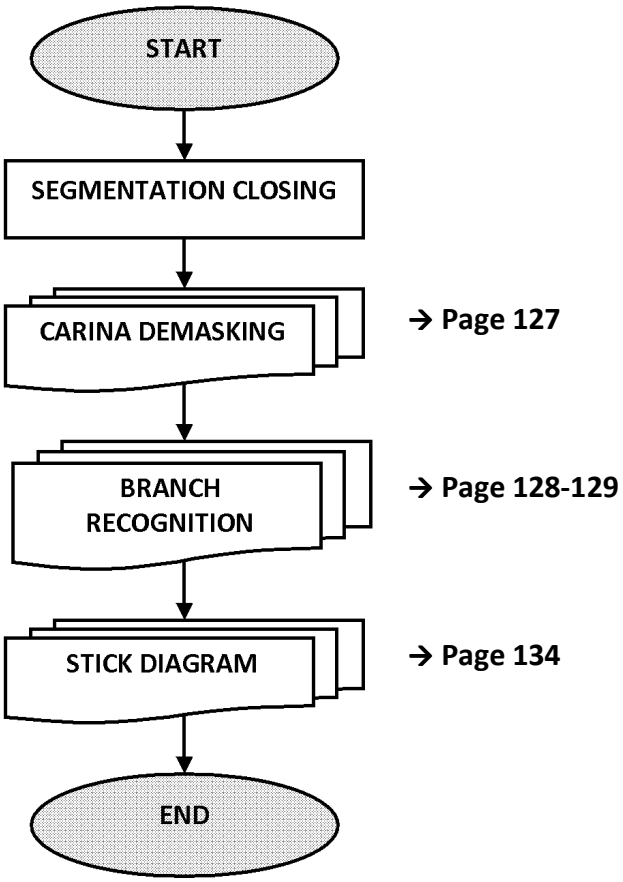

Figure 51 – Linking algorithm flow chart. The output of the linking algorithm is the stick diagram

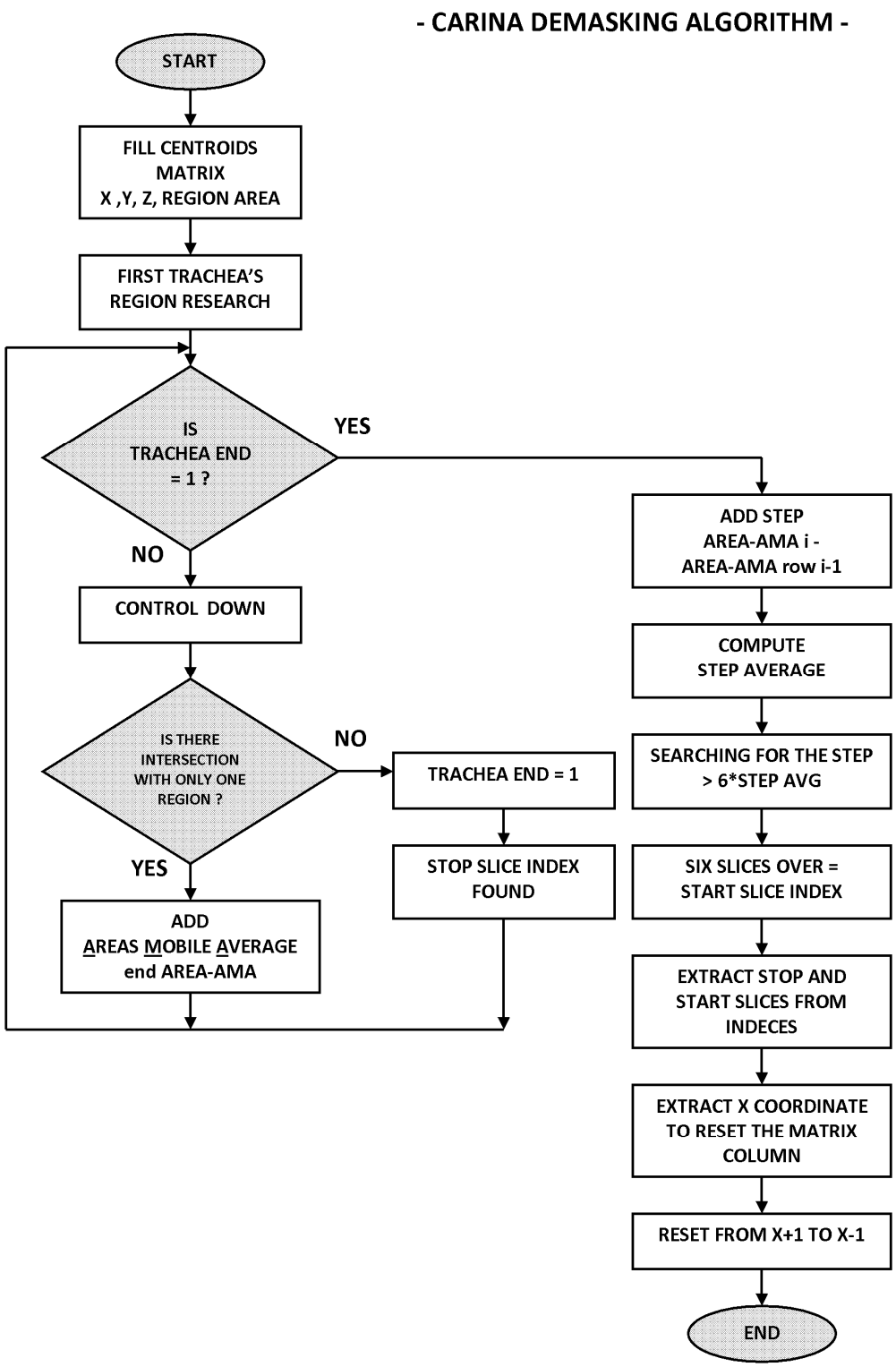

Figure 52 – Carina de-masking algorithm flow chart. The output of the Carina de-masking algorithm is the airways tree segmentation with the correct carina position.

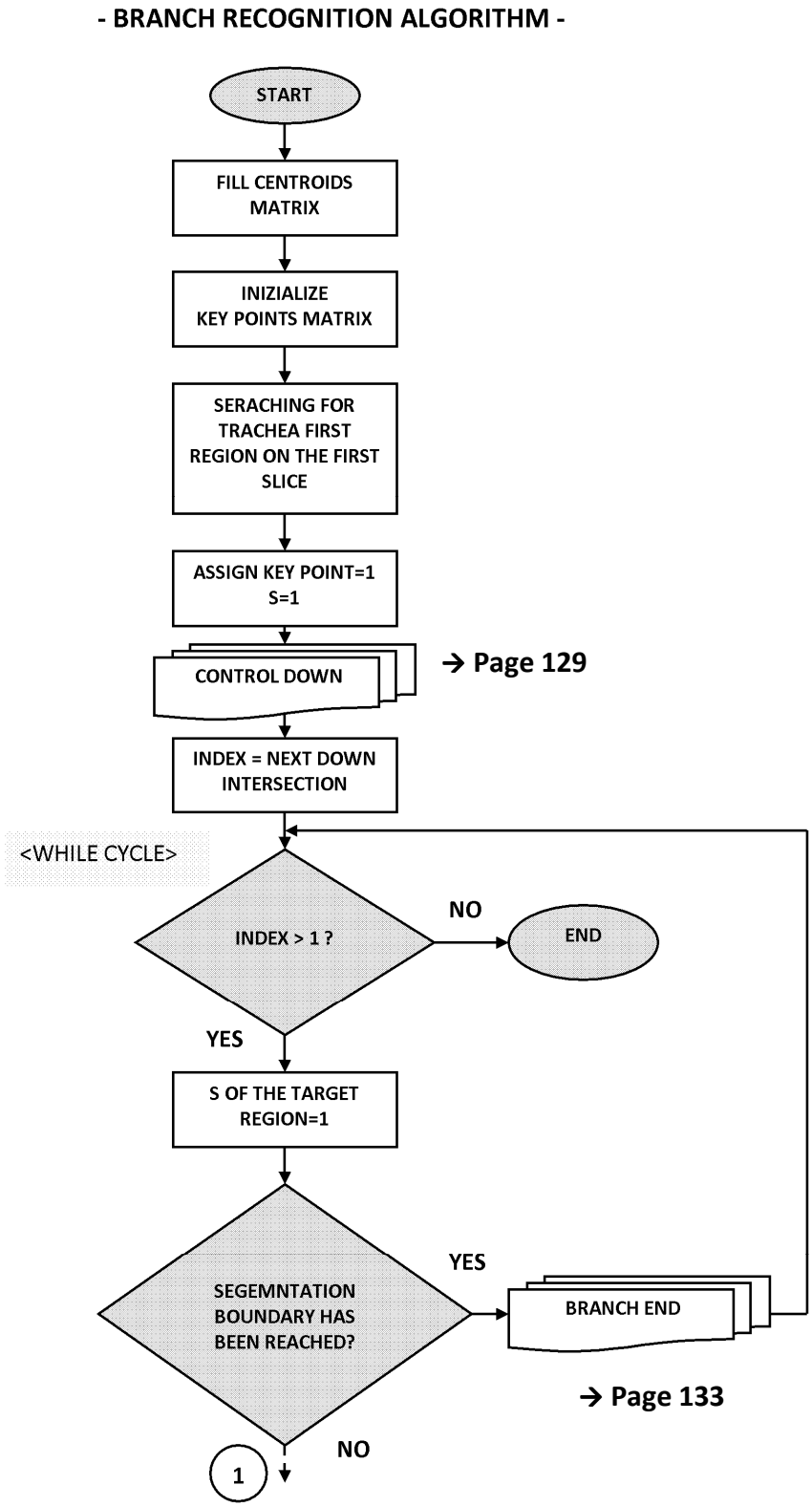

Figure 53 – Branch recognition algorithm flow chart part 1/2. The output of the branch recognition algorithm is the centroids matrix.

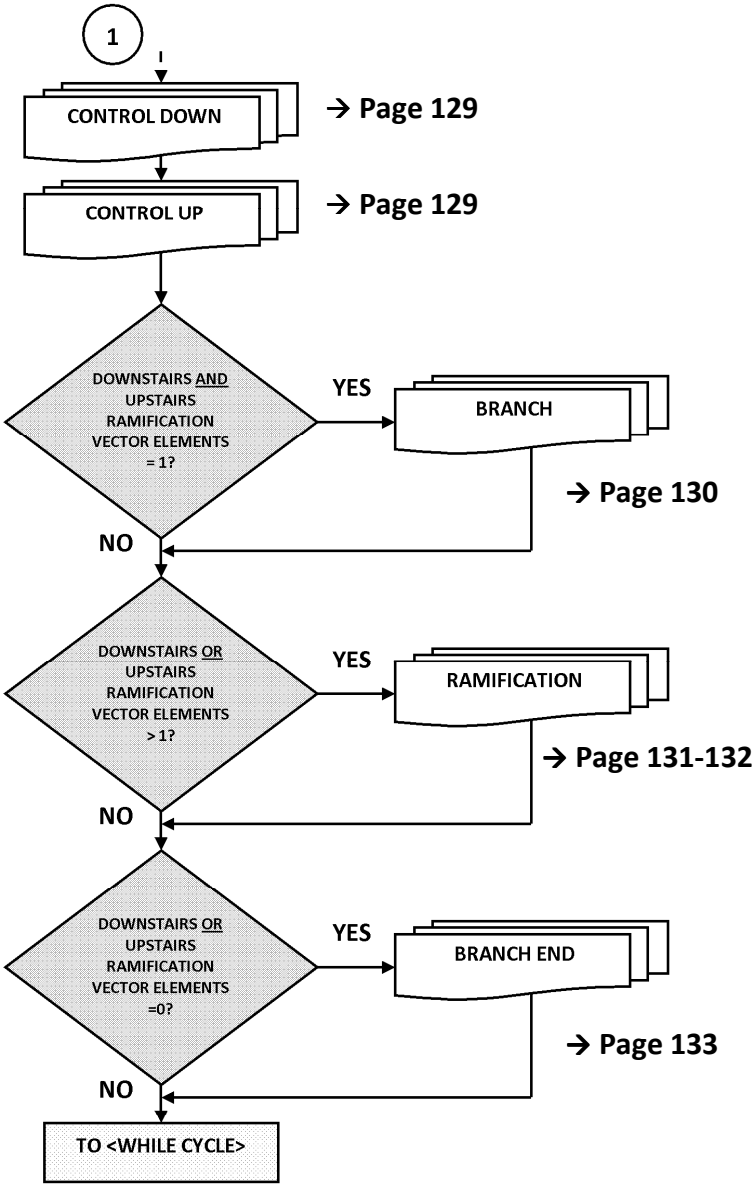

- CONTROL UP AND CONTROL DOWN ALGORITHM -

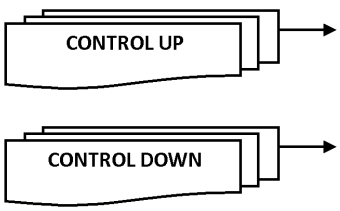

The output of this two functions are the centroids matrix rows that contain centroids of the region intersected downstairs and upstairs by target region. This rows are stored in two vectors called "downstairs ramification vector" and "upstairs ramification vector"

Figure 54 – Branch recognition algorithm flow chart part 2/2 with a little description of the control down and the control up functions.

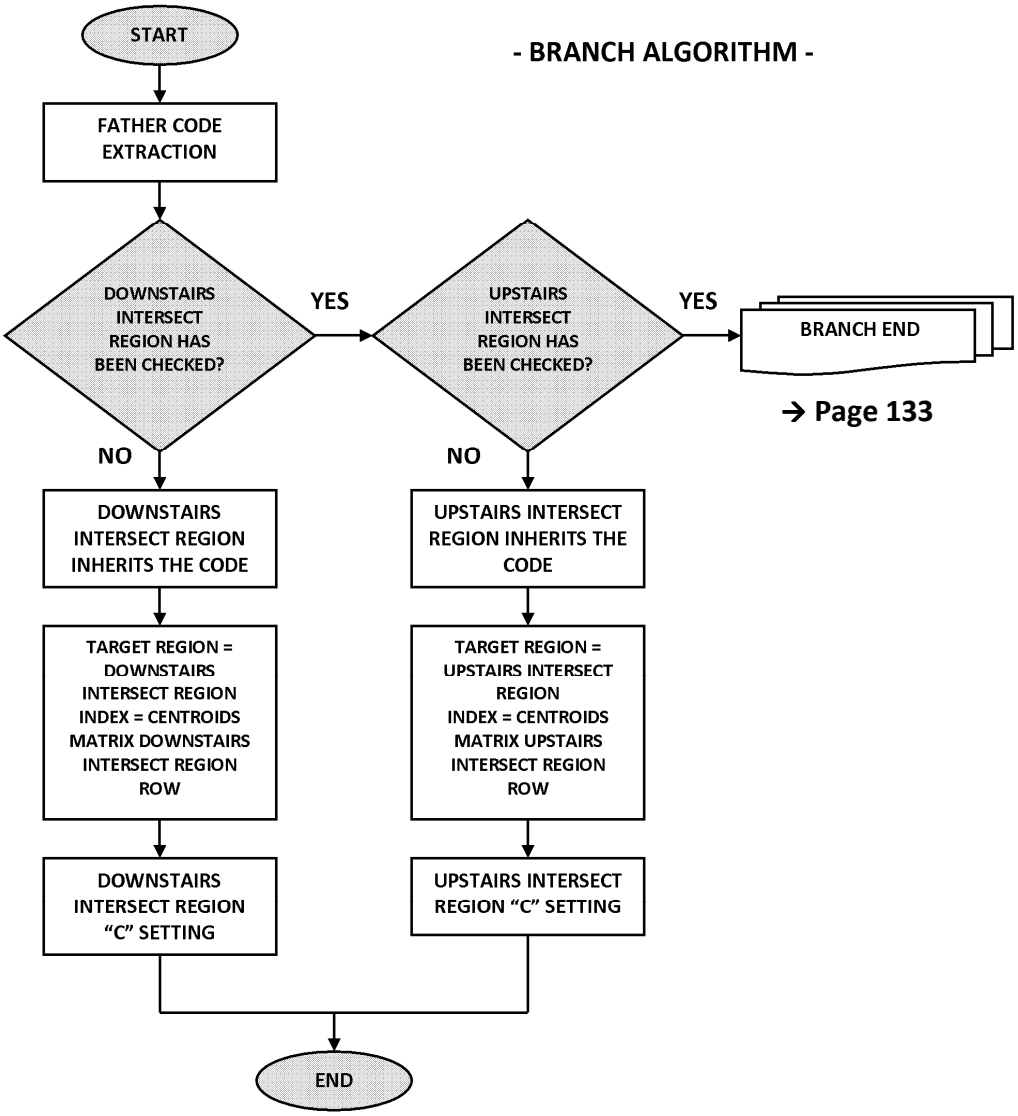

Figure 55 – Branch algorithm flow chart. This function process the branches of the airways tree.

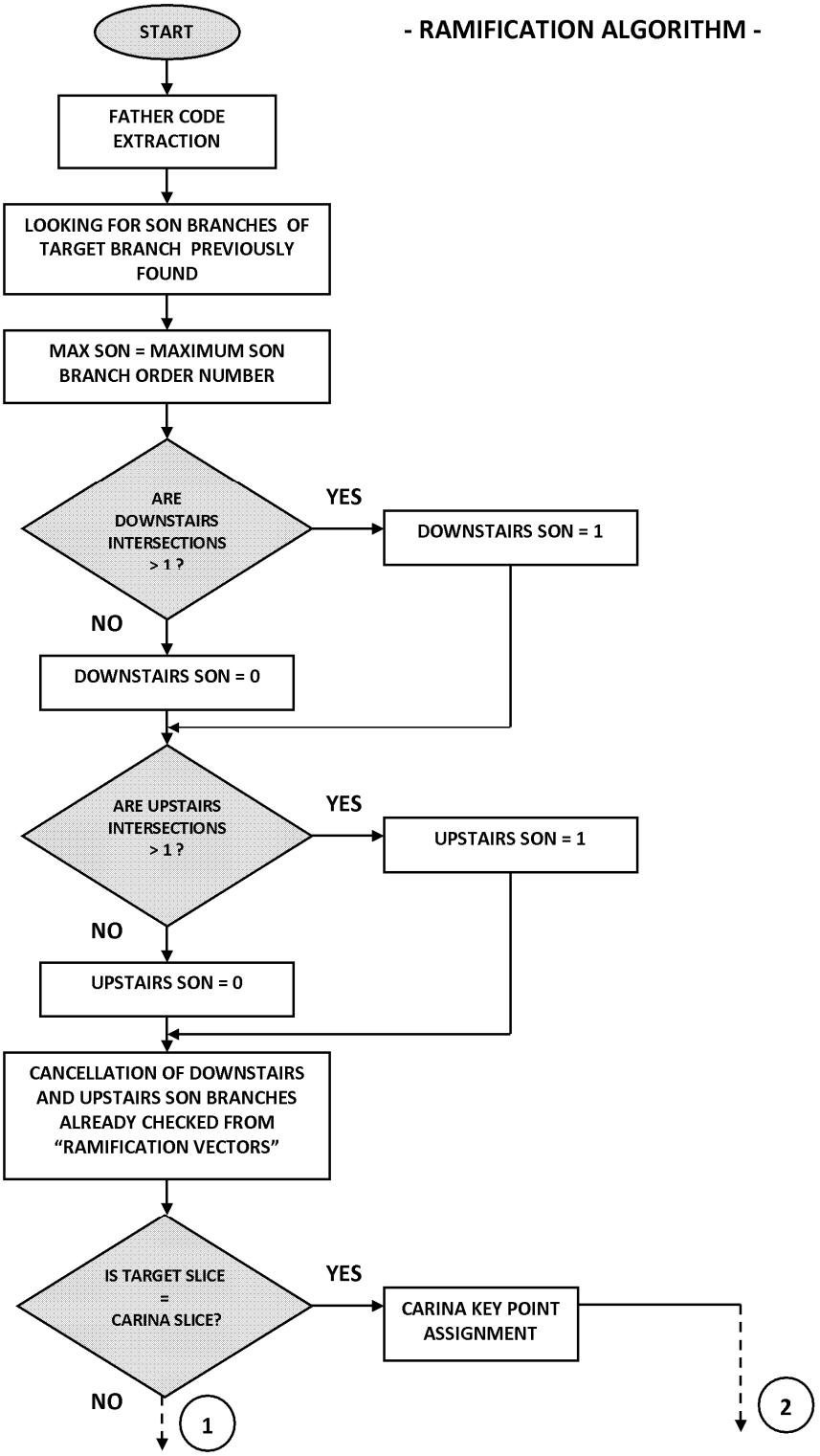

Figure 56 – Ramification algorithm flow chart part 1/2. This function process the ramifications of the airways tree.

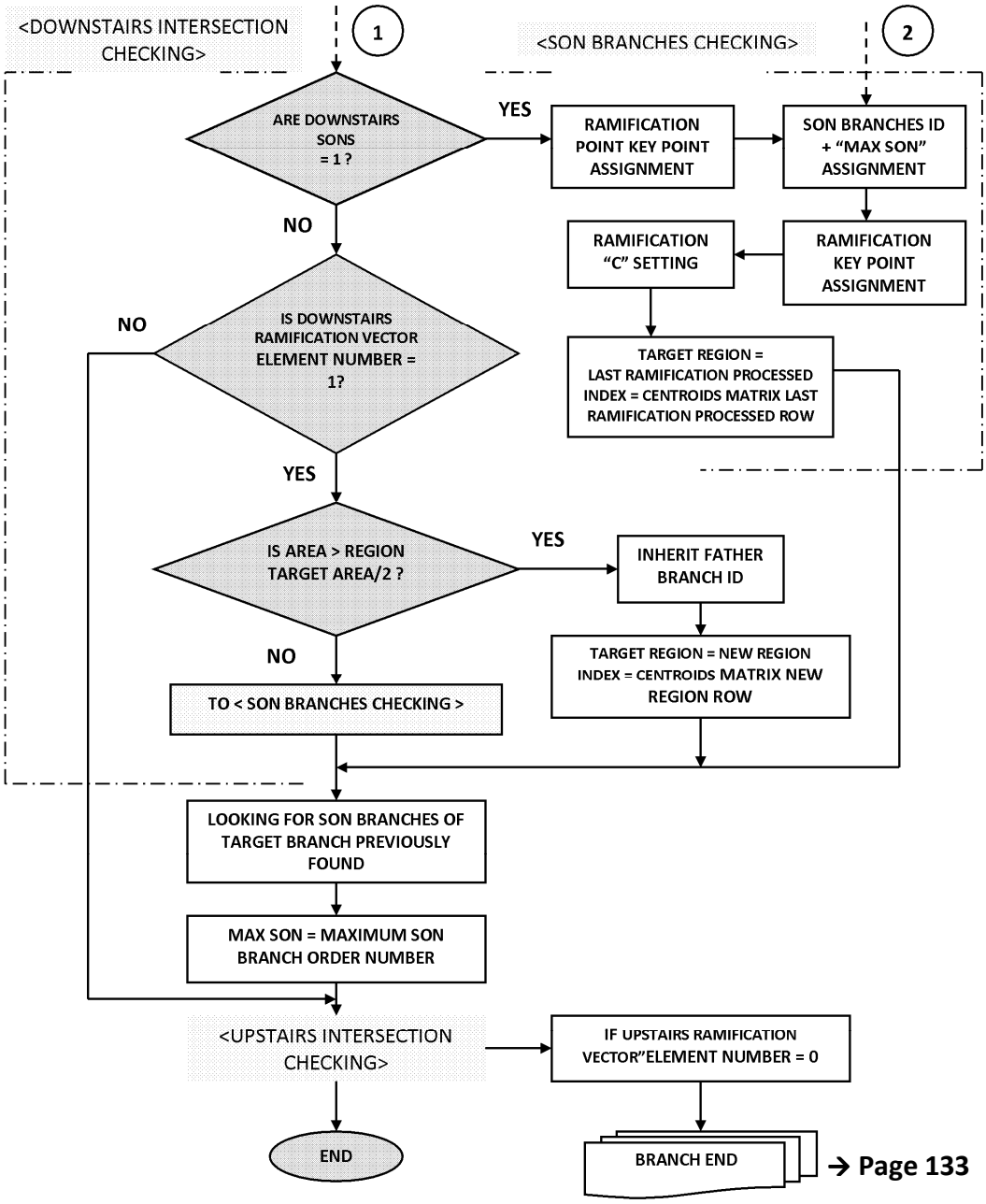

Figure 57 – Ramification algorithm flow chart part 2/2.

- BRANCH END ALGORITHM -

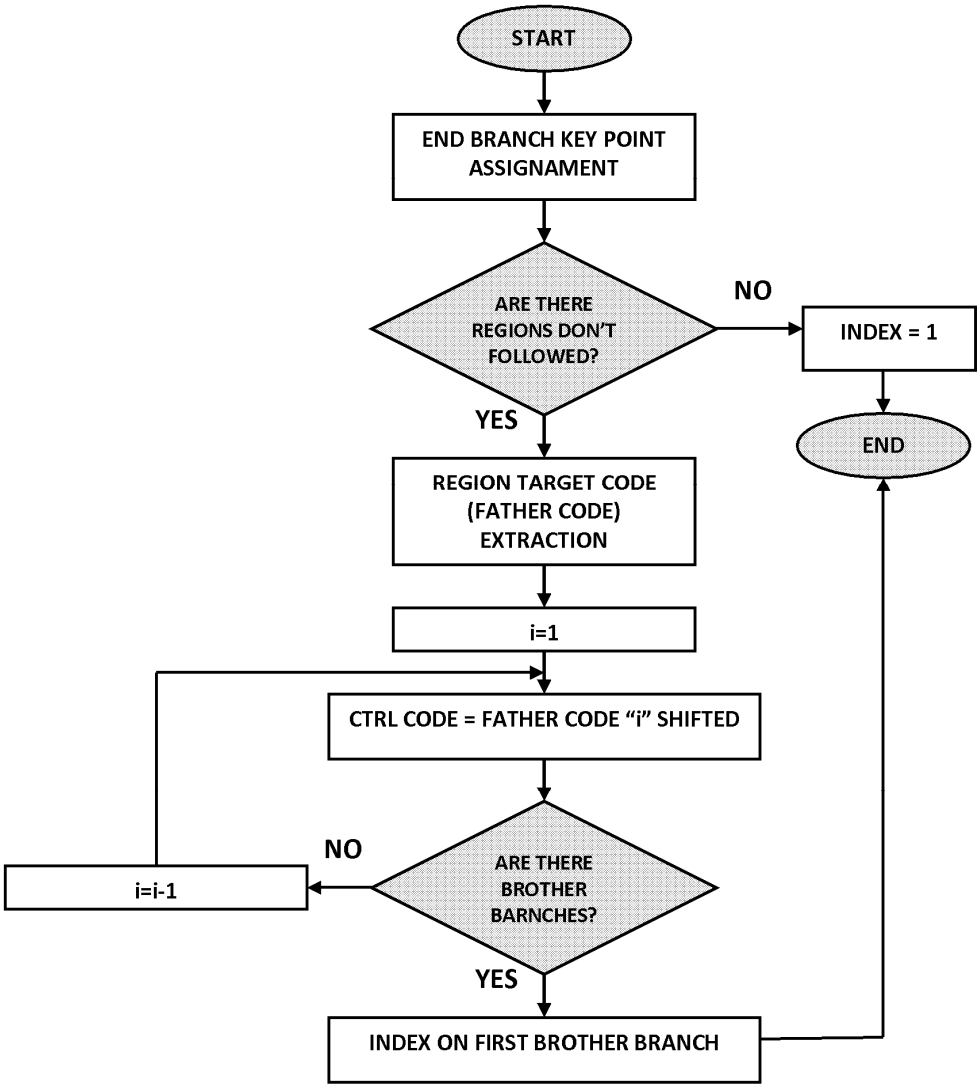

Figure 58 – Branch end algorithm flow chart. This function is used when an end of a branch of the airways tree is reached.

- STICK DIAGRAM ALGORITHM -

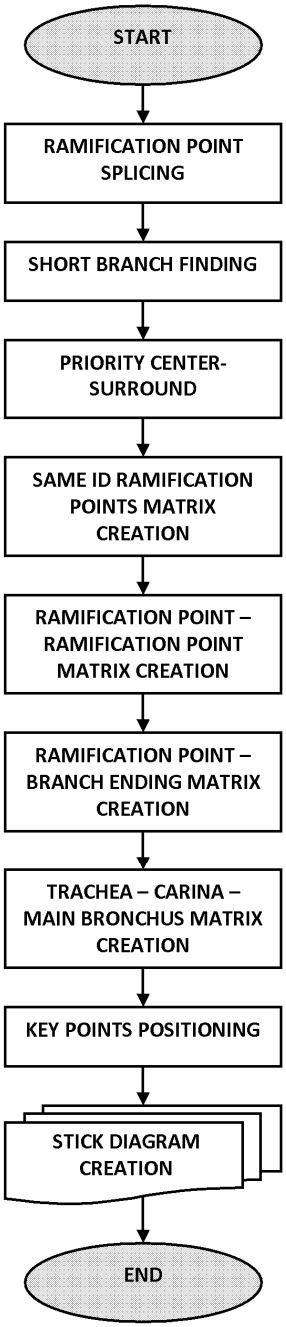

→ **Page 135-137**

Figure 59 – Stick diagram algorithm flow chart. This function includes all the operation of the key points organization and the real final key points linking.

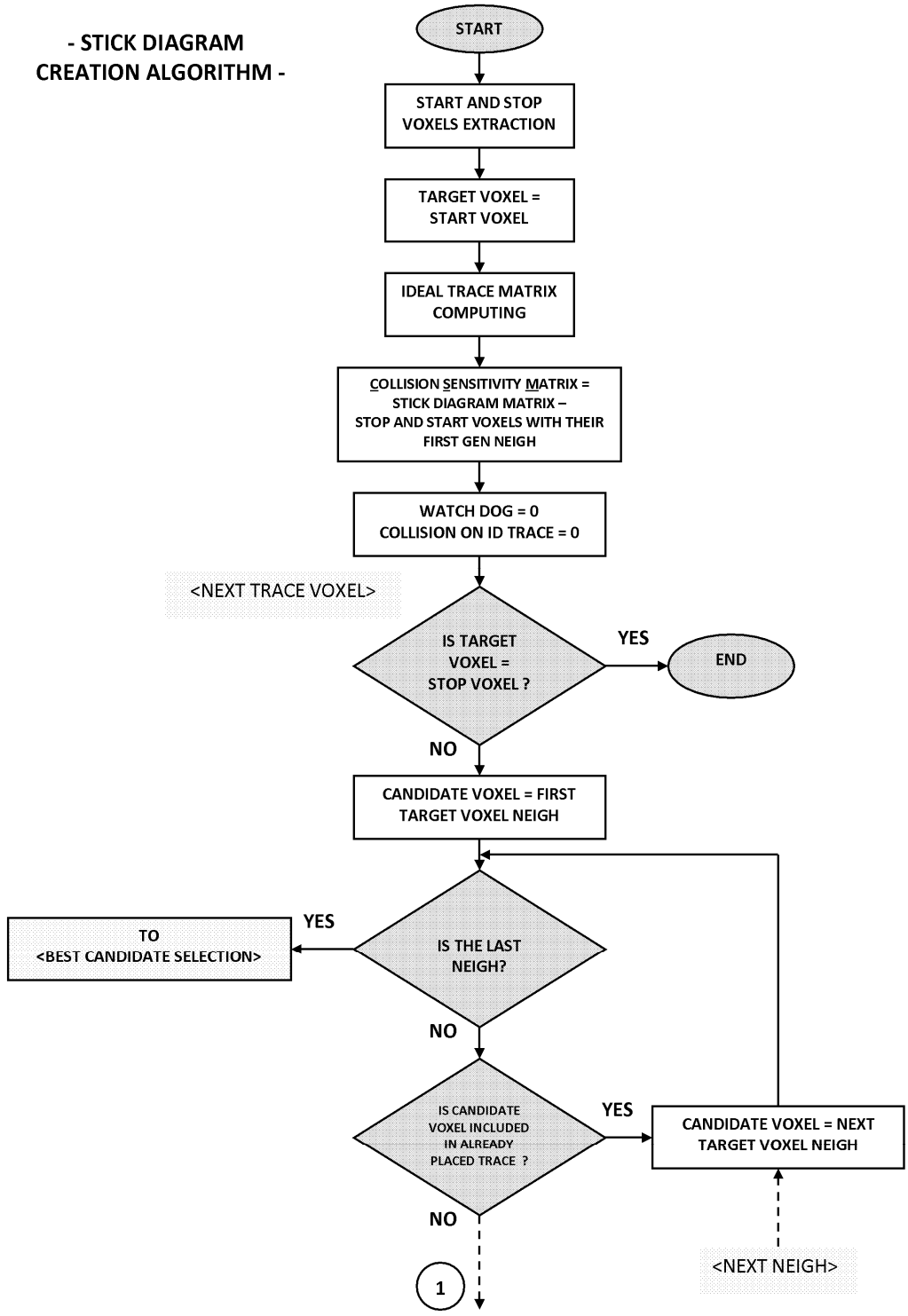

Figure 60 – Stick diagram creation algorithm flow chart part 1/3. This function realizes the key points linking.

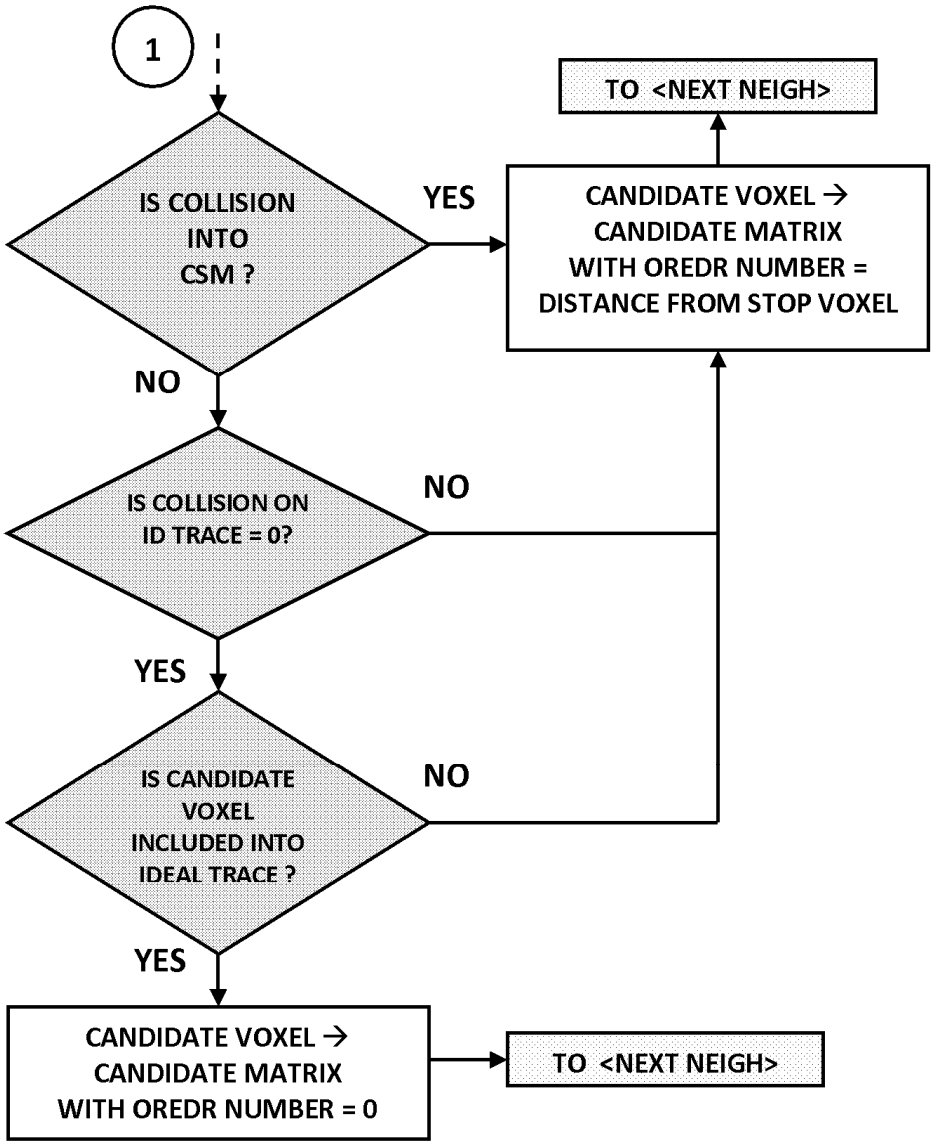

Figure 61 – Stick diagram creation algorithm flow chart part 2/3.

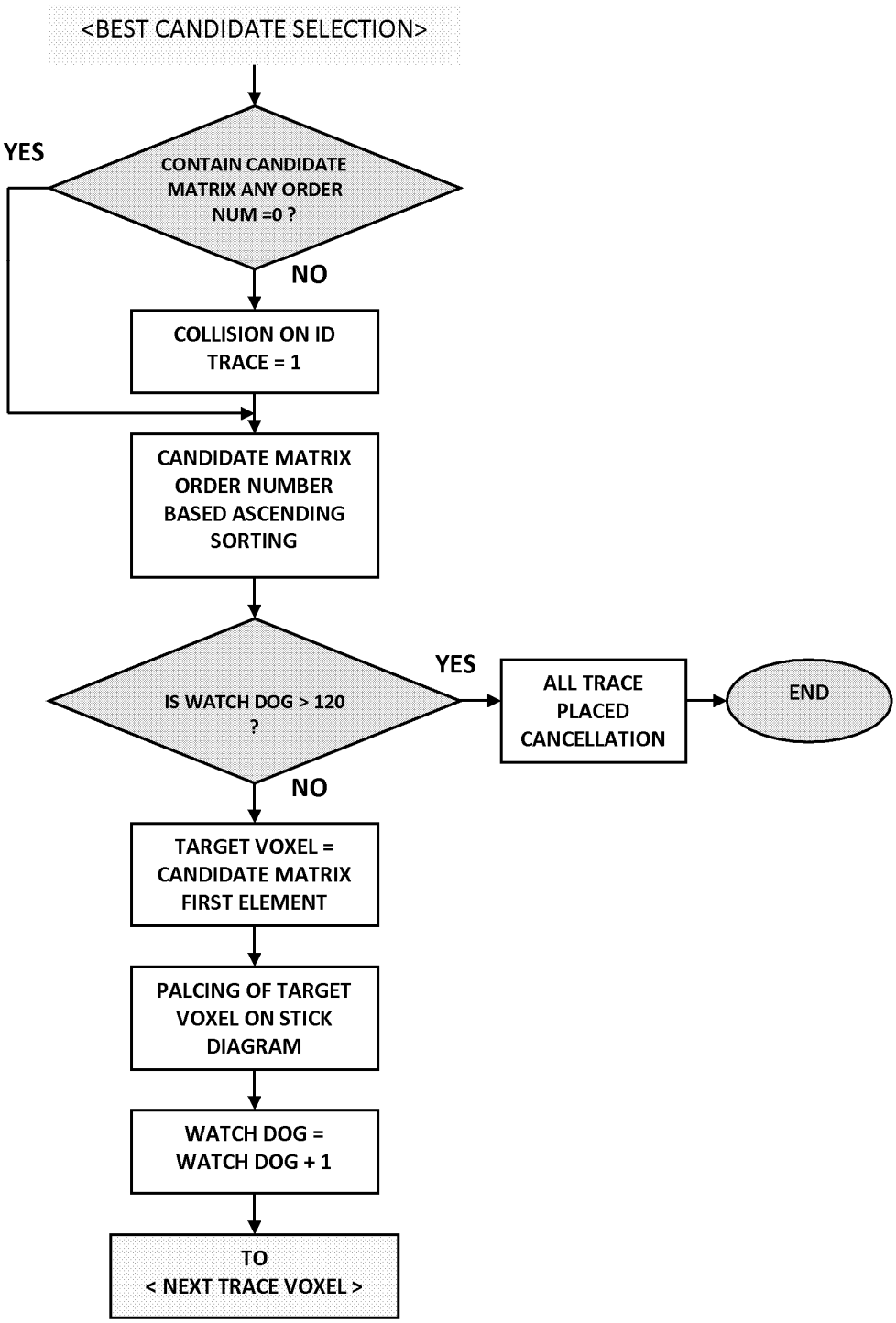

Figure 62 – Stick diagram creation algorithm flow chart part 3/3.

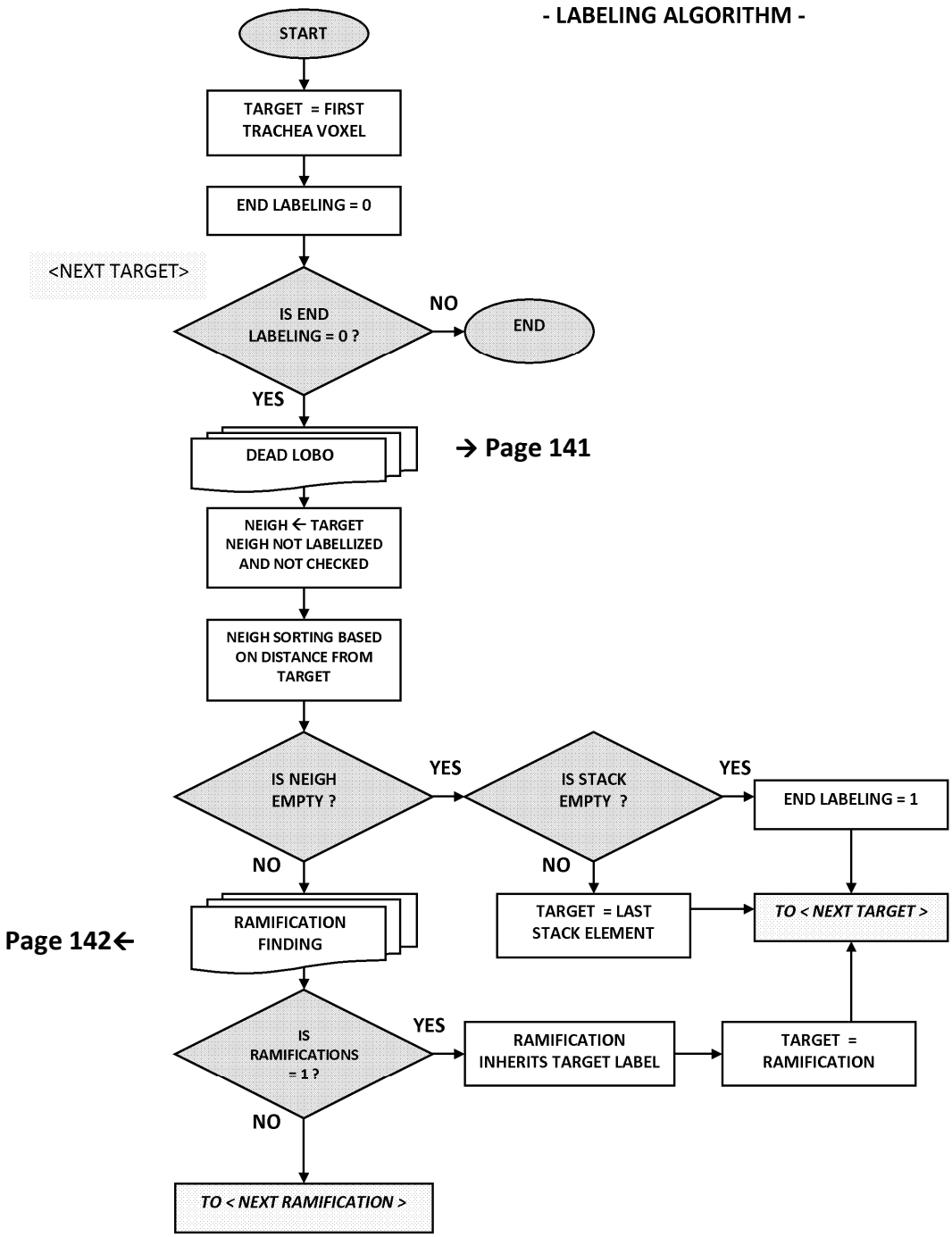

Figure 63 – Labeling algorithm flow chart part 1/3. The output of this function is the labelled stick diagram.

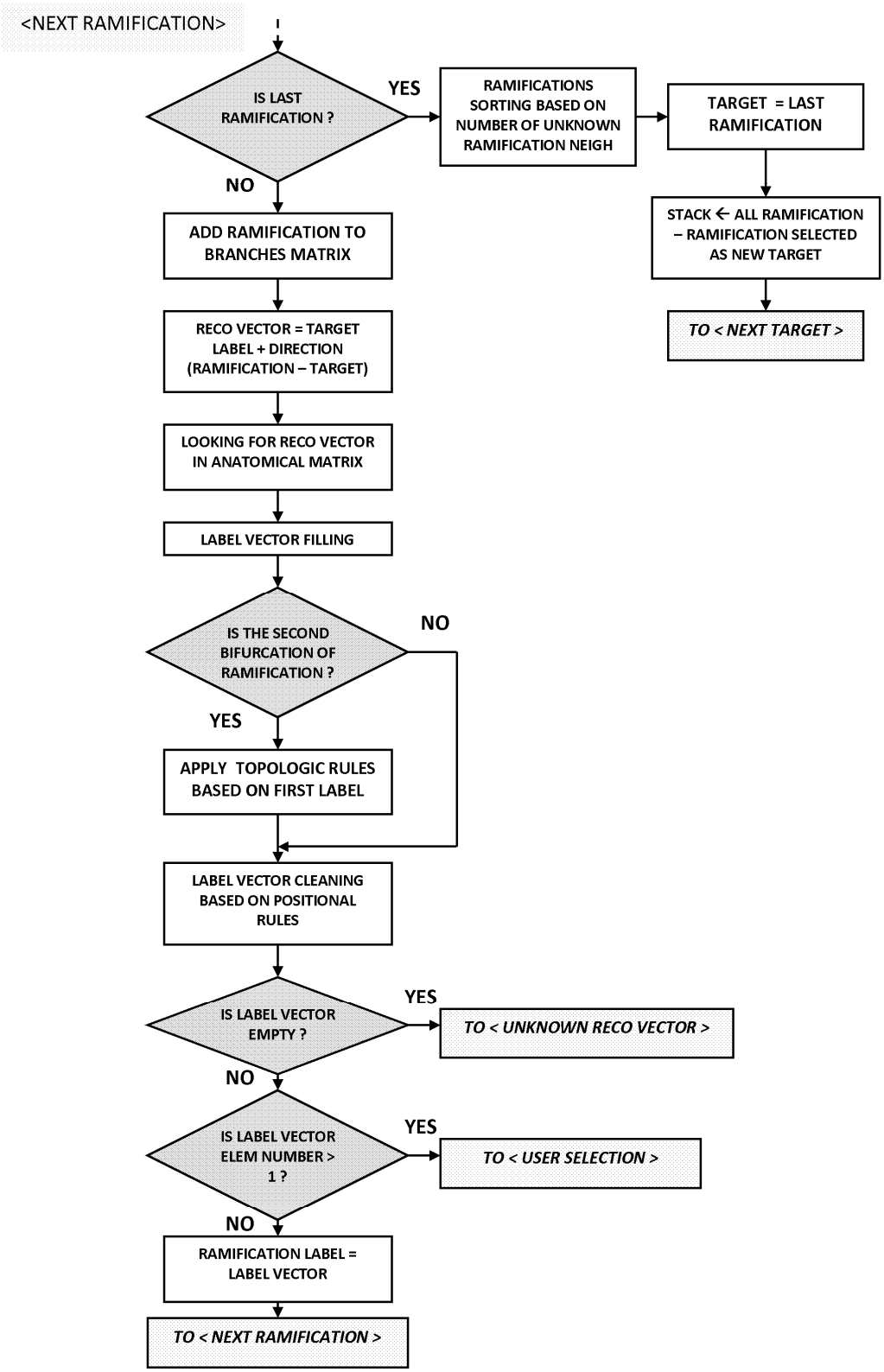

Figure 64 – Labeling algorithm flow chart part 2/3.

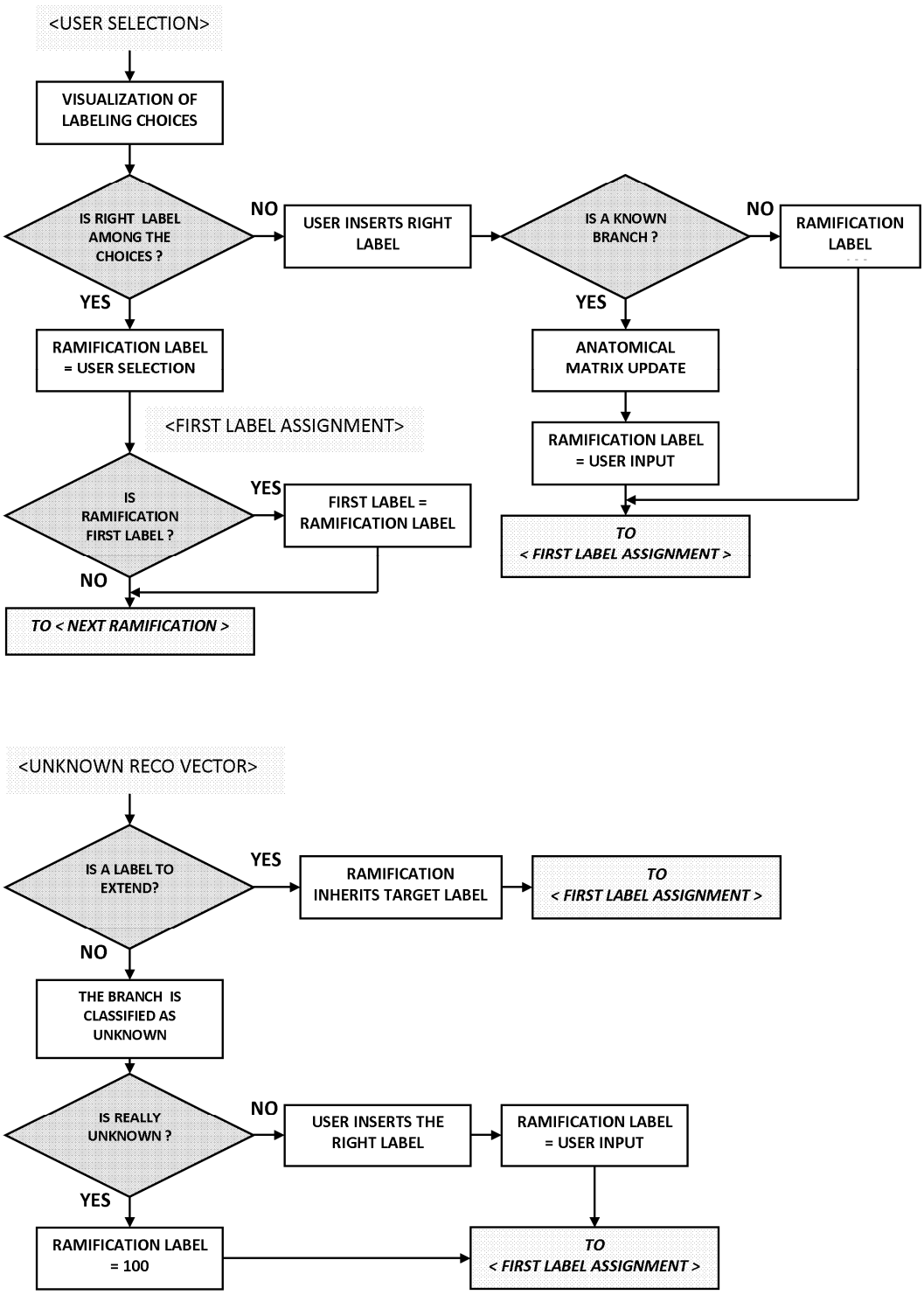

Figure 65 – Labeling algorithm flow chart part 3/3.

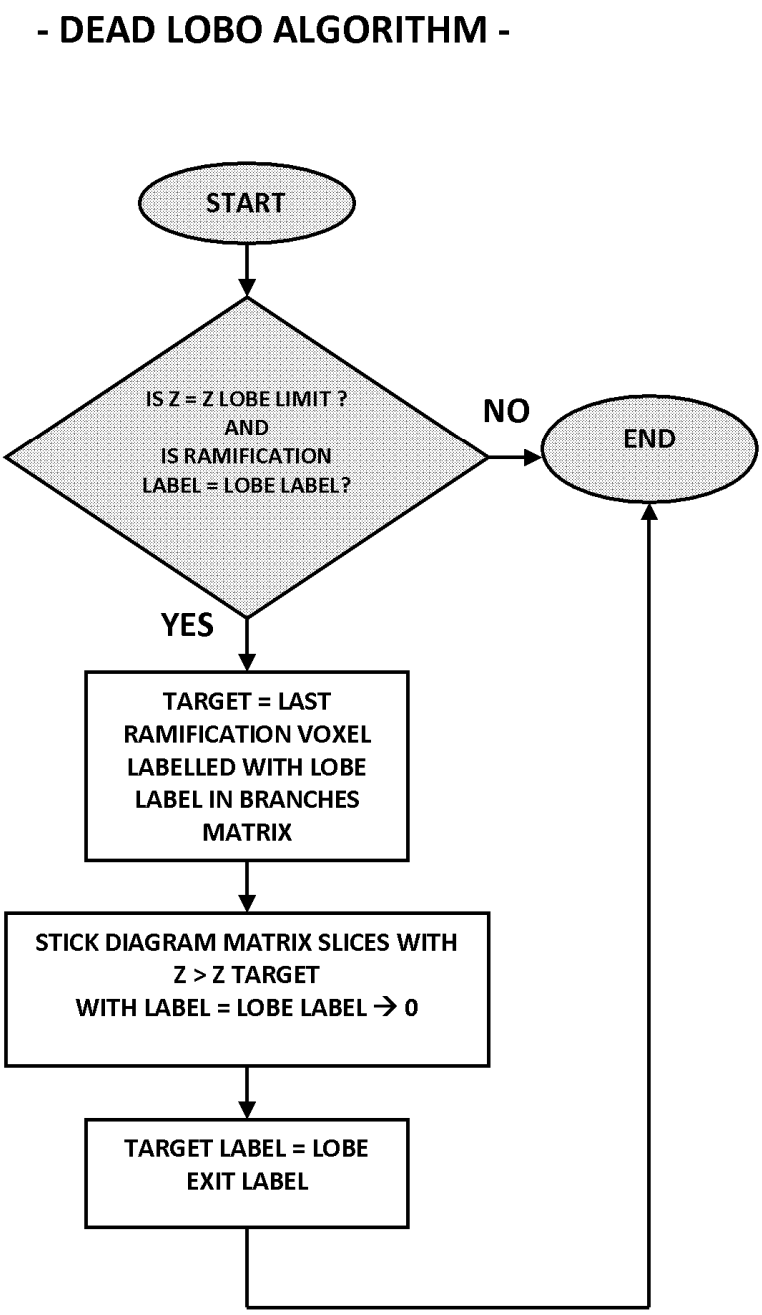

Figure 66 – Dead lobo algorithm flow chart. This function finds the end of upper right lobe real time on the stick diagram.

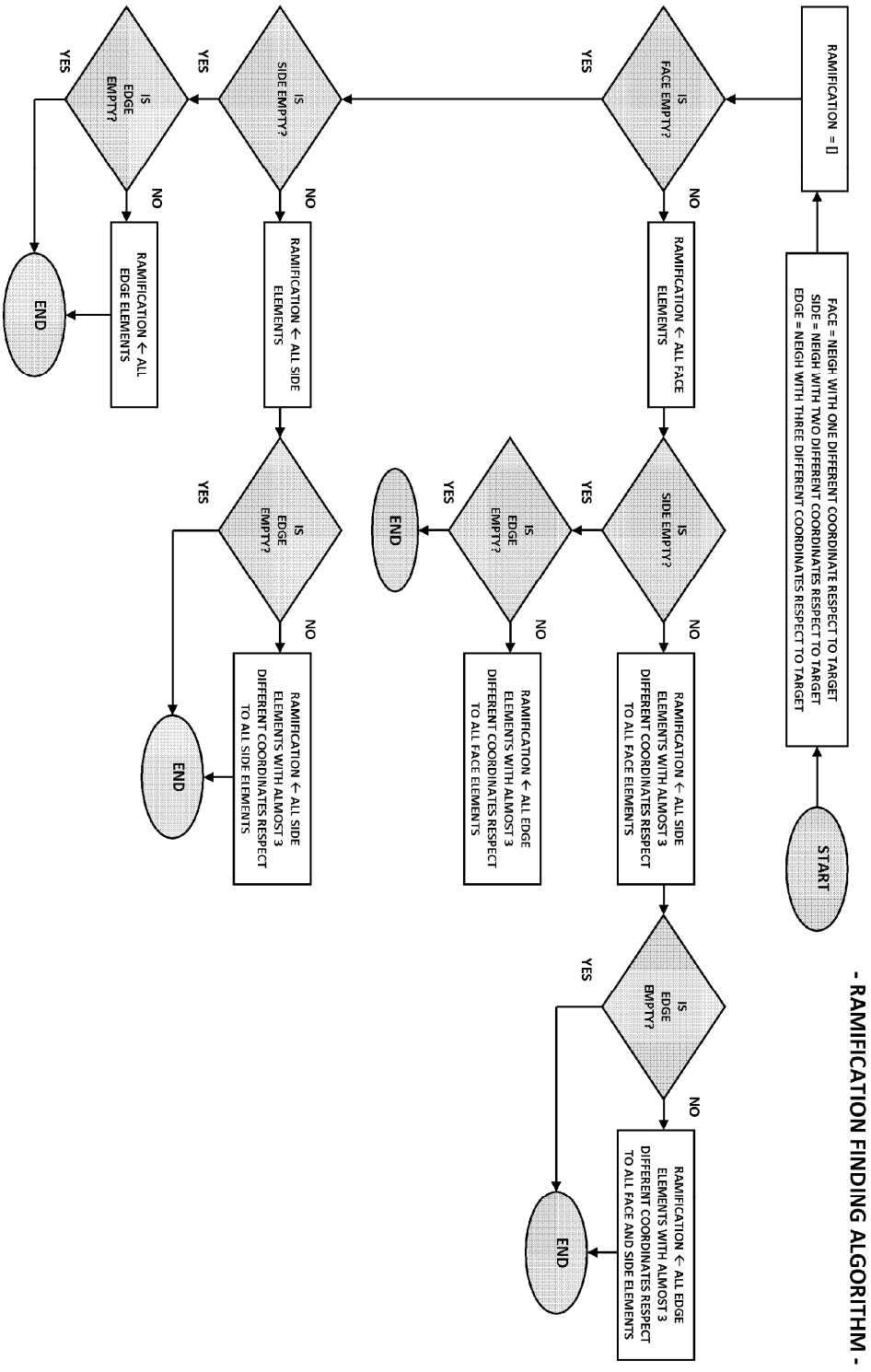

Figure 67 – Ramification finding algorithm flow chart. This function finds the ramification on the stick diagram.

Appendix 2
User interventions

The tables reported in this section contain the user interventions during the labeling of the tracheo-bronchial tree of each subject at TLC and RV volume. The choices are divided for the left and the right lung. For each lung the first column contains the labels candidate list proposed by the software and the second column contains the user choice chose from the list or the label suggested by his experience. When a choice updates the anatomical matrix is indicated by light yellow box.

TLC

Table 18 – User interventions in the automated label of subject 1 tracheo-bronchial tree at TLC volume.

	RIGHT		*LEFT*	
SUBJECT NUMBER	**CANDIDATE LABEL**	**USER CHOICE**	**CANDIDATE LABEL**	**USER CHOICE**
SUBJECT 1	4	23	7	8
	23		8	
	4	4	8	8
	23		36	
	5	5	37	37
	6		39	
	5	24	39	8
	24		310	
			8	
	27	27		
	210		37	39
			39	
	6	6		
	28		8	310
	29		310	
	27	27		
	210			
	6	28		
	28			
	29			

Table 19 – User interventions in the automated label of subject 2 tracheo-bronchial tree at TLC volume.

	RIGHT		*LEFT*	
SUBJECT NUMBER	**CANDIDATE LABEL**	**USER CHOICE**	**CANDIDATE LABEL**	**USER CHOICE**
SUBJECT 2	6	6	8	7
	5		7	
	26			
			8	8
	5	24	7	
	24			
			35	35
	6	6	8	
	28		7	
	29			
			34	34
	100	100	8	
			7	
	6	29		
	29		37	37
			39	
			8	310
			310	

Table 20 – User interventions in the automated label of subject 3 tracheo-bronchial tree at TLC volume.

	RIGHT		*LEFT*	
SUBJECT NUMBER	**CANDIDATE LABEL**	**USER CHOICE**	**CANDIDATE LABEL**	**USER CHOICE**
SUBJECT 3	5	5	31	31
	24		8	
			7	
	5	24		
	24		8	7
			7	
	6	6		
	29		8	8
			7	
	100	100		
			35	35
	6	6	7	
	28			
	29		36	36
			310	
	6	28		
	28		8	36
	29		36	
	6	100	37	37
	210		310	
	6	28	37	37
	28		39	
	29			
	6	6		
	210			
	6	29		
	28			
	29			

Table 21 – User interventions in the automated label of subject 4 tracheo-bronchial tree at TLC volume.

	RIGHT		*LEFT*	
SUBJECT NUMBER	**CANDIDATE LABEL**	**USER CHOICE**	**CANDIDATE LABEL**	**USER CHOICE**
SUBJECT 4	5	24	8	7
	24		7	
	6	6	8	34
	28		7	
	29			
			8	8
	6	210	7	
	27			
	210		8	36
			36	
			37	37
			39	

Table 22 – User interventions in the automated label of subject 5 tracheo-bronchial tree at TLC volume.

	RIGHT		*LEFT*	
SUBJECT NUMBER	**CANDIDATE LABEL**	**USER CHOICE**	**CANDIDATE LABEL**	**USER CHOICE**
SUBJECT 5	5	5	8	7
	26		7	
	6			
			8	7
	5	5	7	
	24		34	
	5	24	100	34
	24			
			35	35
	6	6	8	
	28		7	
	29			
			8	8
	6	28	7	
	28			
	29		36	8
			210	
	6	6		
	210		100	36
	6	28	8	36
	28		36	
	6	210	37	39
	210		39	
	6	29	8	8
	29		310	
	100	210	100	310
	100	29		

Table 23 – User interventions in the automated label of subject 6 tracheo-bronchial tree at TLC volume.

	RIGHT		*LEFT*	
SUBJECT NUMBER	**CANDIDATE LABEL**	**USER CHOICE**	**CANDIDATE LABEL**	**USER CHOICE**
SUBJECT 6	5	24	100	31
	24			
			8	7
	5	5	7	
	26			
	6		35	34
			8	
	5	24	7	
	24			
			8	7
	6	6	7	
	26			
			8	8
	100	24	7	
	5	24	37	37
	6		39	
	6	6	100	8
	28			
	29		8	39
			39	
	100	27	310	
	6	210		
	210			
	6	210		
	210			

Table 24 – User interventions in the automated label of subject 7 tracheo-bronchial tree at TLC volume.

	RIGHT		*LEFT*	
SUBJECT NUMBER	**CANDIDATE LABEL**	**USER CHOICE**	**CANDIDATE LABEL**	**USER CHOICE**
SUBJECT 7			31	31
			8	
			7	
			8	7
			7	
			35	34
			8	
			7	
			34	
			100	34
			8	7
			7	
			8	8
			7	
			35	35
			7	
			34	
			8	36
			36	

Table 25 – User interventions in the automated label of subject 8 tracheo-bronchial tree at TLC volume.

	RIGHT		*LEFT*	
SUBJECT NUMBER	**CANDIDATE LABEL**	**USER CHOICE**	**CANDIDATE LABEL**	**USER CHOICE**
SUBJECT 8	5	24	8	7
	24		7	
	6	6	8	34
	28		7	
	29			
			8	8
	6	27	7	
	27			
	210		37	37
			39	
	6	27		
	27			
	28			
	6	29		
	28			
	29			

RV

Table 26 – User interventions in the automated label of subject 1 tracheo-bronchial tree at RV volume.

	RIGHT		*LEFT*	
SUBJECT NUMBER	**CANDIDATE LABEL**	**USER CHOICE**	**CANDIDATE LABEL**	**USER CHOICE**
SUBJECT 1	5	5	8	31
	6		7	
	24			
			8	8
	100	26	7	
	5	5	37	37
	6		39	
	24			
	5	24		
	24			
	5	24		
	6			

Table 27 – User interventions in the automated label of subject 2 tracheo-bronchial tree at RV volume.

	RIGHT		*LEFT*	
SUBJECT NUMBER	**CANDIDATE LABEL**	**USER CHOICE**	**CANDIDATE LABEL**	**USER CHOICE**
SUBJECT 2	5	5	31	31
	6		8	
	24		7	
	5	24	7	8
	24		8	
	5	6	8	8
	6		39	
			310	
	6	210		
	27		100	36
	100	29	37	37
			39	

Table 28 – User interventions in the automated label of subject 3 tracheo-bronchial tree at RV volume.

	RIGHT		*LEFT*	
SUBJECT NUMBER	**CANDIDATE LABEL**	**USER CHOICE**	**CANDIDATE LABEL**	**USER CHOICE**
SUBJECT 3	5	5	8	8
	6		7	
	24			
			8	36
	5	24	36	
	24			
			37	39
	5	6	39	
	6			
			100	39
	6	6		
	28			
	29			
	27	27		
	28			
	6	28		
	29			
	6	28		
	28			

Table 29 – User interventions in the automated label of subject 4 tracheo-bronchial tree at RV volume.

	RIGHT		*LEFT*	
SUBJECT NUMBER	**CANDIDATE LABEL**	**USER CHOICE**	**CANDIDATE LABEL**	**USER CHOICE**
SUBJECT 4	5	5	8	7
	6		7	
	24		31	
	5	24	100	31
	24			
			8	34
	100	6	7	
			34	
	100	27		
			8	7
	6	29	7	
	28			
	29		8	35
			7	
			34	
			8	8
			7	
			8	8
			36	
			39	37
			310	
			37	39
			39	

Table 30 – User interventions in the automated label of subject 5 tracheo-bronchial tree at RV volume.

	RIGHT		*LEFT*	
SUBJECT NUMBER	**CANDIDATE LABEL**	**USER CHOICE**	**CANDIDATE LABEL**	**USER CHOICE**
SUBJECT 5	4	4	8	7
	23		7	
	5	24	8	35
	24		7	
			34	
	5	6	35	
	6			
			8	8
			7	
			8	36
			36	
			37	37
			39	

Table 31 – User interventions in the automated label of subject 6 tracheo-bronchial tree at RV volume.

	RIGHT		*LEFT*	
SUBJECT NUMBER	**CANDIDATE LABEL**	**USER CHOICE**	**CANDIDATE LABEL**	**USER CHOICE**
SUBJECT 6	5	5	8	7
	24		7	
	5	24	8	8
	24		7	
	5	6	35	34
	6		7	
	24		34	
			8	36
			36	
			8	310
			36	

Table 32 – User interventions in the automated label of subject 7 tracheo-bronchial tree at RV volume.

	RIGHT		*LEFT*	
SUBJECT NUMBER	**CANDIDATE LABEL**	**USER CHOICE**	**CANDIDATE LABEL**	**USER CHOICE**
SUBJECT 7	100	4	8	7
			7	
	5	24		
	24		8	8
			7	
	5	5		
	6		37	8
			39	
	100	26		
			36	36
	5	26	310	
	6			
	24		8	100
			39	
	5	24	310	
	24		37	
	5	6	8	8
	6		310	
	6	27	8	310
	27		36	
			310	
	6	6		
	27			
	210			

Table 33 – User interventions in the automated label of subject 8 tracheo-bronchial tree at RV volume.

	RIGHT		*LEFT*	
SUBJECT NUMBER	**CANDIDATE LABEL**	**USER CHOICE**	**CANDIDATE LABEL**	**USER CHOICE**
SUBJECT 8			8	31
			7	
			31	
			8	8
			7	
			37	8
			39	
			8	
			36	36
			310	
			37	37
			39	
			8	
			37	37
			310	
			8	39
			39	
			310	
			37	

BIBLIOGRAPHY

[1] Hansell D.M., Bankier A.A., MacMahon H., McLoud T.C., Muller N.L., Remy J. *Fleischner Society: Glossary of Terms for Thoracic Imaging Radiology* (246) No. 3. Pp. 697-722. 2008.

[2] Miller W.S. *The lung*. Springfield, IL. Charles C Thomas. 1947.

[3] Webb W.R. *Thin-Section CT of the Secondary Pulmonary Lobule: Anatomy and the Image*. The 2004 Fleischner Lecture Radiology (239), Number 2. May 2006.

[4] Heitzman E.R., Markarian B., Berger I., et al. *The secondary pulmonary lobule: a practical concept for interpretation of radiographs*. I. Roentgen anatomy of the normal secondary pulmonary lobule. Radiology (93). pp. 508–513. 1969

[5] Reid L., Simon G. *The peripheral pattern in the normal bronchogram and its relation to peripheral pulmonary anatomy*. Thorax (13). pp. 103–109. 1958.

[6] Webb W.R., Stein M.G., Finkbeiner W.E., Im J.G., Lynch D. *Normal and diseased isolated lungs: high-resolution CT*. Radiology (166). pp. 81–87. 1988.

[7] Aykac D., Hoffman E.A., McLennan G., Reinhardt J.M. *Segmentation and Analysis of the Human Airways Tree From Three-Dimensional X-Ray CT Images*. IEEE Transactions on medical imaging (22), No. 8. Aug 2003

[8] Weibel E.R. *Looking into the lung: what can it tell us?* American Journal of Roentgenology (133). pp. 1021–1031. 1979.

[9] Weibel E.R. *Design and structure of the human lung. Pulmonary disease and disorders*. Ed. A. P. Fishman. New York: McGraw Hill, pp. 224-271. 1980.

[10] Webb W.R., Muller L.N., Naidich D.P. High *Resolution CT of the Lung, 4th edition*-. Lippincot Williams & Wilkins. 2009.

[11] Jackson C.L., Huber J.F. *Correlated Applied Anatomy of the Bronchial Tree and Lungs With a System of Nomenclature*. American College of Chest Physicians. 1943.

[12] Weibel E.R. *Morphometry of the Human Lung*. Academic Press, New York. 1963.

[13] Yamashita H.: *Roentgenologic Anatomy of the Lung*. Igaku-shoin, Tokyo. 1978.

[14] Moore K.L. *Clinically Oriented Anatomy*. Williams & Willkins. Pp. 49-148. Baltimore. 1985.

[15] Agur A.M.R., Lee M.J. *Grant Atlas of Anatomy*. Williams & Willkins. Pp. 1-76. Baltimore. 1991.

[16] Kitaoka H., Park Y., Tschirren J., Reinhardt J., Sonka M., McLennan G., Hoffman E. A. *Automated Nomenclature Labeling of the Bronchial Tree in 3D-CT Lung Images*. T. Dohi and R. Kikins Eds., MICCAI, LNCS 2489. pp. 1-11. 2002.

[17] Verschakelen J.A., Wever W.D., *Computed Tomography of the Lung - A Pattern Approach*. Springer Berlin Heidelberg Edition. 2007.

[18] Lynch D.A., Newell J.D., Tschomper B.A., et al. *Uncomplicated asthma in adults: comparison of CT appearance of the lungs in asthmatic and healthy subjects*. Radiology (188). pp. 829-833. 1993.

[19] Kim J.S., Muller N.L., Park C.S. et al. *Cylindrical bronchiectasis: diagnostic findings on thin-section CT*. AJR Am J Roentgenol (168). pp. 751–754. 1997.

[20] Murata K., Itoh H., Todo G. et al. *Centrilobular lesions of the lung: demonstration by high-resolution CT and pathologic correlation*. Radiology (161). pp. 641–645. 1986.

[21] Webb W.R., Stein M.G., Finkbeiner W.E., Im J.G., Lynch D. and Gamsu G. *Normal and diseased isolated lungs: high-resolution CT*. Radiology (166). pp. 81-87. 1988.

[22] Itoh H., Murata K., Konishi J., et al. *Diffuse lung disease: pathologic basis for the high-resolution computed tomography findings*. J Thorac Imaging (8). pp. 176-188. 1993.

[23] Mayer D., Bartz D., Fischer J., Ley S., del Rio S., Thust S., Kauczor H.U., Heussel C.P. *Hybrid segmentation and virtual bronchoscopy based on CT images.* Academic Radiology (11), Issue 5. pp. 551-565. May 2004.

[24] San Jose E.R., Reilly J.J., Silverman E.K., Washko G.R. *Three-Dimensional Airways Measurements and Algorithms.* Proceedings of the American Thoracic Society (5). Pp. 905-909. 2008.

[25] Vining D.J., Liu K., Choplin R.H., Haponik E.F. *Virtual bronchoscopy: relationships of virtual reality endo-bronchial simulations to actual bronchoscopic findings*. Chest (109). Pp. 549–553. 1996.

[26] McLennan G., Higgins W., Hoffman E. *Virtual bronchoscopy: impact of the digital revolution.* Pulmonary Perspectives (21). Pp. 1–4. 2004.

[27] Liewald F., Lang G., Fleiter T., Sokiranski R., Halter G., Orend K.H. *Comparison of virtual and fiberoptic bronchoscopy.* Thorac Cardiovasc Surg (46). Pp. 361–364. 1998.

[28] Finkelstein S.E., Summers R.M., Nguyen D.M., Stewart J.H.T., Tretler J.A., Schrump D.S.. *Virtual bronchoscopy for evaluation of malignant tumors of the thorax.* J. Thorac Cardiovasc Surg (123). Pp. 967–972. 2002.

[29] Summers R.M., Aggarwal N.R., Sneller M.C., Cowan M.J., Wood B.J., Langford C.A., Shelhamer J.H. *CT virtual bronchoscopy of the central airways in patients with Wegener's granulomatosis.* Chest (121). Pp. 242–250. 2002.

[30] Scott Ferguson J., McLennan G. *Virtual Bronchoscopy*. Departments of Internal Medicine, Radiology, and Biomedical Engineering. University of Iowa, Iowa City, Iowa. Proc Am Thorac Soc (2). pp 488-505. 2005.

[31] Higgins W.E., Ramaswamy K., Swift R.D., McLennan G., Hoffman E.A. *Virtual bronchoscopy for three–dimensional pulmonary image assessment: state of the art and future needs.* Radiographics (18). Pp. 761–778. 1998.

[32] McAdams H.P., Goodman P.C., Kussin P. *Virtual bronchoscopy for directing transbronchial needle aspiration of hilar and mediastinal lymph nodes: a pilot study*. AJR AmJ Roentgenol (170). Pp. 1361–1364. 1998.

[33] Kiraly A.P., Helferty J.P., Hoffman E.A., McLennan G., Higgins W.E. *Three-dimensional path planning for virtual bronchoscopy.* IEEE Trans Med Imaging (23). Pp. 1365–1379. 2004.

[34] Rooney C.P., Wolf K., McLennan G. *Ultrathin bronchoscopy as an adjunct to standard bronchoscopy in the diagnosis of peripheral lung lesions: a preliminary report*. Respiration (Herrlisheim) (69). Pp. 63–68. 2002.

[35] Snell G.I., Holsworth L., Borrill Z.L., Thomson K.R., Kalff V., Smith J.A., Williams T.J. *The potential for bronchoscopic lung volume reduction using bronchial prostheses: a pilot study.* Chest (124). Pp. 1073–1080. 2003.

[36] Tschirren J., McLennan G., Palágyi K., Hoffman E.A., Sonka M. *Matching and anatomical labeling of human airways tree*. IEEE Trans Med Imaging (24), No. 12. Pp. 1540-1547. Dec 2005.

[37] Palagyi K., Sorantin E., Balogh E., Kuba A., Halmai C., Erdohely, B., Hausegger K. *A sequential 3D Thinning Algorithm and its Medical Applications*. In 17th Int. Conf. IPMI. Pp. 409-415. 2001.

[38] Pelillo M., Siddiqi K., Zucker S.W. *Matching Hierachical Structure Using Association Graph.* IEEE Trans. PAMI. (21). Pp. 1105-1120. 1999.

[39] Mori K., Ota S., Deguchi D., Kitasaka T., Suenaga Y. *Automated Anatomical Labeling of Bronchial Branches Extracted from CT Datasets Based on Machine Learning and Combination Optimization and Its Application to Bronchoscope Guidance*. G.-Z. Yang et al. Eds., MICCAI, Part II, LNCS 5762. pp. 707–714. 2009.

[40] Ota S., Deguchi D., Kitasaka T., Mori K., Suenaga Y. *Augmented Display of Anatomical Names of Bronchial Branches for Bronchoscopy Assistance.* T. Dohi, I. Sakuma, and H. Liao Eds., MIAR, LNCS 5128. pp. 377–384. 2008.

[41] Kitasaka T., Mori K., Hasegawa J., Toriwaki J. *A Method for Extraction of Bronchus Regions from 3D Chest X-ray CT Images by Analyzing Structural Features of the Bronchus*. FORMA (17). Pp.321–338. 2002.

[42] Li L. *Multiclass Boosting with Repartitioning*. In: Proc. of the 23rd Int'l Conf. On Machine Learning. pp. 569–576. 2006.

[43] Barazzetti L. *Reconstruction of the Airways Tree from CT Images for Assessment and Treatment of Emphysema*. Master Thesis. Jul 2009.

[44] Jack E. Bresenham. *Algorithm for computer control of a digital plotter*. IBM Systems Journal (4), No.1. pp. 25–30. Jan 1965.

[45] Frank H. Netter. *Netter Atlas of Anatomy*. Elsevier Masson. 2007.

[46] Asano F., Matsuno Y., Shinagawa N., Yamazaki K. *A Virtual Bronchoscopic Navigation System for Pulmonary Peripheral Lesions*. Chest Journal. pp. 559-566. Aug 2006.

[47] Shinagawa N., Yamazaki K., Onodera Y., Asano F. *Virtual bronchoscopic navigation system shortens the examination time – Feasibility study of virtual bronchoscopic navigation system.* Lung Cancer (56). pp. 201-206. Sep 2006.

[48] Tachihara M., Ishida T., Kanazawa K., Sugawara A. *A virtual bronchoscopic navigation system under X-ray fluoroscopy for transbronchial diagnosis of small peripheral pulmonary lesions*. Cancer (57). pp. 322-327. Jan 2007.